

INFORMATION TO USERS

This manuscript has been reproduced from the microfilm master. UMI films the text directly from the original or copy submitted. Thus, some thesis and dissertation copies are in typewriter face, while others may be from any type of computer printer.

The quality of this reproduction is dependent upon the quality of the copy submitted. Broken or indistinct print, colored or poor quality illustrations and photographs, print bleedthrough, substandard margins, and improper alignment can adversely affect reproduction.

In the unlikely event that the author did not send UMI a complete manuscript and there are missing pages, these will be noted. Also, if unauthorized copyright material had to be removed, a note will indicate the deletion.

Oversize materials (e.g., maps, drawings, charts) are reproduced by sectioning the original, beginning at the upper left-hand corner and continuing from left to right in equal sections with small overlaps.

Photographs included in the original manuscript have been reproduced xerographically in this copy. Higher quality 6" x 9" black and white photographic prints are available for any photographs or illustrations appearing in this copy for an additional charge. Contact UMI directly to order.

**ProQuest Information and Learning
300 North Zeeb Road, Ann Arbor, MI 48106-1346 USA
800-521-0600**

UMI[®]

University of Alberta

OPTIMIZING THE SCID/ α PA MOUSE MODEL FOR HEPATITIS C

by

Dr. Daniel E. Schiller



**A thesis submitted to the Faculty of Graduate Studies and Research in partial fulfillment
of the requirements for the degree of Master Science**

in

Experimental Surgery

Department of Surgery

Edmonton, Alberta

Spring 2002



**National Library
of Canada**

**Acquisitions and
Bibliographic Services**

**385 Wellington Street
Ottawa ON K1A 0N4
Canada**

**Bibliothèque nationale
du Canada**

**Acquisitions et
services bibliographiques**

**385, rue Wellington
Ottawa ON K1A 0N4
Canada**

Your file Votre référence

Our file Notre référence

The author has granted a non-exclusive licence allowing the National Library of Canada to reproduce, loan, distribute or sell copies of this thesis in microform, paper or electronic formats.

The author retains ownership of the copyright in this thesis. Neither the thesis nor substantial extracts from it may be printed or otherwise reproduced without the author's permission.

L'auteur a accordé une licence non exclusive permettant à la Bibliothèque nationale du Canada de reproduire, prêter, distribuer ou vendre des copies de cette thèse sous la forme de microfiche/film, de reproduction sur papier ou sur format électronique.

L'auteur conserve la propriété du droit d'auteur qui protège cette thèse. Ni la thèse ni des extraits substantiels de celle-ci ne doivent être imprimés ou autrement reproduits sans son autorisation.

0-612-69756-8

Canada

University of Alberta

Library Release Form

Name of Author: Dr. Daniel E. Schiller

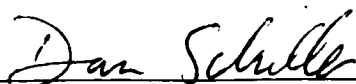
Title of Thesis: Optimizing the SCID/uPA mouse model for Hepatitis C

Degree: Master of Science

Year this Degree Granted: 2002

Permission is hereby granted to the University of Alberta Library to reproduce single copies of this thesis and to lend or sell such copies for private, scholarly or scientific research purposes only.

The author reserves all other publication and other rights in association with the copyright in the thesis, and except as herein before provided, neither the thesis nor any substantial portion thereof may be printed or otherwise reproduced in any material form whatever without the author's prior written permission.



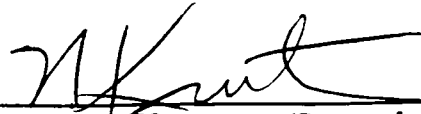
11048 81st Ave,
Edmonton, Alberta
T6G 0S4

Jan 2, 2002

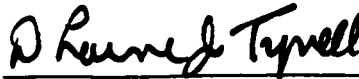
University of Alberta

Faculty of Graduate Studies and Research

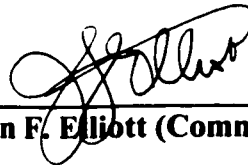
The undersigned certify that they have read, and recommend to the Faculty of Graduate Studies and Research for acceptance, a thesis entitled **Optimizing the SCID/uPA mouse model for hepatitis C** submitted by Daniel E. Schiller in partial fulfillment of the requirements for the degree of **Masters of Science in Experimental Surgery**.



Norman M. Kneteman (Supervisor)
(Committee Chairman)



D. Lorne J. Tyrrell (Committee Member)



John F. Elliott (Committee Member)



Thomas A. Churchill (Committee Member)



Jonathan R.T. Lakey (Committee Member)

Date: June 30, 2001

ABSTRACT

There are many different variables affecting the success of hepatocyte engraftment and subsequent HCV infection in the SCID/uPA mouse. We hypothesized that repopulation of a substantial proportion of mouse liver with human hepatocytes is critical for successful HCV infection.

To test this hypothesis, two quantitative assays were developed to measure the serum levels of human proteins in these mice. A cohort of 21 transplanted mice were followed and serum was collected at various time points for analysis, comparing levels of human proteins in homozygote mice to heterozygotes. The assays were also used to study the different parameters that influence the overall success our model.

The results confirm that a substantial proportion of liver must be repopulated by human hepatocytes to achieve successful HCV infection in this model. Other important factors include the use of freshly isolated hepatocytes and HCV inoculation with fresh serum.

TABLE OF CONTENTS

	Page
INTRODUCTION	
THE CLINICAL PROBLEM: HCV	1
History	1
Virology	1
Epidemiology	7
Transmissibility	8
Immune Response to HCV	9
Diagnostic Tests	10
Clinical Sequelae	13
Pathology	15
Treatment	16
Medical Treatment	16
Interferon	16
Ribavirin	21
Interferon + Ribavirin	22
Interferon + Amantadine	23
Vaccines	25
Protease Inhibitors, Ribozymes, Oligodeoxynucleotides (ODNs)	26
Liver Transplantation	26
 THE SCID/uPA MOUSE MODEL FOR HCV	
The Alb-uPA transgenic mouse	29
The SCID mouse	33
The Beige mouse	34
Hepatocyte Isolation	35
Hepatocyte Cryopreservation	38
Hepatocyte Transplantation	40

OTHER MODELS FOR THE STUDY OF HCV

Animal models	41
Chimpanzee model	41
Tupaia (Tree shrew) model	43
Trimera mouse model	43
RAG/uPA model	44
NOD / SCID model	47
Cell culture-based systems	48
Primary Human Hepatocytes	48
Primary Chimpanzee Hepatocytes	49
Immortalized Tumor Cell Lines.....	49
T-Cell Lines	51
B-Cell Lines	51

HYPOTHESIS	53
-------------------------	-----------

METHODS

SCID/uPA Mouse Breeding	54
Hepatocyte Isolation	55
Hepatocyte Cryopreservation	56
Hepatocyte Transplantation	56
HCV Inoculation	57
Western Blot Assay	58
Quantitative Dot Blot Assay	59
Quantitative ELISA for human Alpha-1 Antitrypsin ELISA (hAAT).....	64
Mouse IgG ELISA for SCID Leakiness	67
Immunohistochemistry	67
Comparing the Dot Blot and hAAT ELISA Assays	69
Correlation of Graft Success with Fresh versus Frozen Hepatocytes	71
Correlation of Graft Success versus HCV Infection Success	71
Correlation of HCV Infection with Fresh versus Frozen Serum Inoculation	71

Long Term Study of Infected SCID/uPA mice.....	72
Demonstration of Transmissibility	72
Effects of Interferon alpha in HCV Infected SCID/uPA mice	72

RESULTS

SCID/uPA Mouse Breeding	75
Hepatocyte Isolation	76
Hepatocyte Cryopreservation	76
Hepatocyte Transplantation	79
Correlating the Dot Blot and hAAT ELISA Assays	79
Correlating Graft Success for Fresh versus Frozen Hepatocytes	87
Correlating Graft Success versus Infection Success	87
Correlating Success of Infection with Fresh versus Frozen Serum	96
Long Term Study of Infected Animals	96
Demonstration of Transmissibility	99
Effects of Interferon alpha on HCV Infected SCID/uPA mice	99

DISCUSSION	105
------------------	-----

CONCLUSION	113
------------------	-----

REFERENCES	114
------------------	-----

APPENDIX	126
----------------	-----

LIST OF TABLES

Number	Title	Page
1	Effect of Antepartum Tranexamic Acid on SCID/uPA Litter Size	75
2	Hepatocyte Isolations from March 2000 – April 2001	77
3	Summary of Cryopreservation / Thaw Results	78
4	Comparison of Three Different Assays for Human Proteins in the Serum of Transplanted SCID/uPA Mice	80
5	Dot Blot and ELISA Serum Assay Results for Homozygotes vs Heterozygotes at 3, 6, 12 Weeks Post-Transplant	83
6	Serum IgG Levels in SCID/uPA Mice	88
7	Comparison of Serum Assay and Estimated Percent Human Chimerism in Liver for 8 SCID/uPA Mice	92

LIST OF FIGURES

Number	Title	Page
1	HCV genome.....	2
2	HIV, HBV, HCV Statistics from 1995	8
3	Natural History of HCV Infection	14
4	Sample Western Blot	60
5	Sample Dot Blot Membrane	62
6	Typical Dot Blot Standard Curve	63
7	Sample hAAT ELISA Plate & Standard Curve.....	66
8	Experimental Design	70
9	Interferon Experiment Design	74
10	Sample Western Blot Results.....	81
11	Average Dot Blot results for Homozygotes vs Heterozygotes	83
12	Average hAAT ELISA Results for Homozygotes vs Heterozygotes	84
13	Scatter Plot Comparing Results From Dot Blot Assay and hAAT ELISA.....	85
14	Repopulation of SCID/uPA Mouse Liver with Human Hepatocytes.....	89
15	Representative H&E Liver Sections at 10 X Magnification of Livers from SCID/uPA Mice Transplanted with Cryopreserved Hepatocytes at 3, 6, and 12 Weeks Post-Transplant (PT).....	90
16	Immunohistochemistry with OCH1E5 Antibody	91
17	Predictive Value of 4 wk Dot Blot > 200µg/ml.....	93
18	Predictive Value of 4 wk Dot Blot > 250µg/ml.....	94
19	Correlating Graft Function with Success of HCV Infection.....	95
20	Long Term Follow Up of HCV-Infected SCID/uPA Mice	97
21	Immunohistochemistry With Anti-HCV Antibody (TORDJI-22).....	98
22	Transmissibility of HCV Infection Between SCID/uPA Mice	100
23	Effect of IFN In HCV-Infected SCID/uPA Mice – treatment vs controls ...	103
24	Effect of IFN In HCV-Infected SCID/uPA Mice – treatment effect According to Genotype	104

LIST OF SYMBOLS AND ABBREVIATIONS

2'5'-OAS	2',5' – Oligoadenylate Synthetase
AMA	Amantadine
Bg	Beige
CHS	Chediak-Higashi Syndrome
CIFN	Consensus Interferon
DB	dot blot Assay
DNA	Deoxyribonucleic acid
EDTA	Ethylene – Diaminetetra-Acetic Acid
ELISA	Enzyme Linked Immunosorbent Assay
ETR	End of Treatment Response
GTP	Guanosine Triphosphate
HA	Human Albumin
hAAT	human alpha-1 antitrypsin
HAV	Hepatitis A Virus
HBV	Hepatitis B Virus
HCV	Hepatitis C Virus
HDV	Hepatitis delta Virus
HGF	Hepatocyte Growth Factor
IFN	Interferon
Ig	Immunoglobulin
IL-1	Interleukin 1
IL-12	Interleukin 12

IM	Intramuscular
IP	Intraperitoneal
IRES	Internal Ribosomal Entry Site
IV	Intravenous
M	million
mM	millimolar
μg	microgram
μl	microliter
NK	Natural Killer
nu	nude
PBMC	Peripheral Blood Mononuclear Cells
PEG	Polyethylene glycol
PI	Post Inoculation
PKR	Protein Kinase
PT	Post Transplant
RAG	Recombinase Activating Gene
RNA	Ribonucleic acid
RV	Ribavirin
SCID	Severe Combined Immune Deficiency
sc	subcutaneous injection
SR	Sustained Response
U.S.	United States
USD	U.S. Dollars

UTR	Untranslated region
uPA	urokinase-plasminogen activator
UW	University of Wisconsin
VAF	Virus & Antigen Free
WHV	Woodchuck hepadnavirus
Zn⁺⁺	Zinc

IV. INTRODUCTION

THE CLINICAL PROBLEM: HCV

HISTORY

After identification of the Hepatitis B virus (HBV) in 1970, followed by the Hepatitis A virus (HAV) in 1973, it became apparent that many patients with hepatitis had neither, and the term non-A, non-B (NANB) hepatitis was coined. In 1989, researchers at a private company in California cloned the hepatitis C virus (HCV) genome using plasma from a chimpanzee animal model (1). Since the discovery of HCV, it has been shown to cause over 90% of post-transfusion NANB hepatitis cases in the United States. There are currently millions of people worldwide infected with this virus and the possible clinical sequelae include cirrhosis, hepatocellular carcinoma, and end stage liver disease causing death. Although the virus was characterized over 12 years ago, efforts to develop effective antiviral agents have so far been severely hampered by the lack of an efficient cell culture system and a robust, small animal model.

VIROLOGY

In 1989 Choo *et al.* at the Chiron Corporation in Emeryville, California identified the HCV virus using a complementary DNA library constructed from infectious chimpanzee plasma (1). Since that time HCV has become an area of intense research and many advances have been made in characterizing and understanding this virus. The HCV virus is a single stranded, positive sense, enveloped RNA virus approximately 9400 nucleotides long. The virus particle is spherical in shape and has a size of 36-62 nm (2). The viral genome is most closely related in organization and protein homology to Flaviviruses (yellow fever, Dengue fever, Japanese Encephalitis), Pestiviruses (Bovine viral diarrhea) and two new RNA viruses (GBV-A, GBV-B) that have recently been discovered in New World primate tamarins (3). HCV has now been designated as the sole member of a distinct genus called “hepacivirus” in the family *Flaviviridae* (4). The HCV genome and protein domain structure are shown in Figure 1.

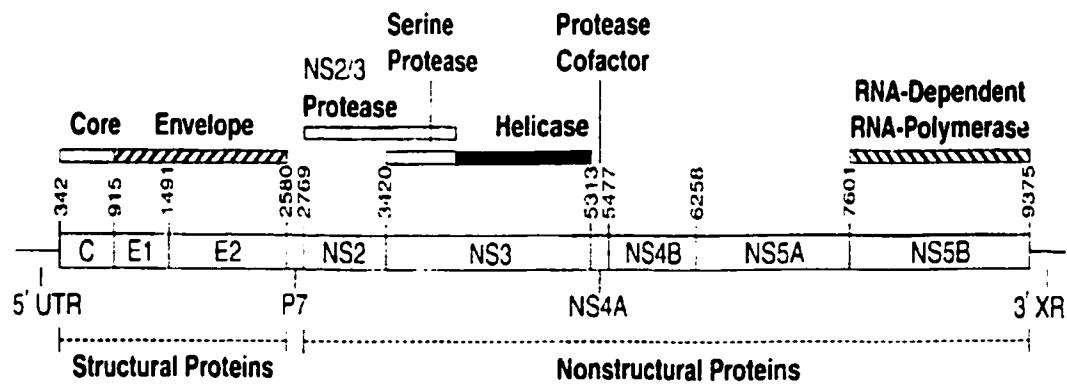


Figure 1. Schematic diagram of the hepatitis C virus genome. The location of HCV genes, proposed functions of gene products, and the 5' and 3' untranslated regions (5' UTR and 3' XR) are shown. Numbering refers to nucleotide positions of genes.

FIGURE 1 – HCV GENOME (from NIH Conference, *Annals of Internal Medicine*, 2000, 132)

The HCV virus consists of a 5' untranslated region (UTR) and a 3' UTR flanking a single large translational open reading frame (ORF) that spans almost the entire genome and encodes a precursor polyprotein of 3010 to 3033 amino acids (3). Since the HCV RNA is located in the cell cytoplasm and is not capped, translation of the genome is termed “cap-independent”. It has been shown that an area of the 5'UTR acts as an internal ribosomal entry site (IRES) that permits direct binding of the 40S ribosome to initiate translation of the genome (4)(5). This is obviously an attractive target for the development of an antiviral agent. The translated polyprotein is proteolytically cleaved into a set of 10 distinct protein products divided into the structural proteins (SP) (located at the 5' end of the genome) and those encoding the nonstructural proteins (NSP) (located at the 3' end). The structural proteins include the core protein (C), and two envelope proteins (E1 and E2). These are released from the polyprotein by host signal peptidases (6). Studies suggest that the core protein binds to HCV genomic RNA and forms the major constituent of the nucleocapsid during formation and release of new virion particles (3). Both the core protein and the 5'UTR are highly conserved among different HCV genotypes, in contrast to the envelope proteins E1 and E2 that are highly variable. E1 and E2 are highly glycosylated transmembrane proteins and may be the

principal target of any humoral immunologic host response to the virus. There are two sequences encoding the amino terminus of the E2 region with marked sequence diversity (7). These two regions are known as the hypervariable regions (HVR) and it is thought that the high variability in these regions may represent a method of “immune escape “ by which the virus can evade the host immune system (8).

The non-structural (NS) proteins are divided into NS1 NS2, NS3, NS4A, NS4B, NS5A, and NS5B. Although the functions of the NS proteins have only been partially elucidated, they have been shown to contain protease, helicase and polymerase functions that are necessary for viral replication. The NS2 region encodes a proteinase that catalyzes the cleavage at the NS2/3 junction. This proteinase may be a metalloproteinase since its activity is enhanced by Zn^{2+} (4). The amino terminus of NS3 contains a serine type proteinase that cleaves at the NS3/4A, NS4A/4B, NS4B/5A and NS5A/B sites. The carboxy terminus domain of the NS3 protein is thought to have helicase activity that may be important in unwinding the double-stranded RNA formed during replication. NS4A has been found to be an essential cofactor for the NS3 serine proteinase. The function of NS4B is as yet unknown. NS5A is a highly phosphorylated protein whose function remains unknown. NS5B represents the viral RNA-dependent RNA polymerase that is needed to replicate the RNA genome (9), which obviously makes this another attractive target for antiviral therapies.

The proposed steps in the life cycle of HCV include: (i) attachment and penetration of the host cell, (ii) uncoating, (iii) translation of RNA into the polyprotein, (iv) processing of the polyprotein to form structural and non-structural proteins, (v) formation of a replicase complex which makes (-) strand RNA from the input RNA, (vi) production of new sense stranded RNA , and finally (vii) additional protein synthesis from the newly synthesized (+) strand RNA for packaging and subsequent release of the virus from the infected cell. Each step in this process is a potential target for antiviral agents designed to interrupt the HCV life cycle.

Attachment and Entry:

In 1998 Pileri *et al.* (10) reported that the HCV envelope protein E2 was found to bind *in vitro* to a human cell surface molecule called CD81. CD81 is a member of the tetraspanin family of cell surface receptors that span the membrane lipid bilayer 4 times. The N and C termini of CD81 are located in the cytoplasm and there are 2 extracellular loops, one small and one large. The binding of E2 has been mapped to the large extracellular loop (LEL) and it is interesting to note that all parts of CD81 **except** the LEL are highly conserved across species. There are a number of amino acid differences between the LEL sequences in humans and rodents so it is not surprising that human but not mouse CD81-LEL will bind to HCV E2. In contrast, there is only a single amino acid difference between the LEL of human CD81 and that of chimpanzees, the only other permissive host for HCV infection. Furthermore, incubation of human cells with serum from chimpanzees that have been vaccinated with recombinant E1 and E2 was shown to block the binding of E2 to CD81 *in vitro* (10). CD81 is an ubiquitous membrane receptor and is found not only on hepatocytes but also on B-cells and various other cell types. In B-cells, CD81 is part of a signaling complex that ultimately leads to B-cell activation and proliferation. It has been suggested that by crosslinking this signaling complex, HCV may lower the threshold for B-cell proliferation (11). This would help explain the various autoimmune disease states associated with chronic HCV infection such as mixed cryoglobulinemia. Whether CD81 is in fact the sole receptor for HCV is a question that remains thus far unanswered. Petracca *et al.* (12) report that some hepatoma lines can bind HCV envelope proteins in the absence of CD81, which suggests that there may be other molecules involved. Meola *et al.* (13) studied the binding affinities of HCV E2 to human CD81 (h-CD81) and tamarin CD81 (t-CD81) that differs from human CD81 at 5 amino acid positions within the LEL. They found that both h-CD81 and t-CD81 bound HCV E2 but t-CD81 binding was stronger even though tamarins are resistant to HCV infection. These results suggest that E2 binding to CD81 does not necessarily correlate with permissiveness of infection.

It has been proposed that HCV may enter host cells by binding to the low density lipoprotein (LDL) receptor since HCV particles have been shown to be associated with B-lipoproteins (4). LDL receptors are known to function as receptors for several viruses

such as the minor-group common cold virus and subgroup A Rous sarcoma virus (14). The HCV-LDL receptor association was seen in studies of mixed cryoglobulinemia, a systemic vasculitis that is associated with HCV. Specifically, HCV-RNA was found in vasculitic skin lesions of HCV-infected patients but not in adjacent normal skin. Furthermore, keratinocytes in the cutaneous vasculitic lesions had upregulated LDL receptors (15). Agnello *et al.* conducted studies with cell lines to better elucidate this association and found that endocytosis of HCV in cultured cells correlated with the level of LDL receptor expression on the cells (15). These authors were also able to inhibit endocytosis of HCV with both an anti-LDL antibody and by adding exogenous LDL to the culture and presumably “flooding” the cell receptors with ligand. IFN is known to induce an IL-1 receptor antagonist which blocks IL-1-receptor-mediated stimulation of IL-1. Since IL-1 is known to increase LDL receptor activity, then one anti-HCV mechanism of action of IFN could plausibly be by indirectly decreasing LDL receptor activity (15). Monazahian *et al.* also showed that addition of purified LDL *in vitro* inhibits the binding of HCV to human fibroblasts completely (14). They also showed that transfection of an African Green Monkey cell line (that is not able to bind HCV) with a vector containing the entire coding sequence of human LDL-receptor enables HCV to bind to these cells. They report that fibroblasts derived from a patient with familial hypercholesterolemia lacking LDL receptors could not bind HCV *in vitro*.

Uncoating & Translation:

Once inside the cell, the virus uncoats (mechanism unknown) and the genomic HCV RNA is translated under direction of the Internal Ribosome Entry Site (IRES) located in the 5'UTR. For most flaviviruses, the host translation machinery recognizes a cap structure at the 5' end of the genome and translation starts at the first AUG codon. In HCV, translation is “cap-independent” and starts at the 4th or 5th AUG codon under the direction of the IRES (16). The polyprotein is translated and is proteolytically processed by both host and viral enzymes. The structural proteins (SP) are cleaved by host proteases, while the non-structural proteins are cleaved by the viral proteases NS2/3 and NS3. Following this, the non-structural proteins NS3-NS5B form a “replicase complex” which produces an antisense or (-) strand RNA from the (+) strand RNA template. This

negative strand HCV RNA then acts as a template for the production of multiple (+) stranded RNA. Detection of the HCV negative strand is indicative of active viral replication. Antisense HCV-RNA sequences have been detected in the liver of infected patients (17). Although the liver is thought to be the main site of viral replication, (-) stranded RNA has been reported in many different sites including serum and peripheral blood mononuclear cells (PBMCs) (18)(19). These reports must be viewed with skepticism since they relied on reverse transcriptase-polymerase chain reaction (RT-PCR) methods that were fraught with problems such as false priming and self-priming that can lead to false positive results. Newer PCR assays using a thermostable reverse transcriptase (rTth) and tagged primers are much more reliable. Using these assays it does appear that (-) stranded RNA can be detected in peripheral blood mononuclear cells (PBMCs) suggesting a true extrahepatic site for viral replication (20). HCV does not appear to produce DNA replication intermediates and thus cannot integrate into the host DNA like some other viruses (e.g. HBV) (21). It is thought that virus particles are formed by core protein interacting with the RNA genome. Virions are released from the cell by an unknown mechanism.

HCV Genotypes:

During replication the RNA dependent RNA polymerase (RdRp) introduces frequent random nucleotide errors which leads to a high rate of spontaneous nucleotide substitutions of $10^{-2} - 10^{-3}$ per site per year (22). This genetic variability is seen in all domains of the HCV genome but predominates in the 5' part of the E2 envelope protein, the hypervariable region (HVR). The genetic variability of HCV has led to its classification into 6 major genotypes numbered 1 to 6 and over 80 subtypes labeled a,b,c. The naming of the different genotypes is related to when they were discovered and thus the genotype originally isolated by Chiron in 1989 is known as 1a. The nucleotide homology between genotypes is 66-69%, and is 77-80% between subtypes (6). Another term – “quasispecies” is used to describe pools of related variants with only minor sequence differences (< 5% of viral genome) (22). An infected patient may have multiple different quasispecies of HCV in their serum at any given time. There are major geographic differences in the distribution of the various genotype. Types 1a, 1b, 2a, 2b

and 3a predominate in North America and Western Europe, and genotype 1b is reportedly the most frequent variant worldwide (8). Genotype 4 is seen mostly in Central Africa, Egypt and the Middle East while 5a is seen predominantly in South Africa (17). Genotype 6 is seen predominantly in Hong Kong.

Genotyping strategies include amplification and analysis of the 5' UTR region, restriction fragment length polymorphism (RFLP) and the use of type-specific probes (6). As will be discussed later, there are significant differences in terms of response to interferon (IFN) between different HCV genotypes with genotype 1b being least responsive.

EPIDEMIOLOGY

It is estimated that greater than 170 million people worldwide are infected with hepatitis C (4). Recent reports from the U.S. estimate that 1.8% of the population is infected, with up to 1/5 of patients seen in inner city emergency departments and 1/3 of prison inmates carrying the virus (23). The annual incidence in the U.S. fell from 180,000 in the mid-1980's before HCV was discovered, to 28,000 in 1995 (23). Intravenous drug use is currently the most common cause for newly acquired infections. HCV infection affects people from all demographic groups but the highest prevalence in North America is seen in 30-40 year old white males. In parts of Africa and Asia, prevalence of HCV is as high as 20% of the population (6). Many people infected with the virus are unaware of their disease and since there is a long asymptomatic period before serious liver dysfunction occurs. HCV has the potential to cause a significant amount of morbidity, mortality and health care costs over the coming decades unless effective treatments are developed. An interesting study from 1995 (See Figure 2) showed that while the number of people infected with HCV far exceeded the number infected with either HIV or HBV, the funding allocated to HCV research was only a fraction of what was allocated for these other diseases (23).

Table 1.—Estimated Prevalence, Economic Cost, and Research Funds in 1995 for Three Chronic Viral Illnesses in the United States

Illness*	People infected (no.)	Annual cost (\$)	Annual funds† (\$)
HIV	900,000	Unknown	1,400,000,000
HBV	1,200,000	360,000,000	14,000,000
HCV	4,000,000	4,000,000,000	1,700,000

*HBV = hepatitis B virus; HCV = hepatitis C virus; HIV = human immunodeficiency virus.

†From the National Institutes of Health.

FIGURE 2 – HIV, HBV, HCV STATISTICS FROM 1995

TRANSMISSIBILITY

Transmission of HCV is most efficient via the parenteral route and classic risk factors include transfusions of blood or blood products, transplantation of tissues or organs from infected donors, intravenous drug abuse with needle sharing, and tattoos placed with poor hygiene. After the discovery of hepatitis A and hepatitis B, it became obvious that the majority of transfusion-associated hepatitis (TAH) was due to another organism – hence the term Non-A-Non-B-Hepatitis (NANBH). Before a specific test became available for NANBH, blood collection agencies in the U.S. began to use surrogate markers of infection such as alanine aminotransferase (ALT) and anti-HBc antibodies to screen for NANBH. The risk of post-transfusion hepatitis before the use of surrogate markers was 0.45% per unit transfused and this fell to 0.19% per unit with the use of these markers (24)(25). In 1990, with the introduction of anti-HCV testing, the risk of post-transfusion HCV infection fell further to 0.03% per unit transfused (25). The risk in 1998 was quoted as 0.001% per unit transfused (26).

The risk of HCV infection from a random needle stick in the hospital is about 0.1%, unless the patient is known to be infected in which case the risk is estimated to be as high as between 5 and 10% (23). No distinction has been made between the risks of a hollow or solid needle stick although one would expect a hollow needle to deliver more inoculum. Sexual transmission of HCV is possible and studies suggest that the transfer of HCV via household contact can occur although the mechanisms are not yet understood. Sexual and household exposures are thought to account for approximately 5-10% of HCV infections in the United States (23). Perinatal transmission of the HCV virus is also possible, although the transmission efficiency is low and the risk of maternal-infant transmission is 5% or less (27). Maternal-infant transmission of HCV is most likely in mothers with serum HCV-RNA concentrations higher than 10^7 genomes per ml (25). Since anti-HCV antibodies may be passed on from the mother, babies of HCV positive mothers should be screened for HCV RNA and not anti-HCV antibodies to detect infection. Breastfeeding is considered to be safe. Transplantation of solid organs such as kidney and heart, as well as bone marrow transplants from infected donors can result in transmission of HCV to other transplant recipients. Depending on the study, anywhere from 5-40% of documented HCV infections claim to have no identifiable risk factors which suggests that a mode of transmission may exist that has yet to be identified.

IMMUNE RESPONSE TO HCV

In order to devise a strategy to develop effective vaccines against HCV, much work has been done looking at the immune response to HCV. In the normal immune response to a viral infection, macrophages and dendritic cells present viral epitopes to B-cells, helper T-cells and cytotoxic T-cells. In many viral infections, B-cells can produce antibodies that can clear circulating virus and protect from re-infection. Antibodies can't eliminate virus that is inside an infected cell and therefore the cellular response is also very important. It is thought that the cellular response mounted by most infected patients against HCV is a weak T-cell response (28). Most of the research looking at the immune response to HCV has been done using chimpanzees which is currently the best available animal model. We know that HCV elicits a humoral response based on the detection of anti-HCV antibodies in the serum of infected patients. In addition, CD4⁺ and CD8⁺ T

cells able to recognize structural and non-structural proteins have been detected in the liver and the peripheral blood of patients with chronic HCV (29). The fact that 15-20 % of humans and 60-70 % of chimpanzees are able to clear their HCV infection suggests that in a subset of patients an effective immune response can be mounted to neutralize the virus. Alternatively, characteristics of the viral strain they were infected with or differences in cell surface receptors may play a role in the ability of these patients to clear the virus. By comparing the class II restricted T-cell response to HCV antigens between patients with acute HCV who succeed in normalizing their biochemical parameters and those who do not, Missale *et al.* (29) showed that a more vigorous T-cell response was seen in the former group. Similar results were found by Lechman *et al.* (30). This suggests that perhaps an efficient and vigorous T-cell response at the early stages of infection may be critical to limit the spread of the virus within the infected host. Finally, it has been shown that patients who clear the HCV infection on their own mount a strong Th1 response and a weak Th2 response. In contrast, patients who develop chronic infection have a milder Th1 response and a stronger Th2 response (31). It has been hypothesized that immunostimulation to promote a Th1 response using stimulatory mediators such as IL-12 may help clear the HCV infection.

It is clear however that in the vast majority of cases the host immune response is not effective in controlling or eliminating the virus. This is evidenced by the high rate of chronicity of the infection despite the formation of anti-HCV antibodies. It has also been shown that chimpanzees can be re-infected repeatedly using both homologous and heterologous HCV strains (32). This correlates with the multiple, repeated episodes of acute hepatitis seen in intravenous drug users and polytransfused thalassemic children (33).

DIAGNOSTIC TESTS

Diagnostic tests for HCV can be divided into serum tests for antibodies to HCV, serum assays for HCV RNA, tissue tests for HCV antigens and tissue tests for HCV RNA.

The first assay to detect anti-HCV antibodies was an enzyme linked immunosorbent assay (ELISA) assay using the C-100-3 recombinant protein derived from the NS4 region

of the HCV-1 isolate (34). Commercially available ELISA assays to detect anti-HCV antibodies are now in their third generation of development and have improved sensitivity and specificity over the original assay by using 4 different HCV-derived proteins. The average time for seroconversion using these assays has decreased from 16 weeks with ELISA-1, to 10 weeks with ELISA-2, to 7-8 weeks with ELISA-3 (35). There are limitations with the ELISA assay in that not only is there a substantial interval between infection and the detection of anti-HCV antibodies but immunocompromised patients may have an active infection without producing detectable antibodies. Also, the ELISA assays still suffer from false positive results in low risk blood donors. To increase the specificity, a radioimmunoblot assay (RIBA) was developed which separated out the 4 HCV-derived protein fragments on separate strips. This test is considered positive if the patient's serum reacts with two or more of the strips. Initial testing is performed using an ELISA assay and if the ELISA is positive, a confirmatory test is performed with the RIBA assay. Commercial kits for the antibody test currently have a sensitivity of 95% (27).

Using molecular biology techniques, HCV RNA can be detected in the serum and liver of infected patients and this is now considered to be the "gold standard" in terms of detecting infection and following response to treatment. The advantage of measuring HCV RNA is that viremia can be detected within only a few days of exposure – long before the elevation of ALT and viral antibody levels are seen (36). Furthermore, levels of HCV RNA in the liver and serum generally correlate with changes in ALT activity (18). Detecting HCV-RNA in the serum is accomplished using RT-PCR technology that can detect minute amounts of viral RNA. A reverse transcriptase step is performed first using specific primers to produce complementary DNA (cDNA) from the viral target RNA. The cDNA can then be amplified by repeated cycles of denaturing, elongation, and annealing. Although some studies have reported detection of negative strand RNA in the serum, these likely represent false positive assay results since: a) this replicative intermediate is thought to exist only **inside** the infected cell and b) it is thought to be unstable in the serum as it would be susceptible to digestion by serum RNases. RT-PCR can be used to measure HCV RNA in the serum both quantitatively or qualitatively.

Qualitative testing is the more sensitive of the two and has a reported detection limit as low as 50 copies / ml (37).

Quantitative RT-PCR methods to measure HCV RNA are quite costly and have reported detection limits of 100-500 viral copies/ml (35). Another quantitative assay known as the branched DNA (bDNA) signal amplification is also available with reported levels of detection in the literature as low as 1000 viral copies per milliliter of serum (25). Yu *et al.* (37) compared two widely used commercial assays for HCV RNA quantification using these 2 different technologies. Sera from 107 HCV-infected patients was used to quantify HCV RNA levels using the Amplicor HCV Monitor assay (Roche) (RT-PCR based) to the Quantiplex HCV RNA 2.0 assay (Chiron) (bDNA based). Results showed that both assays had similar sensitivity and reproducibility but the Amplicor values were on average 1.76 log lower than the Quantiplex results. In addition, genotype 1b was found to have a significantly higher viral load than other genotypes with the Amplicor assay while no genotype-dependent differences in viral load were observed for the bDNA assay. This is interesting since the Amplicor assay uses the most conserved regions of genotype 1 HCV as target sequences for amplification and probe hybridization (37). Serum levels of HCV RNA in infected humans range from 10^3 to 10^8 copies / ml (38).

Detection of HCV RNA in liver tissue is most often performed using RT-PCR technology following RNA extraction. Negative stranded HCV RNA can be detected in the livers of patients with active viral replication but as was mentioned earlier precautions to ensure strand specificity must be taken to avoid false positive results. It is generally accepted that the levels of (-) HCV RNA in the liver are 10-100 times less than the levels of (+) stranded HCV RNA (38)(39). Another method of (-) strand HCV RNA detection is the ribonuclease protection assay. In this assay, a probe is hybridized to the target single stranded RNA which protects this target sequence from digestion by subsequently added RNases. Once all unhybridized single strand RNAs have been digested, the hybridized target RNA is denatured from the annealed radiolabeled probe and undigested radiolabeled probe is resolved by gel electrophoresis and detected by autoradiography. Detection of HCV-RNA in liver tissue is also possible using in-situ hybridization techniques as shown by Negro *et al.* (40).

Many groups have reported the detection of HCV antigens in liver using immunohistochemistry (35), often using sera of HCV infected patients as the primary antibody source (41)(42). TORDJI-22 is a monoclonal antibody specific for the C-100 protein product of the NS3/4 coding region of HCV developed by a company Biogenex (San Ramon, California). This antibody is designed for use with formalin fixed paraffin embedded liver tissue. Studies comparing immunohistochemistry with TORDJI against RT-PCR run on extracted liver RNA have found that immunohistochemistry is 70% sensitive and 80% specific for the detection of HCV (43).

CLINICAL SEQUELAE

The majority of patients infected with HCV do not have symptoms of acute hepatitis such as malaise, fatigue or jaundice. It is estimated that only 10-25% of patients develop acute hepatitis (23). In contrast to hepatitis B in which approximately 5% of patients develop chronic hepatitis, it is estimated that between 60-80% of patients with HCV infection develop chronic hepatitis (27). There is a group of patients with anti-HCV antibodies who appear to be completely asymptomatic, and the idea of a “healthy carrier state” has been proposed. It is unclear whether with enough time all people with HCV infection will develop to progressive disease or not. Gordon *et al.* performed a study in which liver biopsies were performed on 98 apparently healthy, asymptomatic, HCV infected blood donors and 97% were found to have histologic abnormalities on biopsy. Of these, 76% had signs of chronic hepatitis (23). These findings would suggest that truly “healthy carriers” may be very uncommon.

Approximately 20% of chronic carriers will develop cirrhosis of the liver (27) (See Figure 3). The risk of developing cirrhosis is increased 10 fold by heavy alcohol consumption (27). Development of cirrhosis is also associated with ages greater than 40 years at the time of infection, and male sex. The development of cirrhosis often leads to other serious health problems such as ascites, portal hypertension, variceal bleeding and hepatic encephalopathy. After cirrhosis has been established in patients with chronic hepatitis, the lifetime risk of hepatocellular carcinoma is quoted to be 15-20 % (27). A recent Japanese study has shed some light on the time frame of events following HCV infection in terms of chronic hepatitis, cirrhosis and hepatocellular carcinoma. In a long-

term follow-up study of HCV patients, it took an average of 10 years to diagnose chronic hepatitis, 21.2 years to the onset of cirrhosis, and 29 years to the development of hepatocellular carcinoma (23).

While the liver is the primary target of the HCV virus, several extrahepatic manifestations of HCV have been described. Specifically, HCV is associated with porphyria cutanea tarda, aplastic anemia, glomerulonephritis and mixed cryoglobulinemia. Other less convincing associations have been made between HCV and rheumatoid arthritis, pulmonary fibrosis, thyroiditis, and Sjorgren's syndrome (27).

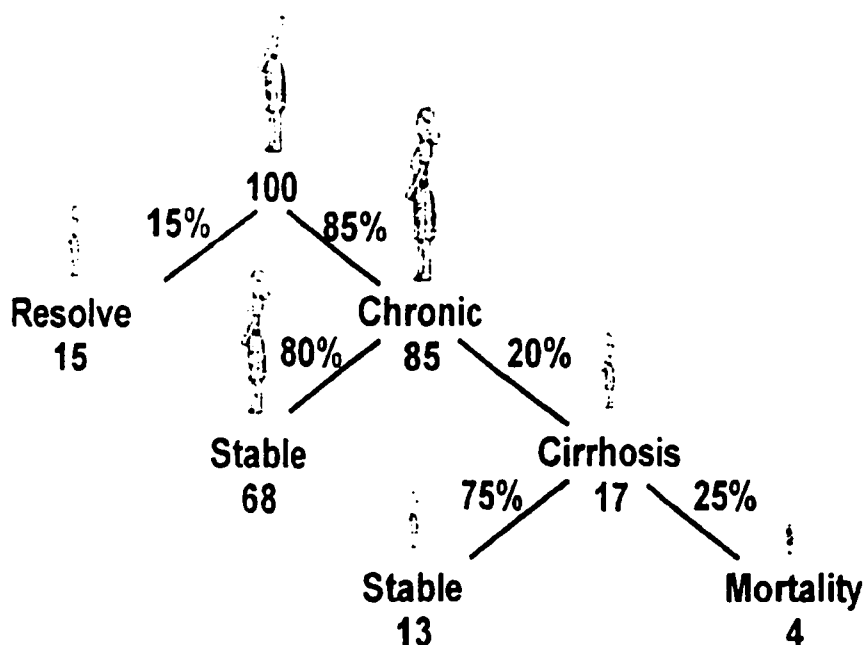


FIGURE 3 – NATURAL HISTORY OF HCV INFECTION. (Taken from Transfusion Service, National Institutes of Health (44))

PATHOLOGY

Liver biopsy remains the “gold standard” to determine the **grade and stage** of liver disease caused by HCV. The grade reported in a liver biopsy refers to the severity of inflammation while the stage describes the degree of fibrosis. It is interesting to note that patient symptoms and serum levels of ALT do not necessarily correspond to the histologic findings on liver biopsy (27). The presence of HCV-RNA however does correspond with histological hepatitis and disappearance of HCV-RNA is usually accompanied by resolution of liver inflammation. A relapse usually coincides with the reappearance of HCV-RNA in the serum (45). While the histologic findings in HCV liver disease are characteristic, they are not pathognomonic and so the final diagnosis of HCV must rely on serological assays to detect anti-HCV antibodies or HCV RNA. The primary mandate of a liver biopsy is to assess the grade and stage of the liver disease and at the same time to rule out other coincidental liver diseases.

Histologic findings of Hepatitis C are mild portal tract inflammation with lymphoid aggregates/follicles and mild periportal piecemeal necrosis, parenchymal steatosis and apoptosis (46). Fibrosis, when present, is often mild in the early stages, with portal-portal and portal-central bridging seen in later stages. An interesting observation is that many of the lymphoid follicles/aggregates are in close proximity to bile ducts but HCV is **not** associated with ductopenia. This distinction is important in distinguishing hepatitis from rejection in the post-transplant setting.

Patients whose biopsies show mild chronic hepatitis with no fibrosis are estimated to have a 50% risk of histologic progression over 10 years with a 10% risk of cirrhosis over this time. Patients showing severe hepatitis with septal fibrosis have a 60-70% risk of cirrhosis over 10 years (27).

The mechanism by which HCV actually causes damage to the liver has been the subject of much debate. Studies of liver biopsies from HCV infected patients reveal that HCV antigens appear in scattered cells or small groups of cells with striking acinus-acinus variation. In fact, in any given tissue, there are likely to be only a few HCV positive cells and these show no consistent relationship with inflammation or necrosis.

The follicles in portal tracts appear to be active B-cell follicles and the areas of piecemeal necrosis appear to contain a predominance of CD4 + cells while the parenchymal infiltrates consist mostly of CD8 + cells (45). A question raised with regard to pathogenesis is whether the hepatocyte damage is immune mediated or directly due to cytotoxic effects of the HCV virus. Evidence to support the immune mediated theory comes from studies in animals that show a decrease in hepatic inflammation with immunosuppression and an increase in inflammation when these agents are withdrawn (47). On the other hand, case reports of subfulminant liver failure associated with very high levels of HCV-RNA following transmission of HCV by organ transplantation have led some to postulate direct cytotoxic effects of the virus (48).

TREATMENT:

a) Medical Treatment:

Treatment of HCV thus far has been disappointing. There are several explanations for the lack of efficient antiviral agents for HCV. The relatively recent discovery of the virus has meant that much of the basic research characterizing the virus is still ongoing. In addition the lack of an effective *in vitro* culture system amenable to high throughput antiviral screening assays, and the lack of a small animal model system for the replication of HCV have been major impediments hampering the development of antiviral strategies and continue to be a problem (9).

The two drugs currently used to treat HCV are interferon-alpha (IFN α) and ribavirin. Unfortunately, for reasons that will be discussed below, results from treatment with these agents are mediocre at best and there is a pressing need for the development of more effective treatment. With increasing knowledge about the different structural and non-structural proteins that make up the HCV genome, new compounds are being developed to target crucial steps in the process of viral translation and replication.

INTERFERON MONOTHERAPY:

Interferons are cytokines that occur naturally in the human body in three forms – interferon alpha, beta and gamma. IFN α is produced by monocytes and transformed B cell lines in response to viruses and antigenic stimuli (49). The gene for IFN α is located

on chromosome number 9. Interferon alpha and beta share the same receptor which is encoded by a gene on chromosome 21. Following binding with its receptor, IFN α is rapidly internalized by receptor-mediated endocytosis and the receptors on these target cells are subsequently downregulated. IFN α is thought to have both direct antiviral and immunomodulatory effects against HCV (49). IFN α exerts direct antiviral effects by inducing production of so called effector proteins such as 2'5'-oligoadenylate synthetase (2'5'-OAS), Mx protein, and double-stranded RNA-activated protein kinase (PKR), each of which directly inhibit viral replication in infected cells. 2'5'-OAS has been shown to lead to the breakdown of single stranded RNA and responders to IFN α therapy have been found to have a larger percent increase in 2'5'-OAS production than non-responders (50). Mx protein is a nuclear protein induced by IFN α which has been shown to inhibit the production of influenza virus in the nucleus of infected cells. IFN α treatment of cells induces PKR activity that catalyzes the phosphorylations of at least 40 cellular proteins. One such protein is the protein synthesis initiation factor known as elongation initiation factor 2- α (eIF2- α) that is directly inhibited by PKR catalyzed phosphorylation (50). As will be discussed later, HCV-derived proteins can bind to and inhibit PKR and lead to IFN resistance.

IFN α also induces multiple immunological changes such as increased expression of class I and class II MHC antigens, activation of cytotoxic T cells and macrophages, enhanced NK cell activity and other more complex interactions with the cytokine cascade (49)(50). IFN α is further thought to have an anti-inflammatory effect by decreasing the production of pro-inflammatory cytokines IL-1 and IL-8 (51).

Several groups have studied the kinetics of HCV RNA following administration of IFN α to learn more about the possible mechanisms of action of IFN α against HCV. These studies have repeatedly shown a biphasic decrease in HCV RNA following administration of IFN (52)(53). The first phase is characterized by a rapid decrease in HCV RNA by as much as 1.5 log in the first 1-2 days after treatment is started. Perelson *et al.* (52) showed that it takes 7-10 hours before any change in HCV RNA is seen which is consistent with the pharmacokinetics of IFN α since the plasma concentration of IFN α does not reach peak levels until 7-10 hours after administration. This first decrease in

HCV viremia is dose-dependent and is thought to be due to IFN α blocking virion production. (53). Following this initial rapid decrease, HCV RNA decreases at a much slower rate and this is thought to be due to the gradual death of infected cells. From these studies, it has been estimated that rate of viral production in infected humans is in the order of $1.8 \times 10^{11} - 10^{12}$ virions per day which explains the emergence of viral escape mutants given the high rate of random nucleotide errors seen during HCV replication. This has led some authors to suggest that much higher doses of IFN α should be used early in treatment to achieve higher rates of HCV eradication, also known as “Induction Therapy”. The half-life of HCV virions in the serum has been estimated from these studies to be 2.7 – 7 hours (52)(54)(55).

Multiple types of recombinant IFN α have been developed for use against HCV including IFN α -2b, IFN α -2a, IFN α n1, and Consensus Interferon (CIFN) (56). IFN α -2a, and 2b are recombinant forms of interferon while IFN α n1 contains multiple alpha interferon subtypes derived from lymphoid cell lines. CIFN is a recombinant compound that was formed by combining the most frequently observed amino acids in each position of several IFN α subtypes to generate a consensus sequence. The NIH Consensus Conference panel on HCV has concluded that all four types of IFN α have comparable efficacy in the treatment of HCV (56). Tong *et al.* (57) reported a multicenter randomized controlled trial comparing CIFN vs IFN α -2b and found that although CIFN showed a greater decrease in HCV RNA during treatment for genotype 1b, the sustained response rates were no different. A new type of IFN α , called PEG-Intron was designed based on the observation that by attaching polyethylene glycol (PEG) to proteins delays their clearance and decreases their immunogenicity. This allows for once weekly IM administration versus the traditional thrice weekly injections needed for the other interferons. The average 1999 cost for 6 months of treatment with IFN α 3 million units (3MU), three times per week is quoted as \$2500 USD (58). In a study published in 1998, Gross *et al.* estimated that the cost of 6 months of IFN therapy was \$2,800 USD per quality-adjusted year of life gained for patients 40 years old, and \$11,100 for patients 60 years old (23). In general the U.S. public has accepted strategies in which the cost per

year of life gained is \$50,000 or less (23). The current cost of IFN treatment for 12 months in Edmonton is between \$10,000 – 20,000 Canadian dollars per patient.

Aside from the inconvenience of thrice weekly injections, IFN is associated with numerous side effects. These can be separated into four main categories: constitutional, hematologic, neuropsychiatric, and autoimmune. Many patients experience an influenza-like illness with fever, chills, myalgias and headaches within 4-8 hours after their first injection (23) (59). These constitutional symptoms can be ameliorated by pre-treatment with acetaminophen and usually improve with subsequent injections. Bone marrow suppression as evidenced by low platelet and white blood cell (WBC) counts are reversible and are most pronounced during the first 4 weeks of treatment. Two to three percent of patients require reductions in IFN α dose for leukopenia and thrombocytopenia. It is recommended that the dose be halved if the neutrophil count drops below 750 cells/mm³ or the platelet count drops below 50,000 cells/mm³. IFN α should be stopped at least temporarily if neutrophils < 500 cells/mm³ or platelets < 30000 cells / mm³ (59). Psychological symptoms are seen in approximately 15% of patients treated with IFN and range from anxiety, irritability, and depression to frank psychosis and suicidal behavior. It is therefore imperative to follow these patients closely and treat symptoms of depression appropriately. Finally, greater than 50% of patients treated for more than 4 months with IFN develop autoantibodies such as antinuclear, anti-smooth muscle, and antithyroid antibodies. Autoimmune thyroiditis develops in 2-5% of treated patients (45). An uncommon side effect of IFN α therapy is worsening hepatitis that is likely due to autoimmune injury to the liver and requires that treatment be discontinued immediately (60). Approximately 5-8 % of patients will need to discontinue IFN treatment due to adverse side effects (23)(28).

Trials studying IFN monotherapy for HCV have been numerous. Interpretation of the results of IFN α must be made with caution as not all authors use the same definition of “response to treatment”. Response to IFN is usually defined as a decrease in serum HCV-RNA (virologic response), serum aminotransferase levels (biochemical response), or both. Clearance of HCV RNA is a more accurate measure of response as it has been shown that only 70-90% of biochemical responders have an actual virologic response (61). Although many patients started on IFN initially appear to respond, it was found that

approximately 50% of responders relapsed soon after the drug was discontinued (44). A sustained response (SR) is defined as having normal levels of ALT and no detectable HCV-RNA for 6 – 12 months after treatment has been stopped, and this is obviously more clinically significant than an end-of-treatment response (ETR). Initial trials using 3M units thrice weekly for 6 months demonstrated an ETR in 46% of treated patients, but a relapse rate of 51% within 6 months of stopping treatment (62). The overall sustained response rate to IFN α monotherapy for chronic HCV was only seen in 20-30% of patients. Predictors of favorable response to IFN therapy have been shown to be: younger age of patient, lack of liver cirrhosis, HCV genotypes 2 and 3, low concentration of iron in the liver pre-treatment, and low levels of circulating HCV-RNA prior to treatment ($< 1 \times 10^6$ genomes / mL) (45)(60). Failure to clear HCV-RNA after 1 month of treatment is a very strong predictor (predictive value 95.3, $p < 0.0001$) of a low ($< 5\%$) probability of sustained response (SR) and suggests that treatment should be discontinued (63). Increasing both the dose and duration of treatment has been shown to be effective in increasing sustained response rates up to 49% by treating for 12 months with an initial dose of 6M units thrice weekly (64). With increased dose and treatment time both cost and side effects also increase. Monotherapy with PEG-Intron has been shown to produce SR rates of 42-44% after 6 months of treatment (65). The most promising direction for IFN therapy in the battle against HCV lies not in its use alone but in combination with other antiviral drugs such as ribavirin.

IFN RESISTANCE

With the somewhat disappointing response to IFN α seen with many HCV infected patients, researchers have begun to try to explain the differences in IFN α sensitivity seen between different patients. Evidence suggests that perhaps differences in the E2 protein between different HCV genotypes may be important. IFN induces a protein known as PKR that can phosphorylate and inhibit the protein synthesis initiation factor eIF2 α resulting in cessation of protein synthesis and death of the infected cell (66). The structural protein E2 contains a 12 amino acid sequence that is very similar to the autophosphorylation site of PKR and the phosphorylation site of eIF2 α . This sequence in E2 is called the PKR-eIF2 α Phosphorylation Homology Domain (PePHD) (67). The

PePHD domains in genotypes 1a and 1b are *more* similar to PKR and eIF2 α than the corresponding sequences of less resistant HCV genotypes. This suggests that for genotypes 1a and 1b, E2 competes with eIF2 α to bind PKR because of sequence homology, thereby allowing eIF2 α to escape phosphorylation and allowing the cell to escape the IFN-induced translation regulation.

By analyzing the NS5a gene of HCV genotype 1b, researchers have found a 40 amino acid stretch in the NS5a protein that has been called the IFN Sensitivity Determining Region (ISDR) (50). It was found that HCV 1b strains with amino acid sequences identical to the prototype HCV1b strain (known as HCV-J following its discovery in Japan) are resistant to IFN α while strains with amino acid substitutions are sensitive. Fukuma *et al.* showed that compared to HCV-J, HCV1b strains with no mutations or 1-3 mutations in the ISDR are resistant to IFN α , while strains with 4 or more mutations in the ISDR are sensitive to IFN α and have lower HCV RNA levels (68). It has been suggested that missense mutations in the ISDR of the NS5a gene are closely associated with increased sensitivity to IFN for certain strains of HCV1b.

RIBAVIRIN:

Ribavirin (1- β -D-ribofuranosyl-1,2,4-triazole-3-carboxamide) is a nucleoside analogue with broad antiviral activity that was originally approved for use in the U.S. as an aerosol to treat infants with severe respiratory syncytial virus (RSV) infections (69). The exact mechanism of action of this compound remains controversial but it has been shown to have antiviral activity against numerous viruses such as the influenza virus, Lassa fever virus, Hantaan virus and HIV. As ribavirin closely resembles guanosine, one hypothesis about its mechanism of action is that it leads to a decrease in the intracellular pool of guanosine triphosphate (GTP) thereby decreasing the synthesis of viral nucleic acid. Another theory is that it results in the synthesis of RNA with abnormal or absent 5' cap structures thereby leading to inefficient translation of viral transcripts. A third hypothesis states that ribavirin has a direct inhibitory effect on viral polymerase activities (69). Ribavirin is taken orally at a daily dose of 1000 to 1200 mg, and the serum half-life is 48 hours. The most notable side effect of ribavirin that occasionally requires stopping treatment is hemolytic anemia. Hemolysis occurs in the first 4 weeks of

treatment and usually causes a drop of hemoglobin of 2-3g/l that returns to normal within 4 weeks after stopping treatment. Fifteen percent of patients taking ribavirin will have a decrease in their hemoglobin concentration by 4 g/l (23) and approximately 8% of patients require a decrease in the dose after developing anemia. The other serious side effect of ribavirin is that it is embryotoxic. It is recommended that both women and men should practice birth control during treatment and for 6 months after completing therapy (59). Additional side effects include a metallic taste, dry mouth, dyspepsia, nausea, headaches and irritability. Used alone against HCV, ribavirin has been shown to cause a decrease in ALT levels but relapse promptly occurs following drug withdrawal. Ribavirin monotherapy has no effect on levels of HCV RNA.

INTERFERON + RIBAVIRIN:

By combining IFN and ribavirin for 6 months, sustained response rates of 36 - 43% have been achieved which represents a 2 to 3 fold improvement over most monotherapy results (70). In comparing 6 vs 12 months of combination therapy, studies have shown sustained response of 41% of patients treated for 12 months with IFN α versus only 33% of patients treated for 6 months (59). Upon subgroup analysis by genotype, SR rates for genotype 1 were 29% and 17% respectively for 12 vs 6 months of treatment and 65% and 66% for genotypes 2 and 3. Comparing patients with high and low viral titers, it was shown that the SR rates to 12 and 6 months of therapy was 38% and 27% respectively for those with pretreatment viral levels of $> 2 \times 10^6$ copies/ml, and 45% and 43% for patients with lower levels. These results suggests that the longer duration of treatment may only truly benefit patients with genotype 1, and those with high pretreatment HCV RNA levels. By combining PEG-Intron and ribavirin for 6 months, Glue *et al.* (65) have shown SR rates of up to 60% at 6 months after stopping treatment which represents the best results to date for medical treatment of HCV. Combination treatment is shown to have a higher incidence of adverse effects compared to IFN monotherapy leading to 17 % vs 13% of patients requiring dose reductions, and 20% versus 8% of patients discontinuing treatment early (28).

There are numerous factors to consider in deciding which patients should receive therapy. Patients with minimal symptoms, normal ALT levels and minimal

inflammation on liver biopsy likely have the best chance of clearing the virus with therapy but many of them will never progress to severe liver disease. It is estimated that only 20-25% of all HCV carriers will ever progress to cirrhosis (71) and these are the patients who will have the poorest response to combination IFN and ribavirin therapy. The NIH consensus regarding asymptomatic patients with normal ALT levels is not to treat these patients. This is based on the fact that the majority will not achieve a sustained response, a minority of patients will actually get worse with treatment and most of these patients have only mild changes on histology (72). All patients with grades 3 and 4 hepatitis are at high risk for progression to hepatitis and should be offered treatment. The difficult decision lies with the patient showing grade 2 hepatitis as no consensus exists in the literature in deciding who should be treated and who should be observed.

Relapse rates within 6 months after treatment with IFN are quite high (73) and relapse usually occurs within the first 6 months after treatment is stopped. Predictors of relapse include: short course of IFN (<6 months), genotype 1, high pre-treatment viral load, cirrhosis, detectable hepatic HCV RNA at the end of treatment, and male sex. Retreatment for relapsers after IFN α monotherapy with combination therapy achieves SR rates of 49% versus 9% if retreated with IFN α monotherapy (73). The question of how to manage relapsers following combination therapy is less clear and remains unanswered.

Patients who are non-responders to IFN α also pose a dilemma in terms of management options. Options include dose escalation, changing the type of IFN α , and phlebotomy. It has been shown that non-responders have a higher hepatic iron concentration than responders and it has been postulated that iron serves as a necessary co-factor for steps in viral replication. By far the most promising approach to patients who do not respond to IFN α monotherapy is to retreat them with combination IFN α and ribavirin (74).

INTERFERON + AMANTADINE

Amantadine hydrochloride (AMA) is an antiviral agent that is active against influenza A. Although the mechanism of action is not exactly clear, recent evidence suggests that these agents block the viral membrane matrix protein, M2, which functions as an ion

channel and is required for internalization of the virus (75). The adverse effects associated with amantadine therapy include cardiac (0.1% - 1%), central nervous system, psychiatric, and convulsions (<5%) (75).

Khalili *et al.* (76) conducted a small (n=29) randomized controlled trial (RCT) of interferon + ribavirin versus interferon + amantadine in patients who had failed interferon monotherapy. The patients were randomized to receive either IFN α 3MU, 3 X per week and 1000 mg of ribavirin per day or the same dose of IFN with amantadine 200 mg/d. After 6 months of treatment the virologic response was 36% in the IFN + RV group versus 0% in the IFN + AMA group. 6 months after the end of treatment, sustained response was seen in 15 % of the first group versus 0 % of the AMA group. These results suggested that IFN + AMA has no useful role in the re-treatment of IFN monotherapy non-responders.

Brillanti *et al.* conducted a prospective RCT to compare IFN + RV + AMA versus IFN + RV in patients who had failed IFN monotherapy (n=60) (77). Patients were treated for 12 months and followed up for an additional 6 months. At the end of follow up, the triple-therapy group receiving IFN + RV + AMA achieved sustained response rates of 48% versus only 5% of the IFN + RV group (p<0.001). Not only do these results confirm the dismal results seen in re-treatment of IFN non-responders with IFN + RV but they support a new treatment regimen which can be offered to this difficult to treat subgroup of patients. The trial that most needs to be done now is an RCT to compare triple therapy with IFN + RV + AMA versus IFN + RV in treatment-naïve patients.

Mangia *et al.* from Italy compared 12 months of IFN + AMA versus IFN alone in newly diagnosed patients (78). Two hundred patients were included in the study and randomized to receive IFN 6 MU, 3 X per week + AMA 200 mg/d or an equivalent dose of IFN alone. The end of treatment response (ETR) rates were 45% in the IFN + AMA group vs 29% in the IFN alone group (p=0.014). Sustained response rates measured at 6 months after discontinuation of treatment were 29% vs 17% (p=0.036) in favor of the IFN + AMA treatment group. Both treatment arms showed similar results when subgroup analysis by genotype was conducted, with significantly lower SR rates seen with genotypes 1 & 4 as compared to genotypes 2 & 3. These findings offer a useful alternative for the treatment of newly diagnosed patients for whom ribavirin treatment

may be contraindicated (thalassemic patients, patients with coronary artery disease, patients unlikely to use effective contraception). The side effect profile was similar in both treatment groups in this study. The use of AMA as an alternative to RV also has important cost implications since 12 months of RV (1000 mg/d) is estimated to cost \$5,986 compared to only \$153 for 12 months of AMA at 200 mg/d (78).

VACCINES:

Although, HCV infection induces the production of cytotoxic lymphocytes and anti-HCV antibodies it is believed that mutant viral variants are able to escape these immune responses (79). The hypervariable region (HVR1) located in the envelope glycoprotein E2 gene is the most variable region of the HCV genome and mutates rapidly *in vivo* suggesting it is under selective pressure from the host defenses. This is reinforced by the observation of a lack of HVR1 variability in an agammaglobulinemic patient followed over a period of 2.5 years (80). The HVR region encodes a protein product only 28 amino acids long but accounts for 50% of the nucleotide changes and 60% of the amino acid substitutions within the HCV genome (81).

Given this lack of protective immunity and the ability of HCV to generate “escape mutants” at such a high rate, the development of an effective vaccine against HCV is a daunting task. Nevertheless, some encouraging progress has been made. Choo *et al.* (82) used recombinant E1 and E2 antigens to immunize 7 chimpanzees that were then challenged 2-3 weeks later with infectious serum of the same strain that was used to generate the vaccine. Five of seven animals achieved high antibody levels prior to inoculation and none of these animals became viremic in the 33 weeks of follow-up. Two animals had lower levels of antibody and became viremic but the viremia was delayed to the third week and they showed lower levels of viremia than the control animals. These results are encouraging even though a low dose of homologous HCV was used as inoculum. Farci *et al.* (80) raised a hyperimmune serum in rabbits following vaccination with a peptide from HVR1. Following *in vitro* incubation of infectious homologous serum with the rabbit hyperimmune serum, 1 of 2 chimpanzees was protected against infection as seen by lack of detectable HCV-RNA (although significance of this is questionable given the small numbers). Success with vaccines thus far is limited and has

only been possible in protecting against homologous strains. To be effective, an HCV vaccine will have to protect against the wide variety of HCV isolates known to infect humans.

PROTEASE INHIBITORS, RIBOZYMES, OLIGODEOXYNUCLEOTIDES

New information about the functions of the non-structural proteins expressed by the HCV genome has led to new ideas about how to combat HCV.

Ribozymes (ribonucleic acid enzymes) are RNA molecules that catalyze sequence-specific cleavage of RNA. By flanking the catalytic sequence with sequences complementary to the target site, specific RNAs can be cleaved. Several groups have shown that ribozymes directed against conserved portions of the HCV genome can significantly decrease HCV RNA levels in both transfected cell lines (83) and in primary human hepatocytes obtained from infected patients (84). Unfortunately, the potential for lethal destruction of non-targeted cellular RNAs is considerable.

Antisense oligodeoxynucleotides (ODNs) are specifically engineered to bind specific sequences in viral RNA, resulting in RNA-RNA hybrids that stop RNA replication. Wakita *et al.* used antisense ODNs targeting the 5' UTR of the HCV genome to inhibit HCV translation in an *in vitro* system using rabbit reticulocyte lysates (85). Presumably antisense ODNs block HCV translation through inhibition of ribosomal binding or other RNA binding proteins. The major problem with using ODNs clinically is delivery to the target cell and susceptibility to endogenous nucleases.

b) Liver Transplantation:

End stage liver disease as a result of HCV has become the most common cause of liver disease requiring liver transplant in North America (48). Orthoptic liver transplant (OLT) due to HCV is estimated to cost the U.S. health care system between \$150 and \$300 million annually (86). The natural course of HCV following liver transplantation has been closely studied since the development of the assays to detect anti-HCV antibodies and HCV-RNA. It is now clear that 100% of patients who are viremic pre-transplant will have a recurrent HCV infection post-transplant (64). It has also been

shown that anti- HCV antibodies decrease and HCV-RNA titers increase post-transplant, presumably as a result of the immunosuppression. Similarly, HCV-RNA titers are also found to be elevated in other immunosuppressed patients such as AIDS patients (63). HCV-RNA levels increase from 10 - 16 fold post-transplant (48)(87) with the rise beginning at 2 weeks post-transplant and peaking at 1-3 months (88). Levels of HCV RNA also were shown to increase steeply in patients treated with steroids (88). There is no definite correlation between the absolute viral titers and histologic changes seen in the liver (63), but some studies have found correlations between the timing of peak HCV RNA levels and episodes of acute graft dysfunction (88). The immunosuppression in post-transplant patients may also allow for more extrahepatic sites of replication as seen by the increased frequency of (-) strand HCV RNA detected in PBMCs post-transplant compared to pre-transplant (20).

Up to 50% of liver transplant patients positive for serum HCV-RNA will have no evidence of hepatitis on liver biopsy at 2 years post-transplant (89). It appears that in most cases the post-transplant HCV infection is mild with a slow rate of progression of liver disease. However, a rapidly progressing form of fibrosing cholestatic hepatitis associated with HCV recurrence has been reported in 6-8% of patients. Some studies suggest that the presence of CMV viremia post-transplant is associated with an increased risk of severe recurrent HCV hepatitis (63). Others have hypothesized that the clearance of HCV-RNA before transplant may help to prevent HCV recurrence after transplantation, but this has not been proven.

Follow up studies of patients transplanted for HCV-induced liver failure initially reported no significant difference in terms of patient survival, graft survival and re-transplantation rates compared to patients transplanted for other causes of liver failure (48). However more recently a study has shown that the 5 year graft survival for HCV transplant patients is significantly less (56.7%) than for patients transplanted for other reasons (65.6%) (90). Longer term follow up of 5 to 7 years has shown that 8-30% of post-transplant HCV infected patients develop cirrhosis (91) suggesting that recurrent infection may not be as benign as previously assumed. Studies indicate that predictors of poor outcome post-transplant are high levels of HCV-RNA post-transplant, severe and early hepatitis, high dose immunosuppression, and non-white patients (91). In the setting

of transplantation it is important to discriminate between hepatitis and rejection on the basis of a liver biopsy. Features suggestive of HCV infection include portal and parenchymal mononuclear infiltrates, areas of necrosis, swollen hepatocytes, and lymphoid aggregates (86) whereas rejection is indicated by endothelitis, bile duct necrosis, and a mixed portal inflammatory infiltrate.

The issue of treatment of recurrent HCV post-transplant is controversial. The option of treating patients pre-transplant in an attempt to decrease viral load is not viable since most patients with decompensated cirrhosis do not tolerate IFN well (92). Another question is whether to treat the infection early post-transplant or to wait until hepatitis develops. IFN causes increased expression of class I and II MHC antigens which could theoretically lead to an increased risk of organ rejection. This was in fact observed in a French trial treating OLT patients post-transplant with IFN where chronic rejection developed in 35% of the IFN-treated group but in only 3% of the non-treated group (63). As long as the medium term survival results remain good (3 year survival rates of 66-74 %) (86), it seems reasonable to continue transplanting these patients while at the same time attempting to find better therapy for the recurrent infection.

Lastly, given the shortage of available organs for transplant and the growing waiting list of patients requiring transplants, the question arises as to whether or not to use livers from HCV infected donors. Vargas *et al.* from Pittsburgh compared patients who had received livers from HCV infected donors with those whose donor was HCV negative (93). They found that both 1-year and 5-year survival were similar in both groups as was the rate of re-transplantation. There was a non-significant trend in the rate of recurring hepatitis favoring the group receiving infected livers who had rates of 47% at 5 years versus 64% in the group receiving non-infected livers. By comparing the donor and recipient strain of HCV to the strain that eventually became dominant in the recipient, they made several interesting observations. Firstly, whenever genotype 1a or 1b was present in the donor : recipient pair, that genotype became predominant. They also found that patients in whom the predominant strain belonged to the donor were significantly less likely to develop recurrent hepatitis than patients with recipient strain predominance. Overall they concluded that the clinical course does not differ significantly for these patients from that of patients receiving uninfected organs. The use

of infected livers will likely have some impact on the supply and demand problem seen with HCV transplants.

THE SCID/uPA MOUSE MODEL FOR HCV

The SCID/uPA mouse model for HCV was originally developed by Dr. David Mercer as part of his PhD work in Dr. Kneteman's lab (94)(95). Given the pressing need for a small animal model to study HCV but faced with the knowledge that only humans and chimpanzees were readily infected with the virus, the first challenge was to somehow achieve long term, stable engraftment of human liver cells in a rodent. Early experiments using SCID.Bg mice met with only transient engraftment of transplanted human cells. This next section will describe the genetic traits of the SCID/uPA mouse that make it possible to achieve long term human hepatocyte engraftment capable of supporting an HCV infection in this model.

The Alb-uPA Transgenic Mouse

The Alb-uPA mouse was originally developed by groups from the Department of Pediatrics at the University of Cincinnati and from the School of Veterinary Medicine at the University of Pennsylvania (96). The conversion of plasminogen to plasmin in the serum initiates the breakdown of fibrinous clot by fibrinolysis. Two different plasminogen activators exist in the form of tissue-type plasminogen activator (t-PA) and urokinase-type plasminogen activator (u-PA). Under normal circumstances, loss of vascular integrity is followed first by formation of a platelet plug followed by the deposition of a fibrin clot, which is subsequently removed by fibrinolysis once vascular integrity has been restored. Bleeding disorders can occur if any of these steps are not functioning properly such as insufficient platelet numbers, platelet malfunction, and low levels of fibrin deposition or high levels of fibrinolysis. It is this last mechanism, which led to the development of the Alb-uPA mouse model in which production of uPA is targeted to the liver resulting in elevated levels of uPA. The elevated uPA results in excessive fibrinolysis and neonatal bleeding deaths.

The Alb-uPA transgene consists of the murine albumin enhancer/promoter, the murine uPA gene body and the 3' untranslated region and flanking sequences of the human growth hormone (hGH). The hGH sequence was added to be able to distinguish

transgene mRNA from endogenous murine mRNA (96). As a result, the production of uPA is targeted to the site of albumin production, the hepatocyte. After breeding two transgenic mice together, researchers found that between one half to two thirds of all transgene positive mice died shortly after birth. All deaths occurred between 3 hours and 84 hours after birth and there was no evidence of intrauterine deaths (96). The cause of death in all cases was found to be a hemorrhagic intraabdominal or intrainestinal event. This is presumably due to birth trauma, umbilical tearing or other trauma. To investigate the exact coagulation disorder, platelet counts were performed and the transgenic animals were found to have normal counts. Plasma uPA levels in transgenic mice were found to be up to 200 times higher than controls, PTT times were elevated and fibrin levels were only 10-20% of normal levels (96). It appears that the hemorrhagic deaths are due to the elevated uPA levels resulting in excessive fibrinolysis and hypofibrinogenemia. Transgenic mice that survived the neonatal period did not bleed later, but passed the bleeding phenotype on to their offspring.

Upon further study of these transgenic mice, it was discovered that the uPA levels and PTT times returned towards normal by 2 months of age in mice that survived the neonatal period. Further investigations to explain this phenomenon began by examining the livers of transgenic mice and these were found to be profoundly abnormal. Grossly they appeared as smooth pale tissue (white liver) surrounding small nodules of more normal, red tissue (red nodules). These red nodules did not appear grossly until 1 week of age and in older mice whose uPA levels had corrected, the entire liver was composed of confluent red nodules. More importantly, analysis of the red nodules revealed clusters of hepatocytes that had spontaneously deleted the transgene. From this set of observations and experiments, it was concluded that the elevated levels of uPA are toxic to the liver and result in a pale, abnormal liver. This creates a "functional liver deficit" (much the same as a partial hepatectomy would) and results in a stimulus for liver growth and regeneration by some unknown signaling process. This growth stimulus is the driving force for repopulation of the liver by the hepatocytes that have deleted the transgene and are thus relieved of its deleterious effects.

Matings of the transgenic mice produce offspring that are both homozygotes and heterozygotes for the transgene. The uPA transgene is inserted into the DNA of these

animals not as a single copy but as a tandem array. Homozygote mice will have twice as many genomic copies of the transgene compared to heterozygote animals. The original studies found that 80% of all homozygotes developed severe edema and died within 3 and 6 weeks of age (97). Analysis of the homozygote liver revealed few to no red nodules which is explained by the fact that in order to initiate a red nodule, a hepatocyte must delete twice as many transgene copies as is the case for a heterozygote. As expected, these homozygous animals have very low levels of serum total protein and albumin. Under light microscopy, tissue from the white liver was found to contain small hepatocytes with prominent cytoplasmic vacuolization (97). When examined by electron microscopy, the ultrastructural defect seems to be transformation of a large part of the rough endoplasmic reticulum (RER) into RER-bounded multivesicular bodies, a lesion which has not been described previously in human liver.

After establishing that transgene-deficient cells had a chronic growth stimulus and were able to repopulate the liver, the next step was to transplant hepatocytes from another mouse into the Alb-uPA mouse and see if they as well would be able to repopulate the liver. For this experiment, transgenic mice carrying a metallothionein-I gene promoter fused to a β -galactosidase structural gene (MT-LacZ) were used as hepatocyte donors. This allowed for differentiation of the donor hepatocytes from the host hepatocytes later by administering the heavy metal cadmium and tissue staining with the substrate 5-bromo-4 chloro-3-indonyl- β -D-galactosidase (X-gal). The stimulus for hepatocyte regeneration was thought to exist as long as the white, transgene-expressing liver remained. Viable hepatocytes (10^4) from adult mouse livers were transplanted into Alb-uPA mice between 5 and 11 days of age by intrasplenic injection. Four to six weeks later the Alb-uPA mice were sacrificed and their livers were appropriately stained and examined by immunohistochemistry revealing that the transplanted cells had repopulated up to 80% of the diseased liver (98). These promising results led the way for xenogeneic hepatocyte transplantation which was successfully performed using rat hepatocytes (99).

To generate immunotolerant Alb-uPA mice, the transgenic animals were crossed with Swiss athymic nude (nu) mice. Adult rat hepatocytes were isolated using a 2-step EDTA collagenase perfusion technique. Between $1-2 \times 10^5$ viable rat hepatocytes were transplanted via intrasplenic injection into the Alb-uPA / nu mice between 10 and 15 days

of age. Transplants were performed in mice that were heterozygous and homozygous for the transgene. The mice were then sacrificed between 6 and 8 weeks (heterozygotes) and 10 and 14 weeks (homozygotes), which is when it was estimated by gross visual inspection that less than 10% of the white liver remained. Analysis of the livers showed that in heterozygote transplant recipients, between 1 and 92% of the liver was of rat origin. Even more impressive, in homozygote transplant recipients, 90-100% of the livers were of rat origin (99). These results show that the Alb-uPA mouse is a potential model for xenogeneic hepatocyte transplants and our lab has shown that human hepatocytes can be successfully transplanted into immunotolerant Alb-uPA mice and engraft in the liver. The Alb-uPA model used in our lab is made immunotolerant by introducing the SCID and Beige traits.

These same authors reported in 1992 that upon close follow-up of the uPA transgenic mice, virtually all mice greater than 1 year of age showed evidence of large hepatic tumors typical for hepatocellular carcinoma (HCC) (100). Analysis of the tumors revealed that transgene expression was not seen in ANY of the tumors suggesting that the tumors were derived from cells that had lost the transgene. They hypothesized that the transgene-associated DNA rearrangements lead to the development of HCCs in these mice, possibly through the co-deletion of the transgene and a linked tumor-suppression gene which would put the affected cell at risk for neoplasia (100). It was also pointed out that the period of intensive mitogenesis that occurs as the red nodules replace the white liver almost certainly enhances tumorigenesis.

Another group of researchers from Wisconsin has made use of the uPA transgenic mouse to study transplantation of cryopreserved hepatocytes (101). In order to avoid the problem of early neonatal bleeding problems, they have created a transgenic mouse in which the uPA gene is targeted to the Major Urinary Protein (MUP) gene promoter instead of the albumin promoter. The advantage of this animal is that expression of the MUP gene is delayed until 2-3 weeks after birth which avoids the problems of neonatal mortality and allows the hepatocyte transplant to be performed on larger, older animals. Using MT-LacZ transgenic mice as donors, this group was able to cryopreserve isolated mouse hepatocytes, thaw the cells, and then transplant 10^5 cells via intrasplenic injection. By histological examination of the livers 8-12 weeks post-transplant, they were able to

show 2 - 32% hepatic repopulation with transplanted hepatocytes. They did not report any serum assays to measure the actual function of these cells.

A. The SCID Mouse

The Severe Combined Immune Deficient (SCID) mutation is an autosomal recessive mutation that was first described in mice in 1983 and occurred spontaneously in the BALB/c C.B17 strain (102). This mouse was found to have extremely low levels of serum Ig and a lack of functional T cells. Functional immunoglobulin and T cell receptor genes are assembled from separate gene elements via somatic gene rearrangement in a process known as **V** (Variable) **D** (Diversity) **J** (Joining) recombination. It is this ability of lymphocyte receptor VDJ gene segments to rearrange that generates much of the receptor diversity that is the hallmark of the immune system (103). VDJ recombination activity is only found in cell lines that represent precursor lymphocytes. Each germ line V,D,J segment is flanked by heptamer-spacer-nonamer sequence elements known as recombination signal (RS) sequences. When two gene segments are to be combined, the RS sequence is first recognized, and then double strand DNA breaks are introduced into each gene at the signal: coding junction resulting in four “loose ends” of DNA. The VDJ recombination machinery recombines these four “loose ends” to form a signal joint and a coding joint. In the SCID defect, the signal joint appears to proceed in a normal fashion but the coding joint formation is abnormal resulting in defective lymphocyte receptors and the lack of functional T or B cells.

In order to serve as a useful animal model for human diseases, it is advantageous to be able to reconstitute an animal's immune system with a “human immune system”. Mosier *et al.* (81) were able to demonstrate this in the SCID model by injecting human peripheral blood lymphocytes (PBL) into the SCID mouse. They reported the reconstitution of a functional human immune system as determined by the production of human Ig at levels of 0.1-1 mg/mL (normal human levels are 7-24 mg/mL) as well as an antibody response following tetanus immunization. Interestingly, the intraperitoneal (IP) route of PBL injection was used as the intravenous route was found to be ineffective. Also, the expected graft-versus-host disease did not pose any significant problem.

Although the SCID model would thus appear to be an ideal animal model for studying both immunodeficient states and xenogeneic transplantation, several limitations exist.

Firstly, experiments using radiation on SCID mice have shown that these mice are not tolerant to radiation and the majority of them die if irradiated. The most plausible explanation for this is due to an inability to repair double stranded DNA breaks that are often seen with radiation. This is analogous to the VDJ recombination event which involves DNA breaks that need to be recombined / repaired and thus it seems that the SCID defect results in a generalized impairment of DNA double stranded breaks (DSB) repair (102). The implication of these findings for this animal model are important in that anti-neoplastic and anti-viral drugs often induce DNA damage and may not be tolerated by these mice.

Secondly, it has become known since 1988 that with age some SCID mice show detectable levels of immunoglobulin, and this tendency increases with age such that in the original SCID strain developed, nearly 100% of mice had detectable levels of Ig at 1 year of age. The term “leaky” is defined differently by different authors but is generally accepted as having $> 5 \mu\text{g/mL}$ or $1 \mu\text{g/ml}$ of Ig detected in the serum. The mean serum Ig levels in CB17 mice is approximately $2670 \mu\text{g/ml}$ (104). Jackson laboratories have introduced the SCID defect into the C3H strain and this new strain, C3H.SCID, has a much lower rate of leakiness which does not increase with age (15% at 3 months of age vs 79% of SCID mice) (102). The mechanism by which leakiness develops is unknown but may be due to spontaneous reversal of the SCID mutation. Alternatively, leakiness may result from the joining of liberated coding joints in pre-B cells by some unknown recombination event that restores what appear to be normal coding joints.

Lastly, although the SCID mouse has no functional T or B cells, other elements of the immune system such as Natural Killer (NK) cells are intact and could theoretically hamper attempts at xenogeneic transplantation. This last problem and that of “leakiness” can be solved by combining the SCID trait with the Beige (bg) trait.

III. The Beige Mouse

The Beige defect, located on murine chromosome 13, is an autosomal recessive disorder resulting in hypopigmentation, bleeding, and immune cell dysfunction. The

original defect arose from a radiation experiment at the Oak Ridge National Laboratory in C57Bl/6 mice but since then many spontaneous mutations have resulted in beige mice (105). The immune defect is the result of selective impairment of naturally occurring killer lymphocytes (NK cells) whereas all other forms of cell mediated lysis are apparently normal. The beige defect is the murine equivalent of the autosomal recessive Chediak-Higashi Syndrome (CHS) found in humans. Patients affected with CHS frequently die at a young age from bacterial infections or lymphoproliferative syndromes resulting from lack of NK cell function. In patients with CHS the NK cell number and target binding appear to be normal but the effector function is defective (106). Similarly, beige mice suffer from decreased coat and eye pigmentation, decreased bacterial activity of granulocytes, decreased NK function, increased susceptibility to bacterial infections, enlarged melanosomes in pigment cells and enlarged lysosomes in many other cell types (106). The pathognomonic picture on peripheral blood smear for both CHS and Beige are “giant azurophilic cytoplasmic inclusions in granulocytes” and this is useful to determine homozygote beige animals phenotypically.

Given that the SCID mouse has no functional T or B cells but still has normal NK cell activity that could damage a xenograft, researchers crossed the SCID and Beige strains in an attempt to create a truly immunodeficient rodent model. An interesting finding upon combining the SCID trait with the Beige trait was that addition of the Beige trait severely depressed the rate of leakiness in the SCID trait. Whereas virtually 100% of the original SCID strain were found to be leaky by one year of age, only 3% of SCID.Bg animals leaked. Thus the SCID.Bg model is a great improvement over the SCID model for xenogeneic transplantation.

IV. Hepatocyte Isolation:

The technique of hepatocyte isolation has been used extensively in the study of liver physiology, liver diseases and cell transplantation. The process by which single, viable parenchymal cells are isolated from the surrounding fibrovascular matrix has evolved considerably over the last four decades. Early attempts to separate hepatocytes from the liver by mechanical and chemical means invariably resulted in dead or damaged cells. The method was improved by Howard *et al.* (1967) who introduced the use of

collagenase to liberate hepatocytes (107). In these early experiments, slices of liver were incubated and shaken in a solution containing both collagenase and hyaluronidase resulting in viable hepatocytes as determined by the trypan blue exclusion test. Although the viability of hepatocytes obtained in this manner was quite high, the yield corresponded to only 5% of the original tissue (107). The most important contribution to hepatocyte isolation came two years later when Berry & Friend (108) introduced the notion of perfusing the liver *in-situ* with the collagenase / hyaluronidase solution after first flushing the blood from the liver. In order to achieve intimate exposure of the intercellular spaces to the collagenase and hyaluronidase, the solution was circulated continuously through the liver via the portal vein at a temperature of 37° C. The collagenase solution contained 0.05 % collagenase and 0.10 % hyaluronidase and was gassed with carbogen (95 % O₂ & 5 % CO₂). This novel technique resulted in the conversion of approximately 50% of the liver into intact, isolated parenchymal cells and became the prototype for most isolation protocols used today. Further work was done in 1973 by Seglen (107) who developed what is known as the “2-step perfusion” method for hepatocyte isolation. By this time it was known that calcium had a role to play in intracellular adhesion, and so calcium chelators such as ethylene-diaminetetra-acetic acid (EDTA) were used to try to separate the liver cells prior to enzymatic digestion. The liver was flushed first with either a solution containing EDTA or a calcium-free solution in an attempt to remove the calcium from the tissue. This calcium removal facilitated subsequent separation of cells by collagenase perfusion presumably due to the washout of some calcium-dependent adhesion factor. This initial flushing also served to flush the blood from the liver that helps prevent any small clots from plugging the vasculature needed to deliver the collagenase. For human specimens obtained from the operating theatre, some groups flush the liver with cold University of Wisconsin (UW) solution to help preserve the hepatocytes (109). It has also been suggested that blood inhibits the action of collagenase and so adequate flushing of the liver before collagenase perfusion is important.

The second of the 2-step perfusions is performed using the collagenase solution. Various other enzymes have been studied in the past for hepatocyte liberation such as trypsin and pronase but collagenase was found to be superior. Although the original

experiments using collagenase for hepatocyte isolation also used the enzyme hyaluronidase, subsequent studies showed that the hyaluronidase had no real impact on the tissue digestion and could be omitted (107). The perfused liver tends to generate CO₂ and thus any solution diffusing through it in a recirculating circuit tends to become acidic with time. It is known that collagenase performs optimally at a pH of 7.5 and so methods to maintain the pH of the collagenase system were developed. The options include the use of a pH-stat which continuously infuses sodium hydroxide (NaOH) into the circuit as needed, or the use of organic buffers such as 4-(2-hydroxyethyl)-1-piperazineethanesulfonic acid (HEPES) in high concentrations. Another important consideration for the optimal performance of collagenase is the addition of calcium. Collagenase is a calcium-dependent enzyme and the optimal concentration has been shown to be approximately 5 mM.

The time taken to adequately digest rat livers using this system is usually in the range of 10 to 15 minutes while human and pig liver biopsies require 30 - 45 minutes for adequate digestion (110)(111)(112). After perfusion of the liver by the collagenase is deemed complete, the capsule of the liver is opened and the hepatocytes are liberated from the fibrovascular matrix by gentle mechanical agitation with a comb, forceps or spatula. Forceful agitation of the liver tissue will only serve to damage cells and liberate non-parenchymal cells. The resulting cell suspension is then shaken in a warm water bath for 15-30 minutes. This serves two purposes: first, in cells that are damaged, the shaking will complete the damage and cause the cells to release their soluble contents or become fragmented, which makes them easier to separate in later steps. Second, small aggregates of cells can theoretically be broken up into single cells with gentle agitation. After shaking, the suspension is passed through filters with successively diminishing mesh width to remove particulate debris and larger clumps of hepatocytes. At this step the suspension is known as the "initial cell suspension" and there are various methods of purification to arrive at the final hepatocyte isolation.

The simplest method of purification is that of differential centrifugation whereby the suspension is centrifuged at 50g for 2-5 minutes repeatedly, discarding the supernatant at each step. This is done based on the knowledge that non-parenchymal cells are smaller and damaged cells are lighter and are therefore more likely to remain in

the supernatant. Viable parenchymal cells are almost certainly lost with each wash and so there is an inevitable decrease in yield seen with each repeated wash to gain purity.

An alternate method of purification uses the concept of “density gradient centrifugation” which is based on the relationship between the density of a cell and its morphological and functional integrity. One such system uses a percoll solution to provide the density gradient. Using this system, viable parenchymal cells will pass through the percoll gradient while non-viable cells and the lighter non-parenchymal cells will remain trapped above the percoll layer. Kreamer *et al.* have shown that for rat hepatocytes, the optimal percoll density is 1.06 g/mL (113). There are no reported studies on the optimal density for human hepatocytes. Dorko *et al.* found that the yield of isolated viable human hepatocytes is inversely proportional to the donor age (114).

The most reliable and simple method to test cellular integrity remains the trypan blue exclusion test. Cells with intact plasma membranes exclude dyes such as trypan blue, nigrosin and eosin, whereas damaged cells become stained, particularly intensely in the nucleus. One should note however that cells may have internal metabolic lesions or small surface alterations that are not revealed by the trypan blue test but that may result in cell death at a later time. The trypan blue exclusion test therefore does not actually measure viability but gross structural integrity at the moment of testing.

The statement in one of the landmark papers that “successful preparation of intact liver cells by perfusion with collagenase is technically quite difficult, and still remains mostly an art” (107) is a reflection of the numerous steps and variables where error can be introduced inadvertently.

V. Hepatocyte Cryopreservation:

Any set of experiments using transplantation of isolated hepatocytes would benefit greatly from a method of cryopreserving large numbers of hepatocytes indefinitely while maintaining their functional and structural integrity. Cryopreservation can overcome problems such as genetic variations in hepatocytes from different patients and non-uniformity of cell preparations (115). As well, transplants of recipient animals at a certain age could be achieved without relying on a source of fresh hepatocytes. The need

to cryopreserve hepatocytes becomes all the more important when they have been isolated from valuable tissue samples such as human liver.

Ideally any cryopreservation system should demonstrate restoration of the thawed hepatocytes to full metabolic activity. The cryopreservation process involves the introduction of a cryoprotectant solution into the cell followed by freezing to very low temperatures. Important variables in the various cryopreservation protocols used include the choice of cryoprotectant and the rate of freezing. Cryoprotectants such as dimethylsulfoxide (DMSO) delay and reduce ice formation during the freezing process resulting in decreased cellular damage. Novicki *et al.* compared two of the most commonly used cryoprotectants, glycerol and DMSO, for rat hepatocyte preservation. They reported DMSO to be superior to glycerol as determined by viability and maintenance of microsomal enzyme function (115). Loretz *et al.* similarly compared various cryoprotectants such as DMSO, glycerol, polyvinylpyrrolidone, and dextrans in the cryopreservation of rat hepatocytes. They determined that the recovery of viable attached cells was optimal with 10% DMSO (116). More recently Adams *et al.* introduced a cryopreservation solution containing 70% University of Wisconsin (UW) solution and 10% DMSO and found it to be superior to the standard 10% DMSO for the preservation of human hepatocytes. They reported viability of >90% in cryopreserved cells but do not report the actual percent of initial cell number that was recovered after cryopreservation (117).

To determine the optimal freezing protocol for hepatocytes, early studies compared preservation of cells at various temperatures ranging from 0° C to -196° C. Cells stored at -196 °C were found to survive the best (113). The rate of freezing cells to -196 °C has also been studied. Gomez *et al.* (118) compared a slow freezing rate to a fast freezing rate for the cryopreservation of rat hepatocytes. The slow freezing protocol consisted of an initial freezing rate of -2 °C per minute to -30°C, followed by a quick freeze down to -196 degrees. The fast freezing protocol entailed freezing directly down to -196 degrees (-39 degrees per minute). They found that cells undergoing the fast freezing protocol fared much better than cells undergoing the slow freezing protocol as determined by numerous parameters including trypan blue exclusion, plating efficiency,

gluconeogenesis, and plasma protein synthesis. In contrast, Loretz *et al.* found that a slower, stepwise cooling process was superior to fast freezing into liquid N₂ (116).

Thawing of hepatocytes is usually performed by immersion in a 37 °C water bath. The cryoprotectant is diluted out and removed from the final cell preparation by repeated centrifugation. It has been suggested that the addition of glucose to the thawing medium improves viability, probably by limiting the osmotic shock caused by the outflow of DMSO (119).

VI. Hepatocyte Transplantation:

There have been many studies performed in recent years to better understand the fate of hepatocytes transplanted into the spleens of rodents. Perhaps the most widely published author in this field is Sanjeev Gupta from Albert Einstein College, The Bronx, NY. Studies by this and other authors have established that although hepatocyte transplantation into extrahepatic sites such as the peritoneal cavity can produce successful engraftment, the transplanted cells do not remain viable for long periods of time. It is generally accepted that the liver offers the most suitable microenvironment for transplanted hepatocytes as they are more likely to benefit from extracellular matrix components, growth factors, nutrients, and interactions with other cells in the liver (115). In rats, it has been shown that intrasplenically transplanted hepatocytes can survive, function and proliferate in the spleen indefinitely. In contrast, in the mouse spleen, which lacks sinusoids, transplanted cells rarely survive (120). Studies have shown that cells transit rapidly from the spleen to the liver via the portal vein and are deposited in peri-portal locations. Electron microscopy has been used to show endothelial cell layer disruption adjacent to transplanted cells allowing the cells to leave the portal vasculature and penetrate the liver parenchyma (120). It is also evident that only a fraction of the cells that are injected into the spleen survive in the liver. Biodistribution of radiolabeled cells in rats have shown that up to 60 % of intrasplenically transplanted hepatocytes in fact migrate to the liver, whereas approximately 10% remained in the spleen and 1-3% were found in the lungs (121).

OTHER MODELS FOR THE STUDY OF HCV

Given the pressing need for the development of effective antiviral agents and vaccines against HCV, it is not surprising that suitable models for the study of human hepatitis viruses are the focus of intense research. The situation is well described by a quote from a paper published by Shimizu *et al.* in 1993: “In spite of the progress in molecular biology of HCV, the biological characteristics of this virus remain obscure. This is primarily because biological assays for HCV have been limited to the experimental inoculation of chimpanzees, which are expensive and restricted in number. It is imperative to develop either a less expensive animal model or an *in vitro* system for propagating HCV “ (122). Although much has been learned since 1993, effective models for this disease are still being sought.

These models can be divided into *in vitro*, (cell culture models), and *in vivo*, or animal models. The animal models include the chimpanzee, the tree shrew (tupaia), the Trimera mouse, the RAG/uPA mouse, and the NOD/SCID mouse with HGF receptor agonist stimulation. The cell culture models studied to date include primary hepatocytes (adult human, fetal human, chimpanzee), immortalized tumor cell lines, T-cell lines and B-cell lines. The next section will attempt to highlight the research findings that have arisen from these different models and specifically focus on the RAG/uPA mouse that is the most similar to our own SCID/uPA model.

I. ANIMAL MODELS:

a) Chimpanzee:

Given that the chimpanzee (*Pan troglodytes*) is the only host permissive for HCV other than human beings, much of the research that has been done to characterize the HCV virus and the immune response it elicits has been done in chimpanzees. Although the chimpanzee is perhaps the best available model for the study of HCV in terms of similarity to humans, there are obvious problems in using these animals for HCV research. Most importantly, chimpanzees are expensive, relatively scarce, and difficult to

handle. Many research centers in the world do not have access to chimpanzee housing facilities even if they could afford the cost of keeping them. There appears to be differences in the natural history of HCV infections in chimpanzees compared to humans since 60-75% of chimpanzees manage to clear their infection as measured by lack of detectable HCV RNA, compared to only 15-20% of humans (123). It has also been reported that chimpanzees don't produce an anti-C22 (core protein) response to HCV infection (124). Nevertheless, important insights have been gained with the chimpanzee model such as the demonstration that chimpanzees can be repeatedly infected with both heterologous and homologous strains of HCV despite the production of anti-HCV antibodies (32). This has led to the theory that HCV persistence is achieved by rapid mutations in regions such as the hypervariable region (HVR) in response to immune pressure as a means of escaping the neutralizing effects of the host immune system. In order to study the sequence variability in a host following inoculation with HCV one needs to know the exact time of inoculation and the exact strains contained within the inoculum. This sort of study is not feasible for human HCV infections because the exact time of infection is often not known, and any infectious serum likely contains a pool of related but slightly different HCV strains, or quasispecies. Major *et al.* were able to study the changes in HVR1 sequence over time by infecting 2 chimpanzees through direct intrahepatic inoculation of recombinant RNA transcribed from a full-length cDNA clone (125). This enables the authors to know the exact sequence of HCV RNA that was used to inoculate the animals. These animals were followed for 60 weeks and both seroconverted and developed persistent HCV infections with peak RNA levels of 10^6 copies/ml. Surprisingly, these authors showed very little change in the HVR1 sequence in either chimpanzee over time which goes against the theory that mutations in this region are important for maintaining persistent infections which is supported by the detection of "escape mutants" seen in human infections. Perhaps the chimpanzee immune response mounted was not strong enough to pressure the virus to mutate. Alternatively, the HVR1 escape mutants seen are just the result of selection of pre-existing variants, which become dominant when the major species is suppressed by the antibody response in the host (125). Vaccination of chimpanzees with recombinant E1 and E2 proteins has led to protection against infection with a low dose, homologous HCV inoculum (82).

b) Tupaia (Tree Shrew) Model:

The tree shrew (tupaia) is a small squirrel-like mammal, which lives in Southeast Asia. Researchers in China and in Spain have tested this animal as a possible model for HCV infection (124). In their first series of experiments, 8 of 23 (35%) animals showed evidence of infection: 2 had transient detection of HCV RNA by RT-PCR, and 6 had intermittent HCV RNA over a period of 27 weeks. Detection was all done by qualitative RT-PCR. Several animals were also found to have detectable anti-HCV antibodies. In the second experiment, the animals were irradiated prior to inoculation with HCV in an attempt to induce immunosuppression. This resulted in a higher rate of HCV RNA detection (50%) although detection was still only transient. Although HCV RNA quantification was not done in these studies, the transient nature of the infection and the presumably low levels of virus present make this animal a suboptimal model for the study of HCV.

c) Trimera Mouse Model:

Researchers in Israel have developed an animal model known as the Trimera mouse, which makes use of the BNX (Beige:Nude:X-linked immunodeficient) mouse (126). The BNX mouse is subjected to lethal doses of irradiation and then “rescued” by transplantation of SCID mouse bone marrow cells. After bone marrow rescue, fragments of human tissue are transplanted under the kidney capsule – this procedure has a 50% mortality rate in these animals with the most common cause of death being excessive bleeding. Human liver fragments from HCV infected patients were transplanted under the kidney capsule. Fifteen of thirty-three animals retained their grafts for at least 12 weeks. HCV RNA levels were detectable in these animals by RT-PCR for approximately 2 months. Normal human liver fragments were infected *ex-vivo* by incubation with infectious human serum and then transplanted under the kidney capsule resulting in detectable HCV levels for 1 month in 20% of animals. The HCV RNA levels detected were in the order of 10^2 - 10^3 copies/ml. Attempts to transplant normal liver fragments and then infect the animals with HCV *in vivo* failed to demonstrate an HCV infection. This model was also used to study HBV by transplanting *ex vivo* infected liver fragments

under the ear pinna or the kidney capsule (127). HBV was detected for up to 25 days with peak serum titers of 2.5×10^5 copies/ml. The authors were also able to show covalently closed circular HBV DNA in the liver fragment transplants 14 days after transplant. Treatment with antiviral agents such as lamivudine (3TC) and β -C-Fdde showed a decrease in the viral load in infected animals with a rebound seen after treatment was stopped. The transient nature of the xenograft in these animals severely limits its usefulness as an animal model for viral hepatitis.

d) The RAG/uPA mouse:

Two genes known as RAG-1 and RAG-2 (Recombinase Activating Genes) need to be expressed simultaneously to generate VDJ recombinase activity in all cell types examined (103). Recombination signal (RS) sequence recognition is mediated by RAG-1 followed by recruitment of RAG-2. The RAGs “nick” the RS sequence at the heptamer / coding border which leads to the double stranded DNA breaks. Strains of mice have been generated with homozygous germline disruptions of these genes – rag-1 and rag-2 knockout mice. These mice have an identical phenotype and have been shown to completely lack functional B and T cells (128). The problem of leakiness is avoided since unlike the SCID defect, the RAG defect precludes the VDJ recombination process ever being initiated. Apart from the defect in T and B cells, these animals appear to be completely normal (102).

The most promising animal model other than the chimpanzee and our SCID/uPA model is being developed by researchers from Albert Einstein College (Bronx, NY) and The University of Hamburg (Hamburg, Germany) (129). This group has crossed the Rag-2 knockout mouse with the uPA transgenic mouse to develop the RAG/uPA mouse model for the study of human hepatitis viruses. This mouse model was first used to study woodchuck hepadnavirus (WHV) (129). Both WHV and Peking duck hepadnavirus are closely related to human hepatitis B virus (HBV).

Woodchuck hepatocytes from non-infected woodchucks were isolated and transplanted ($0.5 - 1.0 \times 10^6$ hepatocytes) into 10-18 day old RAG/uPA mice via intrasplenic injection. Interestingly, in this study, only mice that were hemizygous for the uPA transgene were used, presumably as a result of difficulty in maintaining a

homozygote colony due to excessive neonatal bleeding. By hybridizing test mixtures of woodchuck DNA and mouse DNA in various proportions along with DNA from the transplanted mice, it was estimated that woodchuck hepatocytes constituted between 30 and 95% of the total liver (129). Three months after transplant, the mice were infected with WHV-containing serum and WHV DNA levels were followed indicating active infection to at least 10 months time. Mice were also transplanted with hepatocytes from WHV-infected woodchucks and again active infection was documented after an 8-12 week lag period with WHV DNA levels of up to 10^{11} virions/ml in the serum and covalently closed circular (CCC) WHV DNA detected in the liver. Finally, the authors were able to show in 2 infected mice that treatment with Interferon α -2b (135 IU/g/d) resulted in a decrease in WHV DNA levels of up to 4 log. The titers of WHV DNA in these animals rebounded after treatment was discontinued. Treatment of 1 infected mouse with Dexamethasone resulted in an increase in viral titers of approximately 2 logs (129).

The next relevant study published by this group made use of an immortalized liver cell line developed by transferring the Simian Virus Large T-Antigen into primary human hepatocytes to overcome growth arrest (130). These cells were transfected with circular HBV DNA resulting in a cell line that expresses HBV antigens and replicates the virus. These cells were then transplanted into 6-8 week old homozygous Rag-2 knockout mice (1 million cells) via intrasplenic injection and the mice were followed for up to 5 months post-transplant. Plasma HBV DNA was detected in these mice at levels between 3×10^7 and 3×10^8 virions/ml, and HBsAg was detected in concentrations of up to 7 μ g/ml. DNA analysis of the liver was performed again by generating a standard curve with spiked human DNA and mouse DNA samples of different proportions. By comparing the liver DNA from transplanted mice it was estimated that 0.2 – 0.5 % of the liver mass was replaced by human hepatocytes. This seems like a very small fraction of human chimerism in these mice to produce such a persistent infection with high levels of HBV DNA, which attests to the high level of HBV DNA generated by these immortalized cells. Serum levels of hAAT were measured using an ELISA assay and the authors report that hAAT levels were seen that are 11% - 14% of the level found in normal human plasma samples (normal human levels of hAAT = 0.9 – 2.6 mg/ml) which

is remarkable considering they estimate the transplanted human cell line constitutes only 0.5% of the mouse liver. They do not provide information on levels of hAAT generated by this cell line *in vitro* under standard culture conditions. The authors also make use of a fluorescein-labeled DNA probe for human chromosomes to demonstrate the presence of human derived tissue in the mouse livers by Fluorescent In Situ Hybridization (FISH). Interestingly, in this study there is no mention made of the uPA transgene and one must assume that the mice used were simple Rag-2 knockout mice which may explain the low amount of chimerism seen. The length of documented infection (to 10 months) is surprising however since in our experience we have never been able to achieve long-term engraftment after xenotransplantation into a SCID.Bg mouse. The difference presumably lies in the nature of the cells transplanted (immortalized cell line vs. primary human hepatocytes) or the nature of the immunodeficient background of the mice (Rag-2 knockout vs SCID.BG).

The last study by this group used the RAG/uPA mouse but this time transplanted human hepatocytes in the mice and were able to successfully infect the animals with human HBV (131). Again only mice that were hemizygous for the uPA transgene were used, and they were transplanted at 13-21 days of age with 5×10^5 viable cells via intrasplenic injection. The transplant operation was associated with a 20% mortality rate. The mice were subsequently infected with HBV positive serum (20 μ l sc) **2 days** after transplant. The authors estimated the percentage of human DNA in the mouse liver as described above in their previous 2 studies and estimated that the percentage of human DNA was between 2 and 10 % of the entire liver (131). They also examined cryostat sections of liver stained with antibodies against HBcAg and found that between 5 and 15 % of sections were positive. Levels of HBV DNA were measured up to 4.5×10^8 genome equivalents/ml of serum. Production of human serum albumin (HSA) was quantified using a Western blot procedure with standards made up of known ratios of human and mouse serum and the authors estimated that the levels of human albumin ranged between approximately 1% to 10% with a mean of 5%.

e) NOD/SCID mouse model for HBV

Ohashi *et al.* from Stanford University (132) have developed a mouse model for HBV by combining an immunodeficient mouse with the hepatocyte growth stimulus offered by human hepatocyte growth factor (HGF), known to be a potent mitogen for hepatocytes. Human hepatocytes were isolated and then mixed with an encapsulating substance known as Matrigel. The encapsulated hepatocytes were then transplanted under the kidney capsule of Non-Obese Diabetic (NOD) / SCID mice. Encapsulation of cells has been used before in hepatocyte transplantation (121). The theoretical advantage of encapsulation is that the capsule provides a support matrix for the hepatocytes and also permits the diffusion of small molecules but restricts the passage of host-derived immune cells and thereby protects the hepatocytes from the host immune system. Three days after transplantation the mice were infected with HBV positive serum injected both into the graft and intravenously. The mice were followed and levels of hAAT, HBsAg and HBV DNA were measured in the serum. Usually human hepatocytes transplanted into another species inevitably die within months (even if the animal is immunodeficient) presumably as a result of both non-specific immune attack and the fact that the human cells lack the proper cytokines and growth factors they require to proliferate. HGF is a very potent mitogen of human hepatocytes and earlier experiments in our lab by Dr. David Mercer using SCID.BG mice and implantable HGF pumps suggest that the administration of human HGF significantly improves the survival of transplanted human cells (94). HGF signal transduction occurs by phosphorylation of the HGF receptor known as C-met. Because the half-life of HGF is several minutes and it is very costly, the authors of this study used an agonistic antibody to C-met (not commercially available) that leads to the phosphorylation of human but not murine C-met. Transplanted NOD/SCID mice were given 50 µg of C-Met antibody intravenously every 2 weeks for the first 57 days after transplant (132) in an attempt to increase the survival and proliferation of the transplanted human cells. They were able to demonstrate that mice receiving C-Met antibody had much higher levels of hAAT in their serum than non-treated, transplanted controls. The serum levels of hAAT measured in the treated mice were between 1 – 10 µg/ml. Mice were followed out for 150 days and serum levels of up to 10⁵ viral genome equivalents of HBV DNA were detected. Transmissibility

from mouse to mouse was also shown in this experiment as was superinfection with Hepatitis D Virus (HDV). The demonstration that HGF stimulation can achieve long-term engraftment of human hepatocytes transplanted under the kidney capsule is encouraging and one must assume that human cells growing in the liver of our mouse model would demonstrate a similar survival advantage if exposed to human HGF.

II. CELL CULTURE MODELS OF HCV:

Along with the need for a robust small animal model of HCV, *in vitro* models are also needed for high throughput screening of antiviral agents. As a result, an enormous amount of research has been done in the area of cell-culture models to support active replication of HCV. Detailed discussion of all of the different *in vitro* models that have been studied is beyond the scope of this thesis, but this next section will attempt to highlight some of the more successful models available. It has been shown that HCV can replicate both in the liver and in peripheral blood lymphocytes and this forms the basis of the many *in vitro* models used to study HCV. We can group these into models using: primary hepatocytes (adult human, fetal human, chimpanzee), hepatoma cell lines, T-cell lines, and B-cell lines.

a) Primary Human Hepatocytes:

HCV replication was demonstrated in cultured hepatocytes obtained from patients infected with HCV by Ito *et al.* in 1996 (7). Both positive and negative strand HCV RNA were detected by RT-PCR in the cultured cells out to 28 days, and the supernatant was used to infect an HCV-negative hepatocyte cell culture to demonstrate infectivity. By comparing the HVR1 sequence variations seen in the cell culture and in the donor patient's serum over time, these authors showed that while changes occurred in the patients serum, no variations were seen in the cell culture over a period of months. This finding lends strength to the hypothesis that HVR1 mutates as a result of pressure from the host immune system.

Iacovacci *et al.* (133) have developed a cell culture of primary fetal human hepatocytes that they have been able to maintain for over 3 months with stable levels of albumin, α -fetoprotein, ApoE and α -1 antitrypsin being produced. Inoculating these cells with HCV positive serum resulted in levels of HCV RNA from 10^3 - 10^5 copies/ ml being detected in the supernatant and in the infected cells 30 days post-inoculation. Tagged RT-PCR was used to demonstrate the presence of negative strand HCV RNA in the infected hepatocytes but not in the original donor serum. Immunofluorescence using recombinant antibodies directed against the E2/NS1 protein demonstrated a low (1 – 3 %) percentage of positive cells.

b) Primary Chimpanzee Hepatocytes:

Lanford *et al.* (134) cultured primary chimpanzee hepatocytes and then infected them *in vitro* with HCV positive serum and assayed the cells for positive and negative strand HCV RNA over a period of 25 days. The negative strand HCV RNA detection was performed using both a tagged primer RT-PCR system and the thermostable RT enzyme (rTth). Positive strand HCV RNA was detectable in the cells from days 1 – 25, while negative strand was not present until day 4 and then persisted until day 25. Treatment of the infected cells with interferon α at various doses resulted in a substantial reduction in HCV RNA as seen by decreased signal on a Southern Blot of the PCR products (134). These authors observed that “during our studies we have screened a number of sera from chronically infected individuals and found that many are not infectious. Infectivity did not correlate with PCR titer in these studies. ... the possibility of neutralizing antibodies in some sera cannot be excluded at this time” (134). It would seem that not all patients with high titers of HCV RNA are equally infectious and this has important implications for our model.

c) Immortalized Tumor Cell Lines:

Many groups have used immortalized tumor cell lines to try to study HCV by primary infection of these cells but the infections are usually transient and low in yield (135). Another approach that has been more successful has been to transfect these cells with HCV RNAs that are transcribed *in vitro* from cDNA clones of the virus. Yoo *et al.*.

(135) have used this approach and were the first to show that HCV RNA produced from cloned HCV cDNA was in fact infectious and replication competent. They constructed full length HCV RNA using a T7 RNA polymerase transcription system and transfected the transcripts into a differentiated human hepatoma cell line (Huh7). The transfected cells were incubated with H^3 -UTP and replication was confirmed by detecting negative strand HCV RNA in the cells and by demonstrating de novo incorporation of H^3 -UTP into the HCV RNA. Levels of HCV RNA seen in the Huh7 culture medium were in the order of 10^4 copies/ml.

Dash *et al.* (136) used a similar approach in a well established hepatoblastoma cell line, HepG2. They used *in vitro* transcribed full length (9.6 kb) and near full-length (9.4 kb) HCV RNA transcripts and transfected these into HepG2 cells. Intracellular HCV RNA was detected by RT-PCR as well as by the ribonuclease protection assay similar to the one developed by Dr. Donna Douglas in our lab. Intracellular HCV RNA levels were estimated to be $10^8 - 10^{10}$ HCV copies per mg of total cellular RNA (infected human liver is reported to have HCV RNA levels of $10^5 - 10^{10}$ molecules per milligram of liver RNA). Immunohistochemistry showed finely granular staining in the cytoplasm of 30-60 % of cells at days 30-50 after transfection. Interestingly, the cells showed significant toxicity over 60 days as evidenced by a decrease in cell density.

An alternative approach to full length HCV RNA transcript transfection was taken by Bartenschlager's group from Mainz, Germany who have developed a system using subgenomic selectable RNAs transfected into Huh7 cells. These authors constructed subgenomic replicons composed of the 5' HCV-IRES, the neomycin phosphotransferase gene (neo), the encephalomyocarditis (ECMV) IRES, and HCV sequences from NS2 or NS3 up to the authentic 3' end (137). These replicons are constructed so that they transduce neomycin resistance only to those cells that support HCV replication. The ECMV IRES directs translation of the HCV sequences from NS2 or NS3 to the 3' NTR. Transfection of these replicons into Huh7 cells resulted in active HCV replication with 10^8 copies per mg total cellular RNA of (+) strand HCV RNA detected and a 5- to 10- fold lower amount of (-) strand HCV RNA. An interesting finding from this study was that the structural proteins and NS2 are not required for replication since cells transfected with replicons containing only the NS3-3'UTR region supported HCV replication. This

group has in fact characterized replicon-harboring cell lines that have been cultivated for longer than 1 year showing no signs of cytopathogenicity. They found that high levels of HCV RNA could be preserved in cells passaged under continuous selection. The fact that the highest levels of HCV RNA were found in exponentially growing cells, followed by a decline in resting cells led them to hypothesize that cellular factors required for RNA replication and/or translation vary in abundance and become limiting in resting cells.

d) T-Cell lines:

Reports of T-cell lines being able to support HCV replication had been published soon after the virus was discovered. Shimizu *et al.* reported in 1992 that the human T-cell line MOLT-4 Ma infected with a murine retrovirus was capable of supporting HCV (138). Cells were inoculated with infectious serum, incubated, and then cultured. Cellular RNA was assayed by RT-PCR for both (+) and (-) strand HCV RNA and the authors reported detection of the both the (+) strand and the (-) strand sporadically for 2-3 weeks. Examination of the supernatant revealed sporadic detection of the (+) strand but not the (-) strand. In situ hybridization was also used to show the presence of (-) strand RNA. This group subsequently reported another T-cell line, HPB Ma which showed HCVRNA in the cells for 76 days after inoculation and in the supernatants for 40 days after inoculation (138). Kato *et al.* (139) used a Human T-Lymphotropic Virus Type 1 Infected Cell line, MT-2, and demonstrated intracellular (+) strand HCV RNA for 15 days post-inoculation and (-) strand HCV RNA for 10 days post-inoculation.

e) B-cell lines:

Shimizu and Yoshikura have studied HCV infection in B-cells using an Epstein Barr Virus (EBV) transformed B-lymphoblast line known as the Daudi cell line (140). They have been able to demonstrate production of infectious HCV in primarily infected Daudi cells and the supernatant for more than 2 years (141). They have also inoculated a chimpanzee with culture supernatant from these cells resulting in an active infection in the chimp with HCV RNA detected by RT-PCR in the serum and liver after 5 and 6 weeks respectively. Interestingly, PBMCs from the chimpanzee were collected on week

7 and were positive for HCV RNA as well. The Daudi cells were originally infected with serum from an infected chimp and the sequences of the HVR1 were compared between the original animal, the Daudi cells and the chimpanzee infected with cell culture supernatant. It was found that the majority sequences seen in the first animal were similar to those seen in the serum and liver of the second chimp, but were different than those seen in the cultured cells. PBMCs recovered from the second chimp however, contained the same sequence as the major one found in cell culture suggesting that perhaps certain quasispecies have different cell tropism.

HYPOTHESIS:

When the SCID/uPA mouse model for HCV was first being developed, human hepatocyte graft function was followed by the detection of human albumin (HA) in mouse serum. A Western blot assay was used and showed the presence of an HA signal in most mice within a few weeks after transplant. With time, however, this signal faded out in all but a very few mice. A major advance for this model was the development of the Southern blot assay by Dr. Bill Addison from Dr. Tyrrell's lab. This assay probes digested mouse DNA for both endogenous and transgenic copies of the uPA gene and compares their ratios using autoradiography. For the first time we were able to reliably distinguish homozygotes from heterozygotes and wildtype mice. When comparing the albumin signal of heterozygotes versus homozygotes post-transplant we observed that the signal in homozygous animals lasted longer (> 12 wks) than the signal in heterozygous animals (6-9 wks). This appeared to be because in heterozygous animals the transplanted human hepatocytes are "competing" with the mouse's own "red nodules" to repopulate the liver. In contrast, since there are very few red nodules in a homozygote liver (two sequential mutational events being necessary to delete both tandem arrays of the uPA transgene in the homozygous animals), the only hepatocytes proliferating are the transplanted human hepatocytes and so these cells are able to repopulate more of the mouse liver. When we determined the zygosity of the first 4 animals that were successfully infected with HCV we found that ALL 4 were homozygotes. To date we have never documented an HCV infection in a heterozygous animal. Even when we began to work exclusively with homozygous animals, we had only sporadic success in attempting to infect these animals with HCV. It was apparent that there was more to achieving successful HCV infections than simply transplanting homozygous animals with human hepatocytes and inoculating them with infectious serum. These observations led us to put forth the following hypothesis:

"Repopulation of a substantial proportion of the liver with human hepatocytes is critical for successful HCV infection in the SCID/uPA mouse."

METHODS:

SCID/uPA Mouse Breeding:

The SCID/uPA mice were originally generated by crossing Alb/uPA transgenic mice with SCID.Bg mice as described by Dr. Mercer (94). The homozygosity of the SCID mutation was verified by measuring mouse IgG levels in the offspring to check for “leakiness”. Mice with serum IgG levels $> 1\mu\text{g/ml}$ were considered to be leaky and not used for further breeding. The beige mutation was not followed during this breeding program. The zygosity of the uPA transgene was determined using a Southern blot assay to compare the ratio of endogenous uPA gene copies to transgene uPA copies. When it became apparent that successful HCV infections were only achieved in homozygous animals, breeding was begun using homozygous animals exclusively. Furthermore, since there may be other important factors affecting the success of this model we selectively bred animals demonstrating a strong graft and a successful HCV infection.

The animals were maintained in a virus & antigen free (VAF) biocontainment facility in accordance with the Health Sciences Laboratory Animal Services (HSLAS) policies at the University of Alberta. The mice were checked daily and detailed records were kept with regards to litter size and neonatal mortality.

In an attempt to decrease bleeding-related deaths in the neonatal period, we treated several pregnant mothers with Cyclokapron (Tranexamic Acid, Pharmacia Upjohn), an antifibrinolytic agent that competitively inhibits the activation of plasminogen to plasmin. Tranexamic acid is 40% absorbed through the gastrointestinal tract and according to the product monograph (Pharmacia & Upjohn) crosses the placenta in humans (142). This was done in an attempt to protect the fetuses in the immediate post-partum period from the harmful effects of elevated serum uPA. The tranexamic acid was added in the drinking water of the pregnant mice (30 mg/ml to deliver daily dose of 150 mg) from the time they were known to be pregnant until the time they delivered. Litter size was recorded for both treated and untreated mice.

Hepatocyte Isolation:

Human liver tissue was collected from the operating theater, immediately flushed with cold Calcium & Magnesium Free Dulbecco's Phosphate Buffered Saline (CMF DPBS, Sigma, #D-5652) containing 0.5 mM EDTA, and then transported back to the lab in this same solution. In the lab the largest one to two vessels on the cut surface of the liver were cannulated with a 14-gauge angiocatheter that was sutured in place with 5-0 Dexon suture. After weighing, the liver tissue was flushed again with 500-1000 cc of cold CMF DPBS with EDTA. Next, the circuit was flushed for several minutes with CMF DPBS without EDTA. It is important to flush all the EDTA out of the circuit since the collagenase is delivered in a solution that contains its essential cofactor calcium. After flushing the EDTA from the circuit, the human liver tissue was perfused with a collagenase solution (67 mM NaCl, 7 mM KCl, 5 mM CaCl₂, 100 mM HEPES) in a recirculating 37 ° C circuit for 60-75 minutes, or until the liver appeared to be well digested. The collagenase used was Liberase HI collagenase (Liberase purified enzyme blend for human islet isolation, Boehringer Mannheim, # 1666 720 provided by Dr. J. Lakey) at a concentration of 0.35 mg/ml. Once digested, the liver capsule was opened with a scalpel and the tissue was gently teased away from the underlying fibrovascular scaffolding with sterile pipette tips. The liberated cells were re-suspended in the collagenase solution and placed in a 37 ° C shaking water bath for 30 minutes. The cell suspension was then poured through 200 µm followed by 80 µm screens to remove large clumps and cellular debris.

The cells were washed twice with Hanks Buffered Salt Solution (HBSS) at 80g for 3 minutes and the supernatant was discarded each time. The cells were then centrifuged through a 1.04 g/ml percoll (Sigma, P-1644) gradient at 400g for 5 minutes. The recovered cells were re-suspended in cold UW solution and the yield and viability were measured with a haemocytometer using trypan blue exclusion. Finally, the cells were either used for transplantation , cryopreserved, or both.

Hepatocyte Cryopreservation:

The cryopreservation protocol used was provided by Dr. Jonathan Lakey and is a modified version of the protocol originally developed for the cryopreservation of pancreatic islets. After hepatocyte isolation the cells were centrifuged at 80g for 1 minute and the UW supernatant was removed. The cells were re-suspended in Freeze/Thaw media (10% fetal calf serum (FCS) + 0.5% penicillin - streptomycin (PS) in M199 media (GibcoBRL)) in a volume of 1cc per 10 million hepatocytes. The cells were aliquoted out into 1 ml volumes (10 million cells) in cryopreservation tubes and kept on ice while 2M DMSO was added gradually over 45 minutes to make up a final molarity of 1.5 M DMSO (11.7 % DMSO). Next, the tubes were transferred to a programmable ethanol freezing bath which was pre-set at -7.4°C . Each tube was then “nucleated” by touching it to a superconducting rod that had been stored in liquid nitrogen. This ensured that the tubes all nucleated at the same time and had a uniform rate of freezing. The temperature in the freezing bath was then lowered at a rate of 1°C per minute until the temperature reached -40°C . Once the cells reached -40°C they were plunged into liquid nitrogen (-196°C). The cells were stored in liquid nitrogen until they were needed for transplantation.

At the time of transplant, the cells were removed from the liquid nitrogen and rapidly thawed in a 37°C water bath. The tubes were then centrifuged at 80g for 1 minute and the supernatant was removed. A sucrose solution (0.75 M) was added, followed by the gradual addition of freeze / thaw medium over 30 minutes. Finally the cells were centrifuged again, the supernatant was discarded, and the cells were re-suspended in cold UW solution. Cell counts and viability were determined with the haemocytometer and trypan blue exclusion.

Hepatocyte Transplantation:

SCID/uPA mice were transplanted between 10-15 days of age. Previously we attempted to transplant the mice at a very early age (4-5 days) in order to achieve better engraftment of human hepatocytes during liver repopulation. However we experienced very high mortality rates with transplantation at this age due to bleeding, splenic rupture, and possibly due to portal vein thrombosis.

All work was done under an operating microscope. The mice were anesthetized in the right lateral decubitus position with halothane (MTC Pharmaceuticals, # 00346314) inhalational anesthetic and a small incision was made in the left flank. The peritoneal cavity was entered and the spleen was mobilized into the wound and grasped with a blunt forcep. The hepatocytes were drawn up into a 27 gauge butterfly needle (Becton Dickinson, # 387212) that was inserted into the inferior pole of the spleen under microscopic guidance. After the cells were injected into the spleen, a titanium clip (Ethicon Endo-Surgery, # LT202) was applied across the inferior pole of the spleen for hemostasis. The abdomen was closed in 2 layers with 6-0 silk sutures and the mice were returned to their cage. For the first night after the procedure the baby mice were placed in a heated incubator as baby mice are very susceptible to hypothermia. Detailed records were kept regarding age of transplant, type of cells transplanted (fresh vs frozen / thawed), and post-operative deaths.

HCV Inoculation:

Once the SCID/uPA mice had been transplanted with human hepatocytes, homozygotes with strong graft signals (as determined by serum assays) were inoculated with serum obtained from HCV- positive patients. The research study was explained to the patients and informed consent was obtained prior to drawing blood. The blood was collected in a heparin-free container since heparin is known to interfere with RT-PCR assays used for HCV RNA quantification. The blood was taken to the lab where it was spun down and the serum was collected for inoculation.

The original protocol devised by Dr. Mercer called for 250 μ l of HCV-positive serum to be injected into the jugular vein of 5-6 week old SCID/uPA mice. The Health Science Laboratory Animal Services (HSLAS) recommendation is to never inject more than 100 μ l of volume intravenously into an adult mouse as large volume boluses injected intravenously into small animals can be fatal. Early in our studies we observed several deaths following inoculation of 250 μ l into the jugular vein of 5-6 week old SCID/uPA mice. Presumably this was due to acute right-sided heart failure, or to inadvertent cannulation of the internal jugular artery and delivery of a large serum bolus to the cerebral circulation. Another concern was that this route of inoculation potentially

compromises the internal jugular vein that is the site for serial blood collection in these animals. Because of these problems, mice were inoculated with intraperitoneal (IP) injections of infectious serum and it has been shown that these mice can successfully be infected by this route with as little as 20 μ l of serum (data shown later). Currently, 50 μ l of infectious human serum delivered IP is used to inoculate these mice. Only fresh (versus frozen / thawed) serum is used for inoculation – the reason for this will be presented in a later section

Mice are currently inoculated mice 8 weeks after transplant. This age was chosen for 2 reasons. The first is that, as will be shown later, mice with successful grafts seem to have maximal graft function between 8-12 weeks post-transplant. This is in accordance with the original experiments using the uPA mice where investigators found the liver to be > 90% replaced by transplanted hepatocytes between 10-14 weeks post-transplant in homozygote animals (98). Since we hypothesize that a substantial mass of viable human hepatocytes must be engrafted to support an HCV infection, we reasoned that waiting until 8 weeks post-transplant would likely correspond to a high enough amount of chimerism in the liver for the HCV inoculation to be successful

Western Blot Assay:

The Western blot assay for human albumin (HA) has been previously described in detail by Dr. Mercer (94). Serum (20 μ l) from transplanted mice and from a non-transplanted negative control mouse was immunoprecipitated overnight with a monoclonal mouse antibody specific for HA (clone HSA-9, Sigma, # A-2672) and Protein G agarose beads (Boehringer-Mannheim, #1243233). After washing, the captured protein was then released from the beads by heating in a reducing buffer (20% glycerol, 14mM sodium dodecyl sulphate (SDS), 200mM dithiotreitol (DTT) and bromophenol blue) and loaded onto a 7.5% polyacrylamide gel. A positive control consisting of 1.25 ng of human albumin (HA) was loaded in the first lane of the gel. Following electrophoresis, the protein was transferred onto a nitrocellulose membrane (Schleicher & Schueler, # 10402599) and probed with a biotinylated monoclonal antibody specific for the reduced epitope of HA (clone HSA-11, Sigma, # A6684). Horseradish peroxidase linked to streptavidin (SA-HRP) was added and a signal was

generated by treating with a chemiluminescent solution (SuperSignal Chemiluminescent substrate, Pierce, # 34080). Film (Biomax ML, Kodak, # 868 9358) was exposed to the membrane and developed in a dark room. Figure 4 shows a sample Western blot.

Quantitative Dot Blot Assay:

Although the Western blot assay provided information about whether or not a given mouse was producing HA post-transplant, it did not allow quantification of HA in the serum of a given mouse nor comparison of the levels of serum HA between 2 mice. The need to somehow quantify the amount of human proteins being produced by the human hepatocyte xenograft prompted development of the quantitative dot blot (DB) assay for human albumin. The quantification was performed by generating a standard curve from known concentrations of Human Albumin (HA) diluted in blank (non-transplanted) mouse serum. By expressing the standard curve in the form of an equation, the concentration of HA in transplanted mice was calculated from the linear portion of this curve.

The standards used in the DB assay were made by diluting known amounts of HA (Sigma, # A-1887) in blank mouse serum. Initial experiments revealed that the linear range for the DB assay lies between 25 $\mu\text{g/ml}$ and 800 $\mu\text{g/ml}$ of HA in mouse serum. The set of standards of HA in mouse serum were made by serially diluting the 800 $\mu\text{g/ml}$ concentration 1:1 down to 400, 200, 100, 50, and 25 $\mu\text{g/ml}$ in blank mouse serum. At concentrations greater than 800 $\mu\text{g/ml}$, the standard curve plateaus, and protein begins to run over the membrane away from the blotted area, signifying that the binding capacity of the nitrocellulose membrane (Schleicher & Schuell, pore size 0.45 μm , # 10402599) is maximized. The binding capacity of this membrane is reported by the manufacturer to be 80 μg of protein / cm^2 . The 2 μl blots diffuse out to cover an area of 0.28 cm^2 which should be able to bind a maximum of 22.6 μg of protein.

The standards and serum from transplanted mice were first diluted in a reducing buffer (as in Western blot assay) and heated at 100° C for 5 minutes. This was done because the biotinylated monoclonal antibody for HA that was used (clone HSA-11, Sigma, # A6684) specifically recognizes the reduced epitope of HA. After cooling, 2 μl of each of the samples / standards was blotted by hand onto a piece of dry nitrocellulose

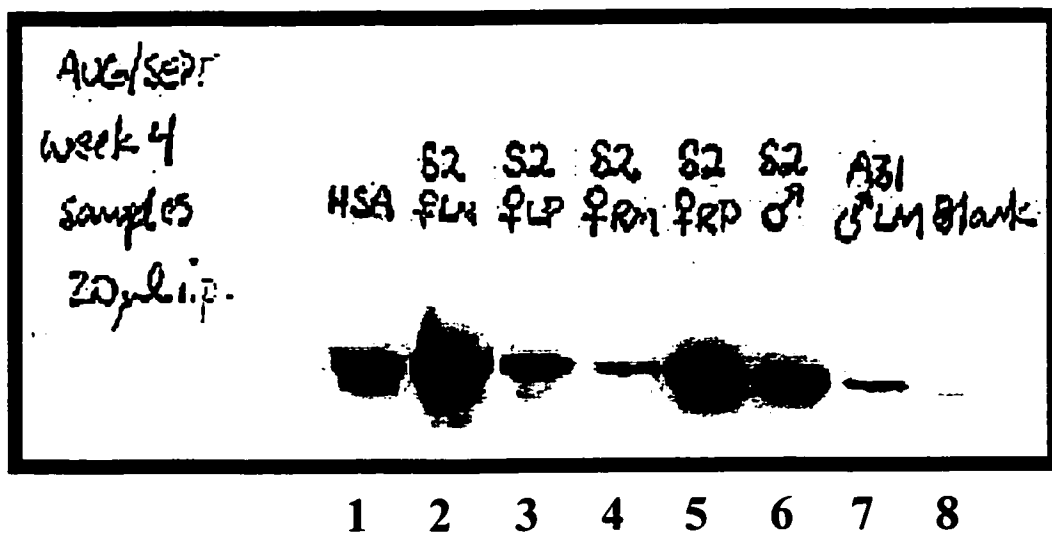


FIGURE 4. Sample Western blot. Western blot assay with positive human serum albumin (HSA) control in lane 1; SCID/uPA mice at 4 weeks post-transplant in lanes 2-7; Negative control = non-transplanted mouse in lane 8. Western blot signals are designated as strong (+++), moderate (++), or weak (+). Mice in lanes 2, 5, 6 have +++ signals. The mouse in lane 3 has a ++ signal. Mice in lanes 4 and 7 have + signals.

membrane in triplicate and allowed to dry for 10 minutes. After drying, the membrane was soaked in a transfer buffer (25 mM TRIS base, 200 mM glycine, 20% v/v methanol) for 20 minutes. The membrane was blocked with 3% phosphate buffered solution / Tween-20 (PBST) for 1 hour which non-specifically blocks free binding sites on the membrane. Next the membrane was covered with a 1:5000 dilution of the biotinylated primary antibody (HSA-11) diluted in 0.5 % PBST and placed on a shaking plate for 2 hours. After three 20 minute washes with 1 % PBST, the membrane was probed with SA-HRP diluted 1:10000 in 0.1% PBST for 2 hours. After six 10 minute washes with 0.1 % PBST the membrane was treated with ECL-PLUS chemiluminescent solution (Amersham Pharmacia Biotech, # RPN 2132) for 2 minutes and the fluorescent signal was detected and quantified using the STORM 860 fluoro/phosphoimager with the Image Quant software package (Molecular Dynamics, Sunnyvale, California) .

The average fluorescent readout was calculated for each set of triplicate blots, and a standard curve was generated by plotting the fluorescent readout for the standard solutions against the log of the HA concentration. The concentration of HA in transplanted SCID/uPA mouse serum was calculated off of this curve. Figures 5 and 6 show a sample dot blot membrane and the corresponding standard curve.

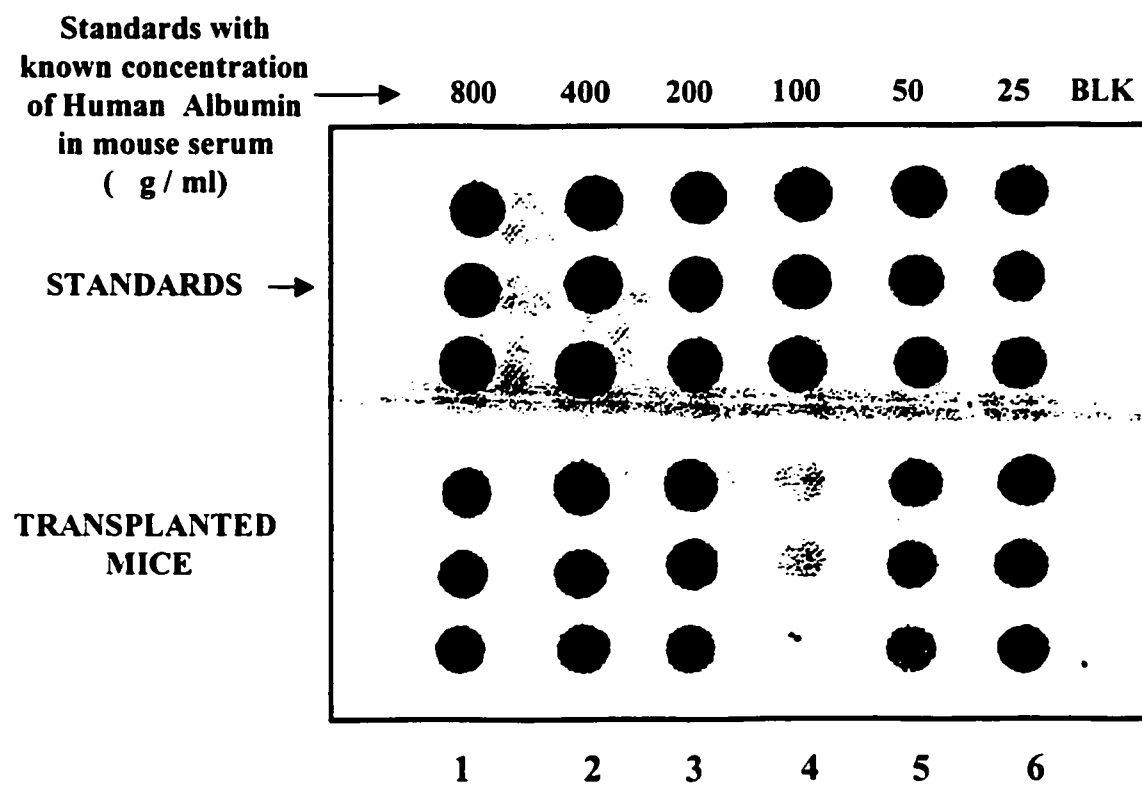


FIGURE 5. Sample Dot Blot Membrane. Standards with known concentrations of Human Albumin (HA) in mouse serum are blotted in triplicate across the top of the membrane. Serum samples from transplanted mice are blotted across the bottom (1-6). Non-transplanted mouse serum serves as a negative control (BLK).

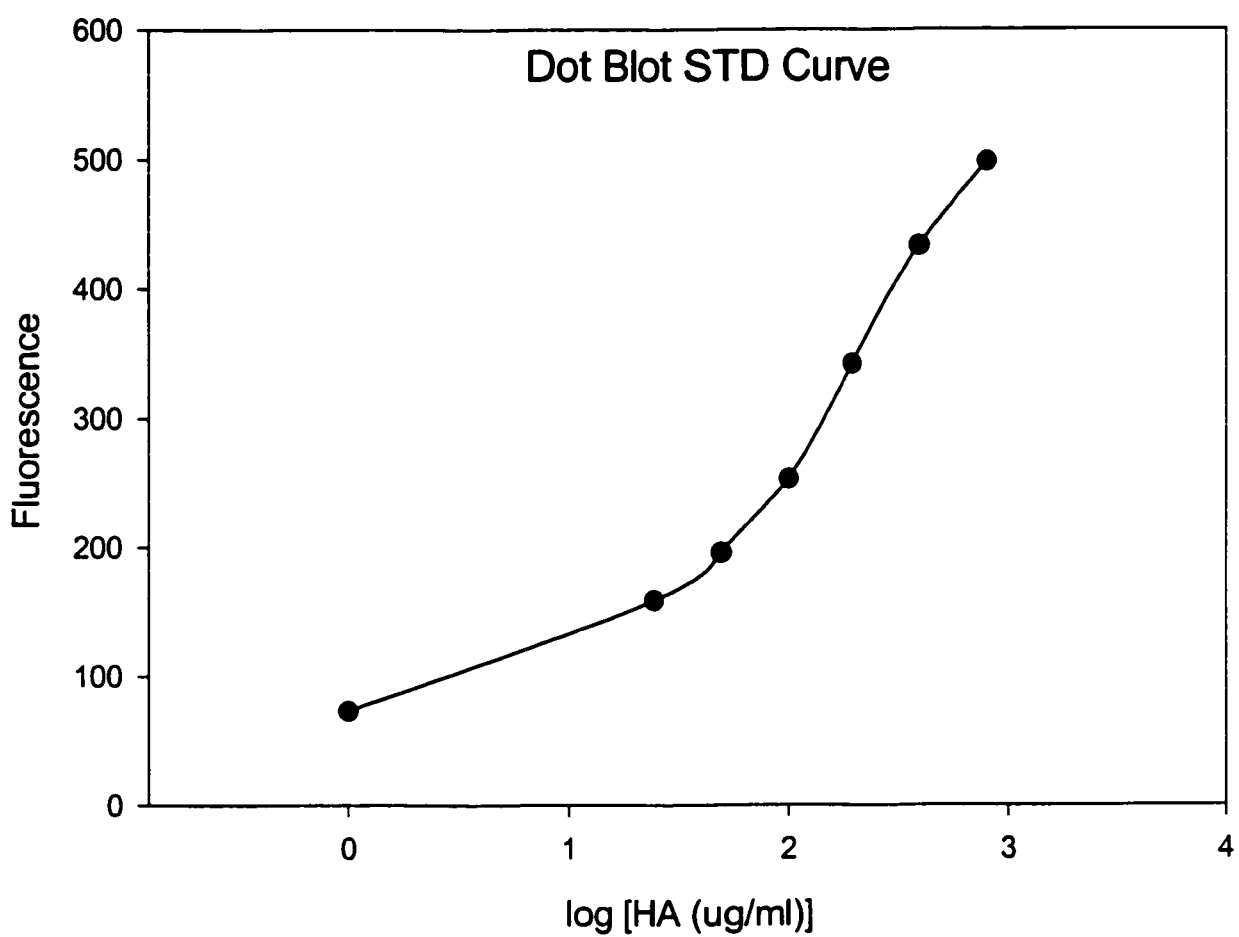


FIGURE 6. Typical Dot Blot Standard Curve. Sample standard curve generated from dot blot assay. Y-axis is average fluorescent readout from STORM 860 for each standard concentration. X-axis is log [concentration of HA in g / ml of mouse serum].

Quantitative ELISA Assay for Human Alpha-1 Antitrypsin (hAAT):

Human Alpha-1 Antitrypsin (hAAT) ELISA – Antibody preparation:

Since the DB assay has many steps that make it prone to run-to-run variability, a means of quantifying human proteins in SCID/uPA mice was sought in the form of an ELISA assay. A literature search revealed several groups that had published quantitative human alpha-1 antitrypsin (hAAT) assays (130)(132) in mouse models, and a research group at Stanford was contacted. Dr. Leonard Meuse kindly provided an outline of their hAAT ELISA protocol. The antibody used in this assay was a polyclonal goat-anti-hAAT antibody (Diasorin, # 81902) which served as both the capture antibody AND the detection antibody in a sandwich ELISA. In order to prepare the antibodies, the azide preservative was first dialyzed out of the antibody solution using 12,000 – 14,000 MW dialysis tubing into a 50 mM K_2HPO_4 dialysis buffer (pH 8.0). Part of the antibody at this stage was aliquoted and frozen to be used as capture antibody, while the remainder was linked to horseradish peroxidase (HRP) using a commercially available HRP-linking kit (EZ Link Plus Activated Peroxidase Kit, Pierce, # 31489) following manufacturers directions. After HRP-linking, the secondary antibody was dialyzed into a 50 mM NaH_2PO_4 buffer (pH 6.8) containing the preservative Thimerosal (0.2%) (Sigma, # T-5125).

hAAT ELISA Protocol:

The wells of a 96-well microtiter plate (Costar, # 3590) were coated with 50 μ l of the capture antibody diluted 1:1000 in coating buffer (0.1 M $NaHCO_3$ pH 9.5). The shipped antibody was measured by spectroscopy to be at a concentration of 20 mg/ml after the first dialysis step, so 50 μ l of a 1:1000 dilution corresponded to 1 μ g of antibody which represents the maximum amount that can be bound to the solid phase of most plastic wells (143). The plate was incubated overnight at 4° C, washed once with tris buffered saline / 0.05% v/v Tween 20 (TBST), and then blocked overnight with TBST containing 5% non-fat dry milk. After blocking, the plate was washed twice with TBST, and the standards / samples were added to the wells. The standard for this assay consisted of a commercially available aliquot of hAAT (Calibrator 4, Diasorin, # 84402) that was

diluted to concentrations from 100 ng/ml to 0.76 ng/ml in milk buffer. The first 2 columns of the plate were reserved for the diluted standards and the remaining columns were used for the SCID/uPA mouse sera. The SCID/uPA mouse serum was diluted 1:100 in the first well of each column with serial 1:3 dilutions in blocking buffer made down the plate resulting in dilutions of 1:100, 1:400, 1:1600, 1:6400 etc. Serum from a non-transplanted mouse was included as a negative control. After 2 hours of incubation with the standards / samples, the plate was washed three times with TBST and then the HRP-linked secondary antibody was added at a 1:300 dilution in milk buffer for 2 hours. The substrate used to react with the HRP to produce a color change in this assay was 3,3',5,5'-Tetramethylbenzidine (TMBD, Sigma, # T-3405). After washing 3 times with TBST the TMBD solution was added to the wells in timed additions and the reaction was allowed to proceed for 5-7 minutes. The reaction was stopped by timed additions of 1 M H_2SO_4 and then the plate was read using an ELISA plate reader at 450 nm. A standard curve was generated as for the dot blot assay, and the concentrations of hAAT in the SCID/uPA mouse samples were calculated. Figure 7 shows a sample ELISA plate readout and the corresponding standard curve.

	BLK 1	QAL 2	CAL 3	M1 4	M2 5	M3 6	M4 7	M5 8	M6 9	M7 10	M8 11	BALB/c 12
A	0.081	0.444	0.401	0.501	0.128	0.510	0.447	0.481	0.452	0.433	0.432	0.079
B	0.084	0.361	0.371	0.481	0.103	0.515	0.465	0.527	0.426	0.293	0.403	0.087
C	0.079	0.299	0.279	0.459	0.111	0.483	0.449	0.475	0.334	0.138	0.315	0.098
D	0.075	0.198	0.213	0.414	0.083	0.397	0.293	0.344	0.176	0.118	0.171	0.090
E	0.068	0.151	0.140	0.198	0.070	0.247	0.163	0.212	0.100	0.091	0.118	0.107
F	0.065	0.120	0.108	0.124	0.084	0.140	0.108	0.140	0.123	0.085	0.084	0.101
G	0.075	0.098	0.122	0.090	0.087	0.100	0.109	0.098	0.080	0.081	0.112	0.111
H	0.085	0.089	0.082	0.081	0.058	0.075	0.073	0.057	0.071	0.090	0.070	0.088

— STDS — SCID/uPA mice —

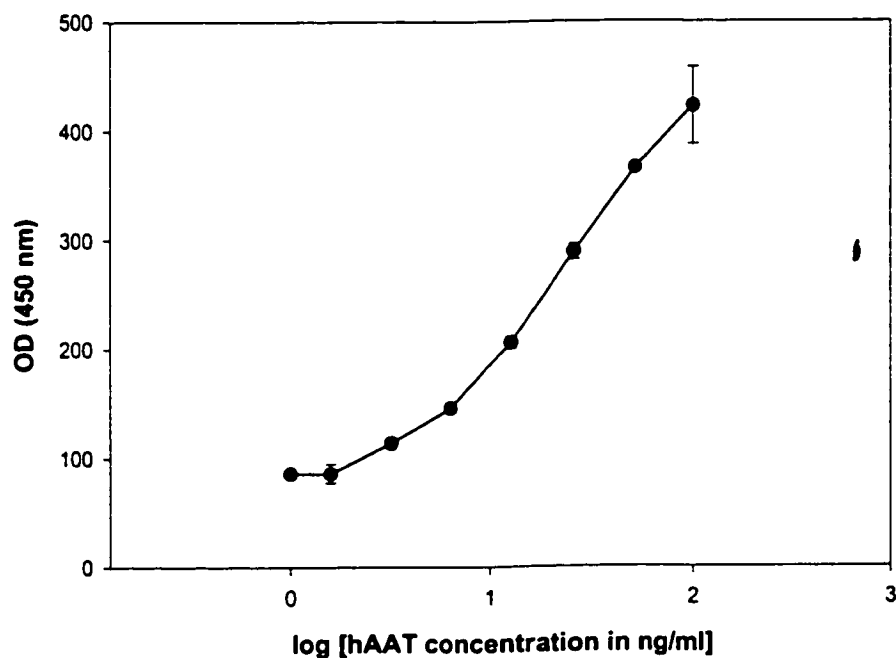


FIGURE 7. Sample hAAT ELISA plate & Standard Curve: a) ELISA plate: Columns 2 & 3 represent Standards with hAAT concentrations from 100 ng/ml down to 0.76 ng/ml (1:1 dilutions). Mouse samples are diluted 1:100 in row 1 and serially diluted 1:3 down the plate. Column 1 is blank. Column 12 represents a non-transplanted BALB/c mouse. Dilutions of mouse serum that correspond to the most linear portion of the standard curve are circled. b) Sample standard curve generated from Standards in columns 2,3. The Y-axis is the Optical Density (OD) readout for the wells in the standard lanes (450 nm). The X-axis is log [serum concentration of hAAT in ng/ml]. Error bars represent Standard Error (SE).

Mouse IgG ELISA for SCID Leakiness:

Serum from SCID/uPA mice was assayed for levels of mouse IgG using an ELISA protocol provided by Dr. G. Korbitt. There are different definitions of leakiness reported in the literature but the most widely used definition is a level of serum IgG > 1 µg/ml. The multi-well plate was first coated with a sheep anti-mouse IgG capture antibody (ICN, # 55485) diluted 1:1000 in coating buffer (50mM NaHCO₃, pH 9.5) and incubated overnight. After washing with TBS / 0.1% Tween-20 (TBST), wells were blocked with PBS / 2% bovine serum albumin (BSA) for 1 hour and then washed again. The standard (purified mouse IgG1, ICN, # 50327) was serially diluted 1:2 down the plate starting with a dilution of 1:10,000. The mouse samples were serially diluted down the plate 1:2 starting with a dilution of 1:100 in the first row. PBS / 1% BSA was used as the diluent. After incubation and washing, the secondary antibody consisting of HRP-linked-sheep anti-mouse-IgG antibody (ICN, # 55558) was added for a 2 hour incubation. The substrate o-Phenylenediamine (OPD, Sigma, # P-1526) was added and the reaction was allowed to run for 10 minutes before the plate was read at 490 nm. A standard curve was generated and the appropriate calculations were made.

Immunohistochemistry:

Immunohistochemistry was performed in an attempt to demonstrate two important features in the chimeric livers of the SCID/uPA mice. The first objective was to be able to clearly and reliably differentiate human from mouse hepatocytes in the livers of chimeric SCID/uPA mice. Moderate success was achieved in this area thanks to Dr. Chunhai Hao from the department of Pathology. The second goal was to demonstrate clearly and reliably the presence of HCV antigens within human hepatocytes in the livers of HCV-infected mice. Limited success was achieved in this endeavor.

Staining Human Cells in Mouse Liver:

The first technique that was utilized to demonstrate the presence of human cells in our SCID/uPA mouse livers involved staining cryostat sections of liver with a biotinylated antibody specific for human MHC class I antigen. The antibody used was a monoclonal antibody expressed in the cell line BB7.7 (ATCC HB 94). Because it was

believed that MHC class I antigen would not be preserved by formalin fixation, liver samples were stored in frozen specimen embedding medium (Cryomatrix, Shandon, #6769006) at -20°C. After many months of negative results despite the support provided by Dr. G. Korbitt's lab this approach was eventually abandoned and a collaboration was developed with Dr. Chunhai Hao from the department of Pathology, University of Alberta Hospitals. Using both frozen and formalin-fixed tissue sections, numerous commercially available antibodies to human liver derived proteins were tested and many of them seemed to cross react with the background mouse tissue. Finally Dr. Hao found a monoclonal mouse antibody specific for human hepatocytes (Clone OCH1E5, DAKO, # M 7158) hereafter referred to as OCH1E5. This antibody works best on formalin fixed tissues and gives very clear demarcation between human nodules and background mouse liver. Non-transplanted mouse liver was used as a negative control.

Five micrometer sections of paraffin-fixed tissue were mounted on glass slides. The slides were heated at 60°C for 10 minutes and then deparaffinized with xylene and rehydrated through absolute ethanol, to 90% ethanol, to 70% ethanol, and finally to water. Next the slides were placed in a solution of hydrogen peroxide and methanol for 6 minutes to quench the endogenous peroxidases. After pre-treatment with the proteolytic enzyme pepsin to "unmask" the antigens, the slides were counterstained with hematoxylin, and then blocked with 20% normal goat serum for 15 minutes. The OCH1E5 antibody was applied at a 1:10 dilution and then a biotin-labeled secondary antibody directed against mouse IgG was added. Finally, an HRP-linked-avidin-biotin complex was added which binds to the secondary antibody, and the substrate 3,3',-diaminobenzidine tetrahydrochloride (DAB) was added to generate a brown colored signal.

Percent chimerism in the liver was estimated by viewing 1-4 sections of each liver sample under 2.5 X magnification and quantifying the percent of human tissue in 10 random microscopic fields. These results were averaged to get a rough estimate of percent human chimerism. Microscopic images were captured using a camera (Coolsnap, Roper Scientific Photometrics) mounted onto a microscope (HBO 100, Zeiss) and quantification was performed using the software package IP LAB, version 3.2 (Scanalytics Inc, Fairfax, VA).

Detection of HCV Antigens in Mouse Liver:

A monoclonal mouse antibody specific for the C-100 protein product of the NS3/4 region of the HCV genome (TORDJI-22, BioGenex) was used to detect HCV antigens in the liver of infected SCID/uPA mice. Slides were prepared from formalin fixed, paraffin embedded tissues. The immunohistochemistry protocol used was as described above using the TORDJI-22 antibody at a 1:50 dilution as the primary antibody. An anti-mouse IgG antibody was used as the secondary antibody with DAB as the colorimetric detection substrate.

Comparing the Dot Blot and hAAT ELISA Assays

Once the two quantitative serum assays had been developed, they were used to follow a series of 21 mice that were generated from homozygote x heterozygote matings. Thus all 21 mice were either heterozygous (n=6) or homozygous (n=15) for the uPA transgene. The mice were transplanted at 10-12 days of age with 5×10^5 cryopreserved human hepatocytes from the same human donor. The mice were randomly divided into 3 groups and followed for 3, 6, and 12 weeks post-transplant (PT) before being sacrificed. Blood was collected at various timepoints and at sacrifice the liver was harvested. The serum was analyzed using the dot blot assay for human albumin (HA) and the ELISA assay for human alpha-1 antitrypsin (hAAT). Immunohistochemistry was performed using the OCH1E5 antibody against human hepatocytes. IgG levels were also measured on all the mice where serum was available to check for leakiness. The results of the two quantitative assays for each available sample were compared in a scatter plot (ELISA value on Y-axis versus dot blot value on X-axis, 38 samples) and the Spearman rank correlation coefficient was calculated. Figure 8 illustrates the experimental design.

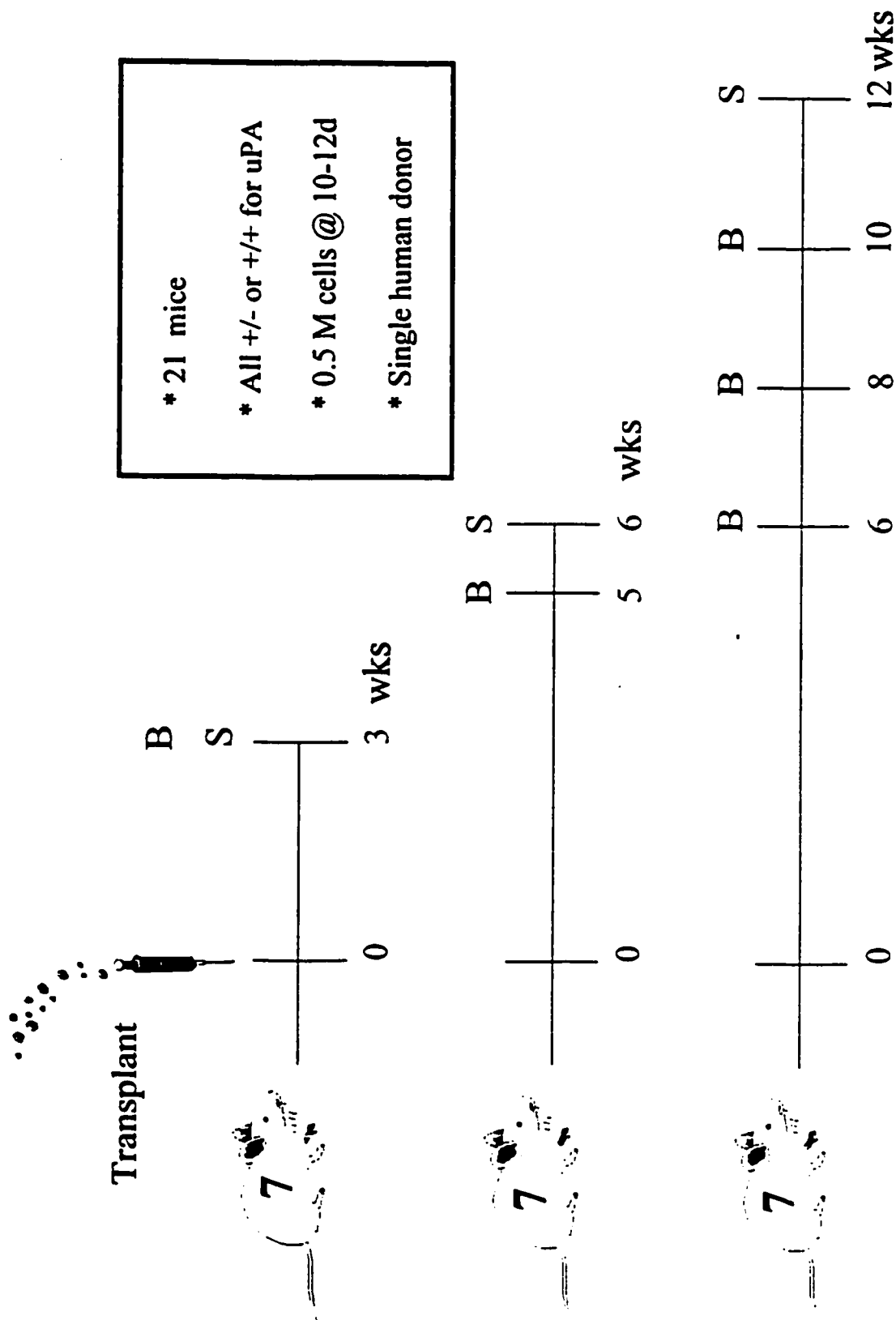


FIGURE 8: 21 mice transplanted at 10-12 days, followed for 3, 6, 12 weeks before sacrifice. B= blood collection; S=sacrifice

Correlation of Graft Success with Fresh versus Frozen Hepatocytes

A total of 162 homozygous animals were transplanted as previously described, and had serum drawn at 4 weeks post-transplant for dot blot (DB) Analysis. The result of the 4 week DB assay was compared for mice who had received fresh versus frozen hepatocytes. Statistical analysis was performed using SPSS 10.

Correlation of Graft success versus HCV Infection success

Of the 162 animals described above, 63 mice were inoculated with serum from HCV-positive patients between 5 and 10 weeks post-transplant. Mice with a 4 week serum DB signal greater than 200 µg/ml were compared to those with signals below this level in terms of whether or not they were successfully infected with HCV as determined by serum RT-PCR analysis. This analysis was also repeated using a serum DB signal cutoff of 250 µg/ml. All RT-PCR analysis was performed by the Provincial Laboratory at the University of Alberta Hospital using the Cobas Amplicor kit (Roche Diagnostics) (qualitative RT-PCR) or the Cobas Amplicor HCV Monitor v2.0 (Roche Diagnostics) (quantitative RT-PCR). The assays were performed following manufacturer instructions provided by the manufacturer. Statistical analysis was performed using SPSS 10.

Correlation of HCV Infection Success with Fresh versus Frozen Serum Inoculation

A total of 59 transplanted mice with 4 week serum DB signals greater than 200 µg/ml HA were inoculated with either fresh or frozen serum from HCV-positive patients. Success of HCV infection as determined by RT-PCR analysis was compared in mice receiving fresh serum versus mice receiving frozen serum. This analysis was also repeated using a serum DB signal cutoff of 250 µg/ml. Statistical analysis was performed using SPSS 10.

Long Term Follow Up of Infected SCID/uPA mice

Four homozygous siblings were transplanted at 12 days of age with 5×10^5 fresh human hepatocytes as previously described. Seven weeks post transplant these animals were inoculated via intravenous injection with 250 μ l of freshly collected HCV-positive serum. Serum was collected for quantitative HCV analysis starting at 1 week post-inoculation, and for graft signal quantification starting at 7 weeks post-inoculation (14 weeks post-transplant). At 29 weeks post-transplant, all four mice underwent a partial hepatectomy under general anesthesia. The liver tissue was fixed in formalin and studied using the immunohistochemical techniques previously described.

Demonstration of Transmissibility

Some of the critics of this model have suggested that perhaps the HCV RNA that is measured in the serum of these animals is simply carry over from the inoculum of infectious serum and that the virus is somehow "associated" with the human hepatocyte graft but not actually replicating in these mice. Once the quantitative assays allowed selection of animals with strong grafts, transmissibility was demonstrated in this model in response to these criticisms. Mice were initially infected with serum from an HCV-positive patient. Once infection was documented, the mice were either phlebotomized, or in a few cases sacrificed, and their serum was used to inoculate another mouse that had demonstrated a strong graft signal by analysis of serum HA level. This was repeated in up to three successive mice.

Effects of Interferon alpha Administration in HCV Infected SCID/uPA mice

Interferon alpha (IFN α), in combination with ribavirin, is currently the best available form of medical treatment for patients with chronic HCV. Researchers at Albert Einstein College of Medicine (Bronx, NY), using a RAG/uPA mouse model of WHV have demonstrated that treatment with IFN α -2b @ 135 IU/g/day IM for 15 days resulted in a significant decrease in the levels of WHV DNA in their model (129). We studied the effects of IFN α -2b (Schering, # 02238674) treatment in HCV-infected SCID/uPA mice. The study animals all had successful human hepatocyte engraftment (as evidenced by DB signals > 200 μ g/ml at 4 weeks PT), and were inoculated with HCV-positive serum at 8

weeks PT. Eight mice were infected with genotype 3a, while the remaining seven mice were infected with genotype 1b. The treatment groups consisted of: sham saline injections (n=5), 135 IU/g/d of IFN α -2b (n=1) and 1350 IU/g/d of IFN α -2b (n=9) and treatment duration was 2 weeks. At the start of treatment, end of treatment and 2 and 4 weeks after the end of treatment, blood was collected for analysis of graft function (hAAT ELISA) and for quantification of HCV RNA by RT-PCR. Figure 9 illustrates the Interferon experiment.

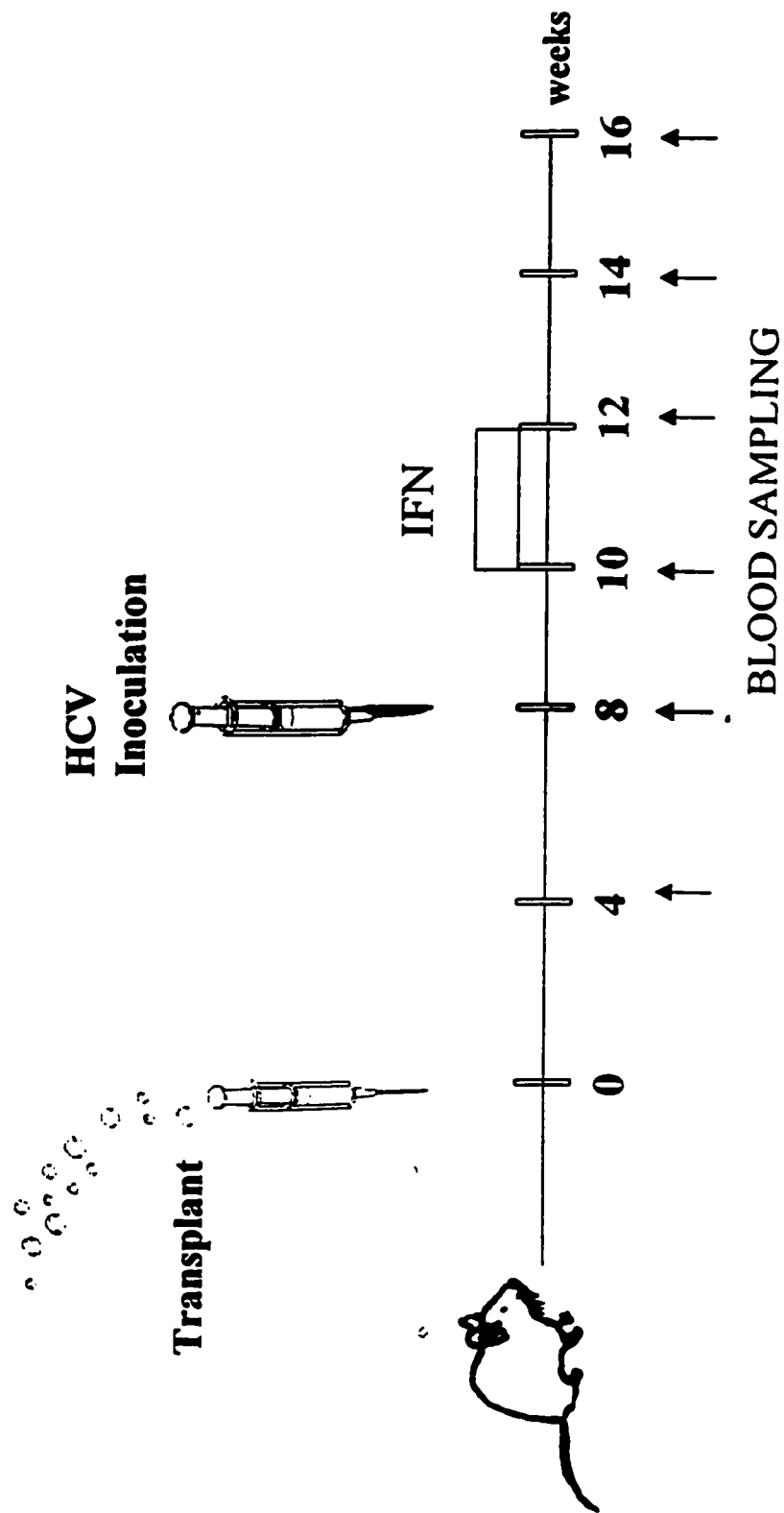


FIGURE 9: Transplanted mice with strong graft signals are inoculated with HCV at 8 weeks post-transplant (PT). At 10 weeks PT, mice are treated with: (a) normal saline, (b) IFN 135 IU/g/d or (c) IFN 1350 IU/g/d for 14 days. Serum is collected and levels of HCV RNA are measured using RT-PCR analysis.

RESULTS:

I. SCID/uPA Mouse Breeding:

The results of our colony production and transplant activities have been analyzed from February 2000 to March 2001. The average litter size was 5.7 (+/- 2.4, SD). Of the 477 mice born during this period, 362 survived to transplant age, giving a neonatal mortality rate of 25%. Occasionally mother mice cannibalized their entire litters which skewed the neonatal mortality somewhat. If we remove cases where the entire litter was found missing or dead, the neonatal mortality decreases to 12 %.

Comparison of litter size from 4 pregnant mothers treated antepartum with tranexamic acid versus 8 untreated mothers is given in Table 1.

TABLE 1 – EFFECT OF ANTEPARTUM TRANEXAMIC ACID ON SCID/uPA LITTER SIZE

Treated with Tranexamic Acid (Litter size)	Not Treated (Litter size)
6	2
1	7
7	5
3	4
	6
	8
	8
	5
AVG = 4.3 +/- 2.4 (SD)	AVG = 5.6 +/- 1.9 (SD)

II. Hepatocyte Isolation

Table 2 summarizes the results in hepatocyte isolation from March 30, 2000 until April 6, 2001. Only isolations for which all the required information was available were included. Note that warm ischemia time represents the time the liver tissue was not being perfused while still in the patient (i.e. clamp time). Cold ischemia time represents the time from when we collected the liver tissue in the operating theater until the collagenase perfusion was begun. One isolation was from part of a donor liver from a 9 year old boy being transplanted into a 1 year old child. The liver had been harvested, flushed with cold UW and kept on ice overnight which is why the cold ischemia time is documented as 10 hours = 600 minutes. This value was not included in the calculation of average cold ischemia time as it is a distant outlier.

III. Hepatocyte Cryopreservation

Table 3 shows the results from cryopreservation and thawing of isolated human hepatocytes. Hepatocytes were cryopreserved either the same day that they were isolated (S) or the next day (N) after overnight storage in cold UW solution. The post-thaw viability for cells frozen on the same day was superior compared to cells frozen after storage in cold UW solution overnight (68.6 % \pm 13.6% vs. 48.2 % \pm 15.2%, $p=0.041$ by Mann-Whitney test). The pre-cryopreservation viabilities were similar for both groups (82.4 % \pm 4.4 % vs. 84.8% \pm 8.6%, $p=0.383$ by Mann-Whitney test). Similarly the percent of cells recovered (number of viable cells upon thawing / number of viable cells frozen) was found to be higher on in the same-day group versus the next-day frozen group (0.6 \pm 0.1 vs 0.4 \pm 0.2, $p=0.02$ by Mann-Whitney test).

TABLE 3
SUMMARY OF CRYOPRESERVATION / THAW RESULTS

Same (S) or Next (N) Day Freeze	Number of Viable cells Frozen (Million)	Cell Viability Before Freeze (%)	Number of Viable Cells Recovered (Million)	Percent Yield Recovered (%)	Cell Viability Post-Thaw (%)
S	20	85	7.2	0.36	75.0
S	20	85	8.9	0.45	89.0
S	20	84	12.5	0.63	63.0
S	44	86	10	0.23	68.0
S	20	72	14	0.7	75.0
S	40	72	33	0.83	65.0
S	40	81	17	0.43	70.0
S	20	83	11.7	0.59	85.0
S	40	82	34	0.85	68.0
S	60	82	40	0.67	72.0
S	20	82	13.5	0.68	63.0
S	42	86	30	0.71	72.0
S	30	82	29	0.97	68.0
S	42	86	11.4	0.27	27.0
MEAN		82		0.6	68.6
SD		4.4		0.2	13.6
N	20	78	4.5	0.23	50.0
N	68	93	37	0.54	45.0
N	30	84	8.7	0.29	79.0
N	35	70	10.5	0.3	46.0
N	102	93	36	0.35	29.0
N	20	91	8	0.4	40.0
MEAN		84.8		0.4	48.2
SD		8.6		0.1	15.3

IV. Hepatocyte Transplantation:

Mortality associated with the transplant procedure was 12.3 %, with most of these deaths occurring in the first 48 hours post-transplant. Presumably most of these deaths were bleeding or anesthetic related but some deaths may have also been caused by the mother mouse either killing the babies or neglecting them post-op and refusing to let them nurse. Previously when we attempted to transplant mice at 4-5 days of age we observed a higher mortality rate, mostly due to splenic rupture and bleeding. Interestingly in several cases where we attempted to transplant mice at a much older age (>16 days old) we also saw a higher mortality rate that may have been anesthetic related.

V. Correlating the Dot Blot and hAAT ELISA Assays:

Serum Assays:

Table 4 shows the results of the serum assays for the 3 groups of mice that were followed with the dot blot and ELISA assays. One mouse from group 3 died after the 8 week blood sampling. All other mice survived until sacrifice. As seen in Table 4, the results from the Western blot do not correlate well with the other two assays. Mice who were found to have very low levels of serum human proteins still demonstrated signal on the Western blot. This is likely because the Western blot assay uses such a large volume of serum (20 μ l) and overloads the nitrocellulose membrane (See Figure 10). Table 5 was generated by grouping the quantitative serum assay results for homozygotes and heterozygotes at each time point. The results from table 5 are graphically represented in Figures 11 and 12. The correlation between the dot blot and ELISA assays is seen in Figure 13. Both serum assays showed the following trend: a) at 3 weeks PT the average graft signal was similar in both groups, b) as the mice get older, the average graft signal in the heterozygote group decreased to barely detectable levels whereas the homozygotes maintained a strong signal, and c) the average level of serum human albumin measured in the heterozygote group was always less than 200 μ g/ml.

TABLE 4
COMPARISON OF THREE DIFFERENT ASSAYS FOR HUMAN
PROTEINS IN THE SERUM OF TRANSPLANTED SCID/UPA MICE

Group 1		3 w Wtara	3 w DB	ELISA										
Mouse		(ug/ml)	(ug/ml)	(ug/ml)										
ARM (H)		+++	125	15										
AmLP (H)		+++	71	18										
BIRP (H)		++	< 25	22										
CIRA (H)		++	< 25	LO										
CIRBoh (h)		+++	47	10										
DIRA (H)		+++	109	19										
DmLP (H)		+++	35	5										
Group 2		5 w Wtara	5 w DB	5 w ELISA	6 w Wtara	6 w DB	6 w ELISA							
Mouse		(ug/ml)	(ug/ml)	(ug/ml)	(ug/ml)	(ug/ml)	(ug/ml)							
AmLA (H)		+++	1863	139	+++	1472	306							
ARA (h)		+++	303	32	+++	221	13							
BIRN (h)		++	47	3	+++	< 25	1							
CmBoh (H)		+++	176	12	+++	304	39							
CULM (H)		+++	203	26	+++	434	38							
DmLM (H)		+++	217	17	+++	374	38							
DIRM (h)		+++	67	3	+++	52	2							
Group 3		6 w Wtara	6 w DB	6 w ELISA	8 w Wtara	8 w DB	8 w ELISA	10 w Wtara	10 w DB	10 w ELISA	12 w Wtara	12 w DB	12 w ELISA	
Mouse		(ug/ml)	(ug/ml)	(ug/ml)	(ug/ml)	(ug/ml)	(ug/ml)	(ug/ml)	(ug/ml)	(ug/ml)	(ug/ml)	(ug/ml)	(ug/ml)	(ug/ml)
AmLM (h)		+++	200	15	+++	99	6	+++	36	3	+++	< 25	2	
AIRP (h)		+++	99	7	+++	NES	NES	+++	NES	1	++	< 25	2	
BmLP (H)		+++	608	68	+++	513	133	+++	983	161	+++	767	98	
BILM (H)		+++	154	8	+++	259	26	+++	356	40	+++	382	40	
CIRN (H)		++	< 25	1	++	< 25	2	DEAD	DEAD	DEAD	DEAD	DEAD	DEAD	
CIRP (H)		+++	385	32	+++	NES	NES	+++	1020	137	+++	594	74	
DIRP (H)		+++	2283	183	+++	2195	270	+++	2028	260	+++	1717	173	

NOTE:

- (H) = homozygote
- (h) = heterozygote
- NES = Not enough serum to perform assay
- w = weeks post transplant
- Wtara = Western blot to detect human albumin
- ELISA = ELISA assay to detect human alpha-1 antitrypsin
- DB = dot blot assay to detect human albumin
- Western blot signals categorized as strong (+++), moderate (++), or weak (+)

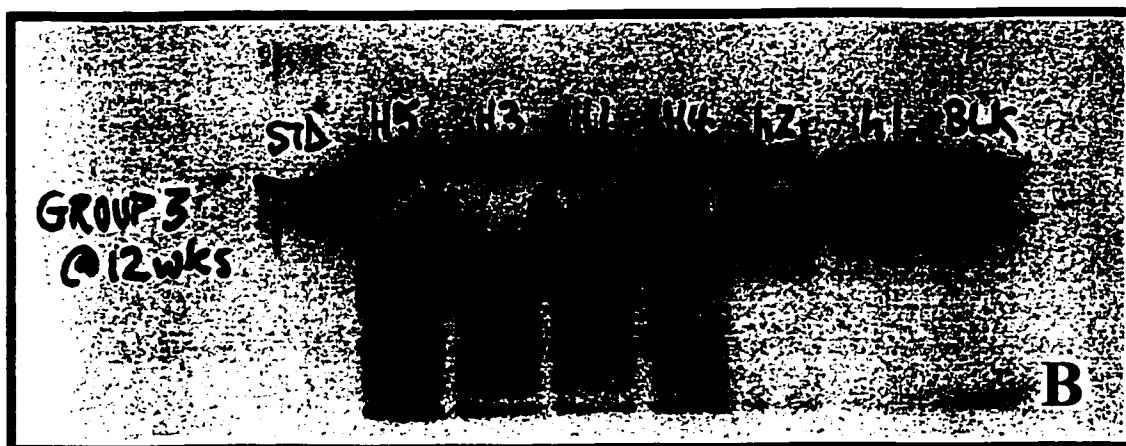
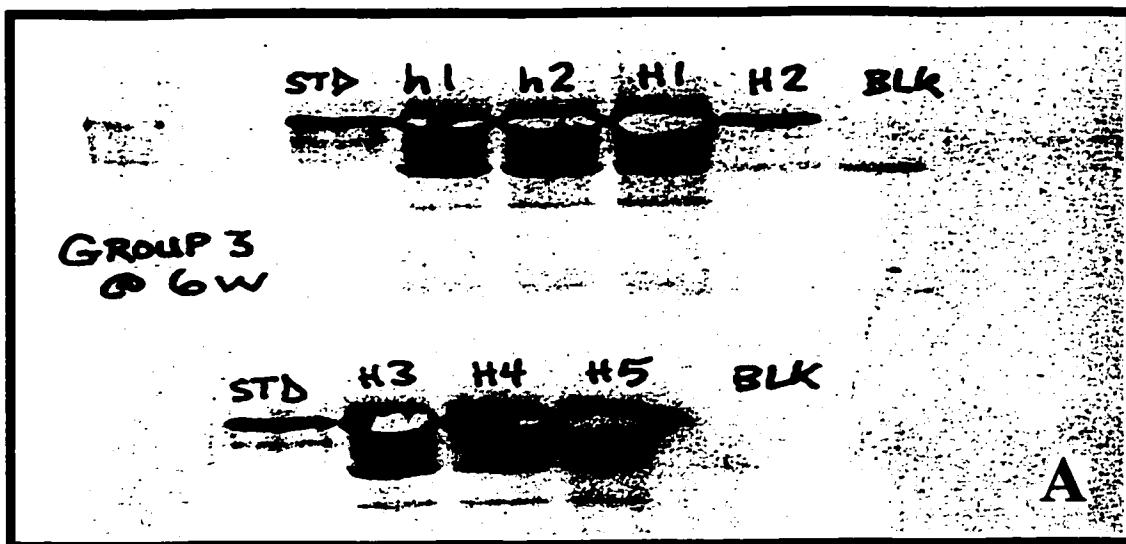


FIGURE 10. Western blot results for group 3 at 6 (A) and 12 (B) weeks post-transplant: Homozygous mice are H1 (DfRP), H2 (CfRM), H3 (BfLM), H4 (CfRP), H5 (BmLP). Mouse H2 died after 8 week blood sampling. Heterozygous mice are h1 (AfRP), h2 (AmLM). Human albumin (HA) Standard loaded in first lane, negative control serum = BLANK in last lane. In Figure A, H2 has ++ signal while other mice have +++ signals. Note the excessively strong signals at 12 weeks with h1 and h2 and even the BLANK lane showing signal. (PT = Post-transplant)

TABLE 5
DOT BLOT AND ELISA SERUM ASSAY RESULTS FOR HOMOZYGOTES vs HETEROZYGOTES
AT 3, 5, 6, 8, 10, 12 WEEKS POST-TRANSPLANT

Wks PT	Dot Blot Assay (ug/ml)				HAAT ELISA Assay (ug/ml)		
	Homozygotes	Heterozygotes	Difference Between Groups*		Homozygotes	Heterozygotes	Difference Between Groups*
3 wks	109	47			18.5	10.3	
	71				17.8		
	0				0		
	35				4.8		
	125				15.3		
	0				22.5		
AVG	56.7	47	NS		13.2	10.3	NS
SE	20.1	0			3.3	0	
5 wks	1863	303			138.8	32.3	
	176	47			12.3	3	
	203	67			26.3	2.5	
	217				16.8		
AVG	614.8	139	NS		48.6	12.6	NS
SE	360.4	67.1			26.2	8	
6 wks	1472	221			306.3	12.5	
	304	0			38.8	1.3	
	424	52			38	2	
	374	99			37.8	6.8	
	2283	200			182.5	14.8	
	385				32.3		
	0				0.8		
	154				8		
	608				67.8		
AVG	667.1	114.4	p=0.039		79.1	7.5	p=0.033
SE	231.1	37.9			31.6	2.4	
8 wks	2195	99			270.3	6	
	0				1.8		
	259				26.3		
	513				133		
AVG	741.8	99	NS		107.9	6	NS
SE	429.2	0			53	0	
10 wks	2028	36			260	1	
	1020				137	3	
	356				40		
	983				160.8		
12 wks	1717	0			173	1.5	
	594	0			73.5	1.5	
	382				40.3		
	767				96		
AVG	980.9	12	p=0.014		122.6	1.75	p=0.006
SE	201	9.8			24.9	0.4	

* Statistical analysis using Mann-Whitney test. NS = Not Significant. 10 and 12 week data combined for statistical analysis.

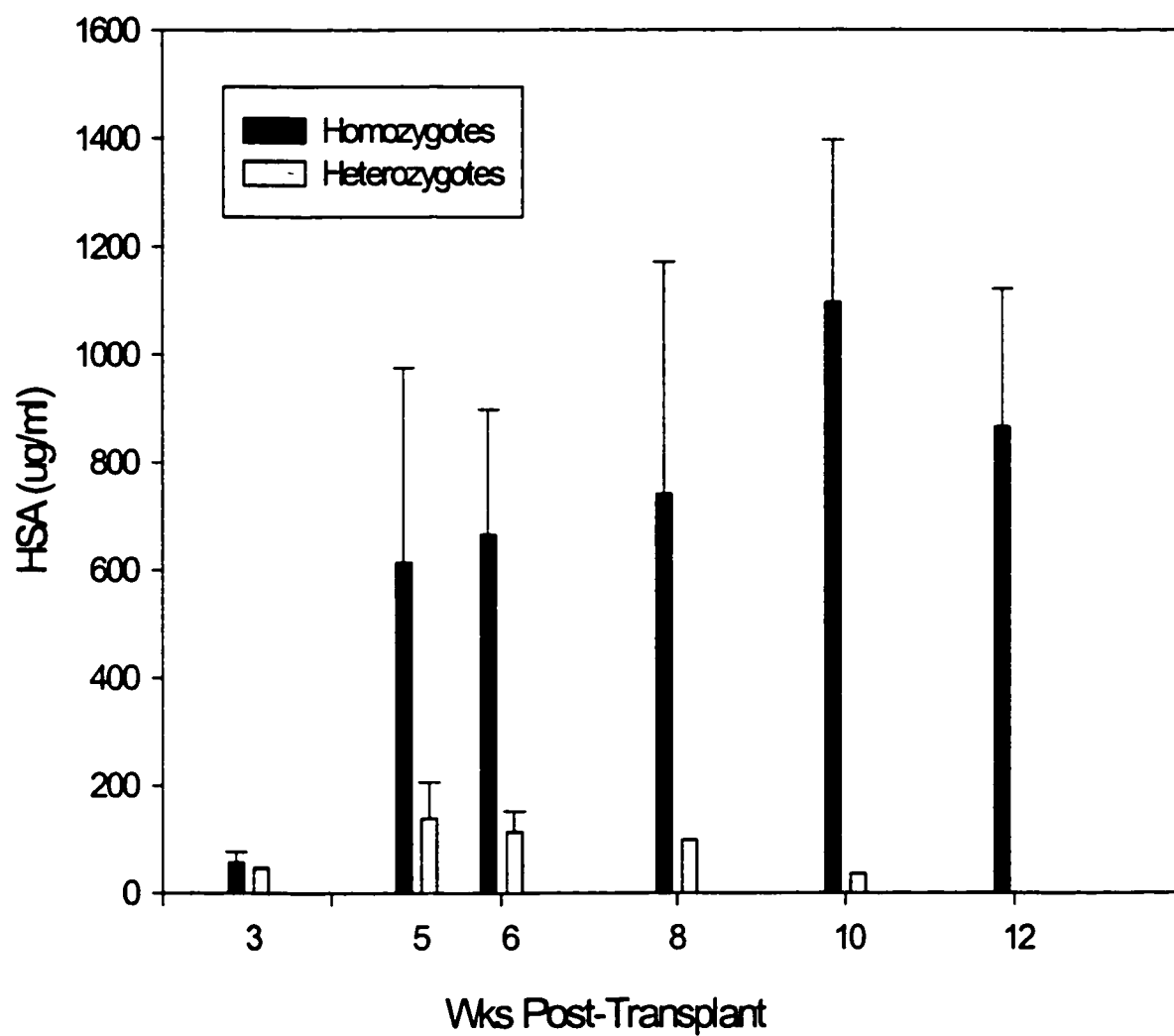


FIGURE 11. Average dot blot results for homozygotes versus heterozygotes. X – axis represents number of weeks post-transplant. Y-axis represents average serum level of serum human albumin (ug/ml) for homozygotes and heterozygotes. Error bars represent Standard Error (SE).

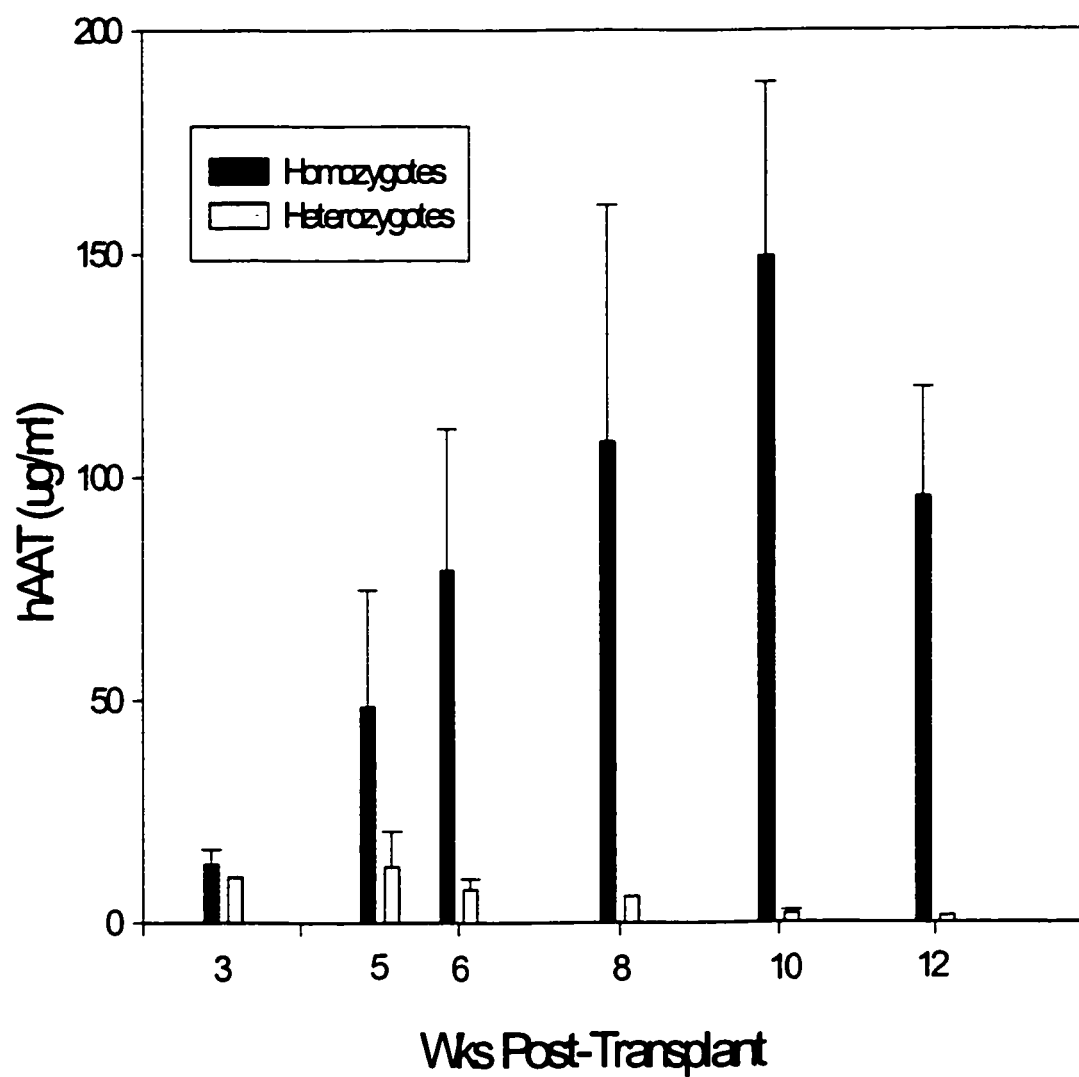


FIGURE 12. Average hAAT ELISA results for homozygotes versus heterozygotes. X – axis represents number of weeks post-transplant. Y-axis represents average serum level of human alpha-1 antitrypsin (µg/ml) for homozygotes and heterozygotes. Error bars represent Standard Error (SE).

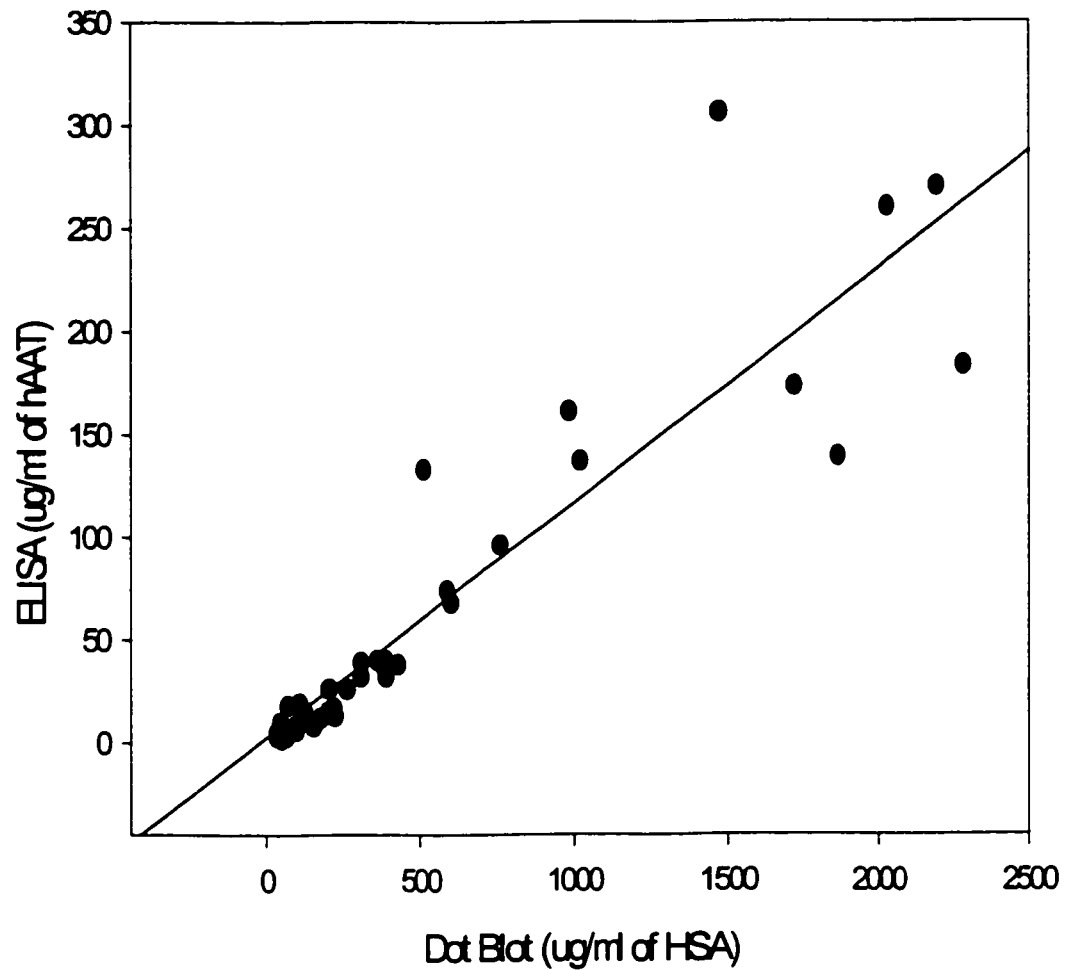


FIGURE 13. Scatter plot comparing results from dot blot assay and hAAT ELISA. All collected serum samples from Table 4 for which a result was available from both serum assays (n=38) were used. Dot blot values are plotted on the X-axis, hAAT ELISA values are plotted on the Y-axis. The two assays correlate very strongly (Spearman rank correlation coefficient = 0.946, significant at the 0.01 level).

Serum IgG levels are shown in Table 6. One mouse in group 1, 2 mice in group 2, and 3 mice in group 3 were found to be leaky as defined by serum IgG levels greater than 1 µg/ml, although the levels measured were all quite low compared to a normal CB17 mouse (average IgG level = 2670 µg/ml, (136)).

Immunohistochemistry:

On gross examination at time of sacrifice there was no discernible difference between the livers of the homozygous and heterozygous animals at 3 weeks post-transplant; both appeared pale with barely visible tiny punctate spots on the surface of the liver. At 6 weeks, the homozygote livers had definite pink nodules spread out in a pale background, while the heterozygote livers appeared mostly red with scattered areas of pale, yellowish liver. At 12 weeks, the homozygote livers had multiple large red nodules in a pale liver background, while the heterozygote livers were completely red, with a nodular appearance and had multiple fine red vessels seen on the liver surface. An example of human nodule expansion in a homozygous SCID/uPA mouse liver is seen in Figure 14.

Figure 15 shows hematoxylin and eosin (H&E) slides of representative heterozygote and homozygote livers at 3, 6, and 12 weeks post-transplant. At 6 and 12 weeks post transplant one can see nodules in the livers of homozygous animals, but not at 3 weeks PT. There are no distinct nodules seen in the livers of heterozygous animals at any timepoint with H&E staining. Unfortunately, we were unable to obtain any good quality staining for human hepatocytes in the livers of these 21 mice. After many months of hard work, Dr. Hao finally got the human hepatocyte marker working well in formalin fixed tissue (See Figure 16), but despite many variations, the protocol was never successful in these frozen liver sections. Some of the liver specimens suffered desiccation after prolonged freezer storage in suboptimal freezing containers and this likely contributed to the poor results.

In order to obtain correlative data between the serum assays and the immunohistochemistry, liver was collected from 8 mice and fixed in formalin. Immunohistochemistry with OCH1E5 was performed and percent human chimerism was

estimated as described above. Serum was collected at or near the time of tissue collection and was analyzed via the hAAT ELISA assay. The results are shown in Table 7.

VI. Correlating Graft Success for Fresh versus Frozen Hepatocytes

A total of 162 mice had DB serum analysis at 4 weeks post-transplant and 73 mice were subsequently inoculated with HCV (Figures 17, 18). Of the 105 mice transplanted with fresh hepatocytes that had serum analyzed by Dot Blot assay at 4-5 weeks post-transplant, 67 had serum HA values greater than 200 $\mu\text{g/ml}$ compared to only 21 of 57 mice transplanted with frozen / thawed hepatocytes (64% vs 37%, $p < 0.001$ by Chi-square analysis). A similar analysis shows that a higher percentage of mice transplanted with fresh hepatocytes have 4 week PT serum HA levels greater than 250 $\mu\text{g/ml}$ compared to mice receiving frozen / thawed hepatocytes (54% vs 32%, $p = 0.006$ by Chi-square analysis).

VII. Correlating Graft Success versus Infection Success

Comparison was made between mice with 4 weeks PT serum DB signal $> 200 \mu\text{g/ml}$, and mice with weaker grafts with respect to success of HCV infection. This analysis was also repeated using 250 $\mu\text{g/ml}$ serum HA as the cutoff. Mice with a DB signal over 200 $\mu\text{g/ml}$ at 4 weeks achieved a successful HCV infection 64% of the time when inoculated with fresh serum compared to only 21% of mice with a weaker graft signal ($p = 0.008$ by Chi-square analysis). Mice with a DB signal over 250 $\mu\text{g/ml}$ at 4 weeks achieved a successful HCV infection 75% of the time when inoculated with fresh serum compared to only 16% of mice with a weaker graft signal ($p < 0.001$ by Chi square analysis). Results for the 250 $\mu\text{g/ml}$ cutoff are shown graphically in Figure 19.

TABLE 6
SERUM IgG LEVELS IN SCID/uPA MICE

Group 1 (3 weeks)	IgG (ug/ml)	Group 2 (6 weeks)	IgG (ug/ml)	Group 3 (12 weeks)	IgG (ug/ml)
AfRM (H)	LO	AmLA (H)	6.6	BmLP (H)	15.6
AmLP (H)	2.1	CmBOTH (H)	0.9	BfLM (H)	1.5
BfRP (H)	NES	CfLM (H)	LO	CfRM (H)	NES
CfRA (H)	0.2	DmLM (H)	LO	CfRP (H)	0.5
DfRA (H)	LO	AfRA (h)	LO	DfRP (H)	0.5
DmLP (H)	LO	BfRM (h)	LO	AmLM (h)	0.3
CfBOTH (h)	LO	DfRM (h)	1.5	AfRP (h)	1.2
NOTE: NES = Not enough serum to run assay; LO = undetectable levels					
H = homozygote; h = heterozygote					



6 WEEKS PT



12 WEEKS PT



15 WEEKS PT



17 WEEKS PT

Figure 14. Repopulation of SCID/uPA Mouse Liver with Human Hepatocytes. This mouse received 10^6 cryopreserved human hepatocytes at 16 days of age and the liver was repeatedly examined and photographed.

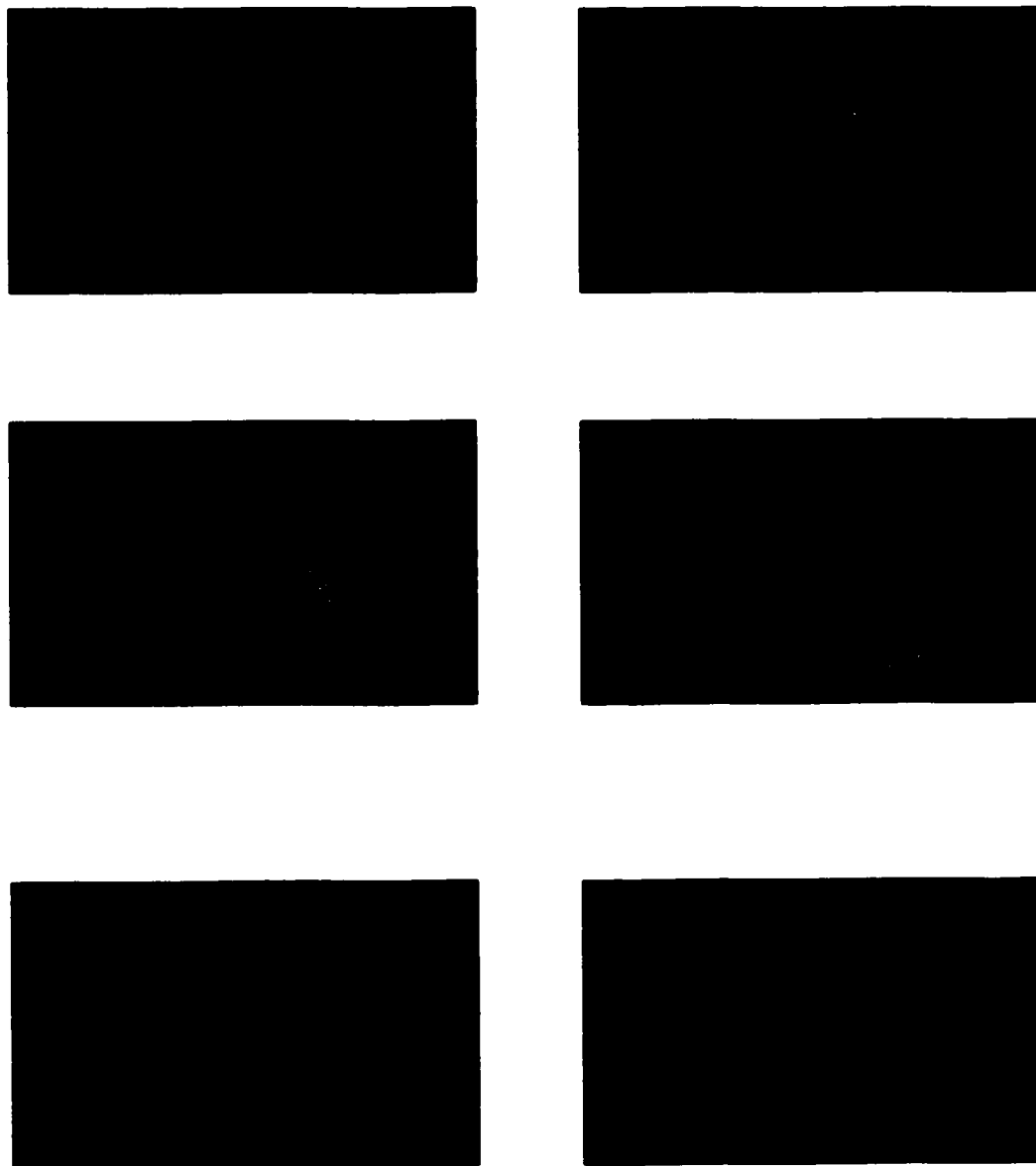


Figure 15. Representative H&E sections at 10 X magnification of livers from SCID/uPA mice transplanted with cryopreserved hepatocytes at 3, 6, and 12 weeks post-transplant (PT). A, C, E - heterozygote at 3, 6, 12 weeks PT. B, D, F - homozygote at 3, 6, 12 weeks PT. No nodules are seen in the livers of heterozygous animals at any time while nodules are visible in homozygous livers at 6 and 12 weeks PT.

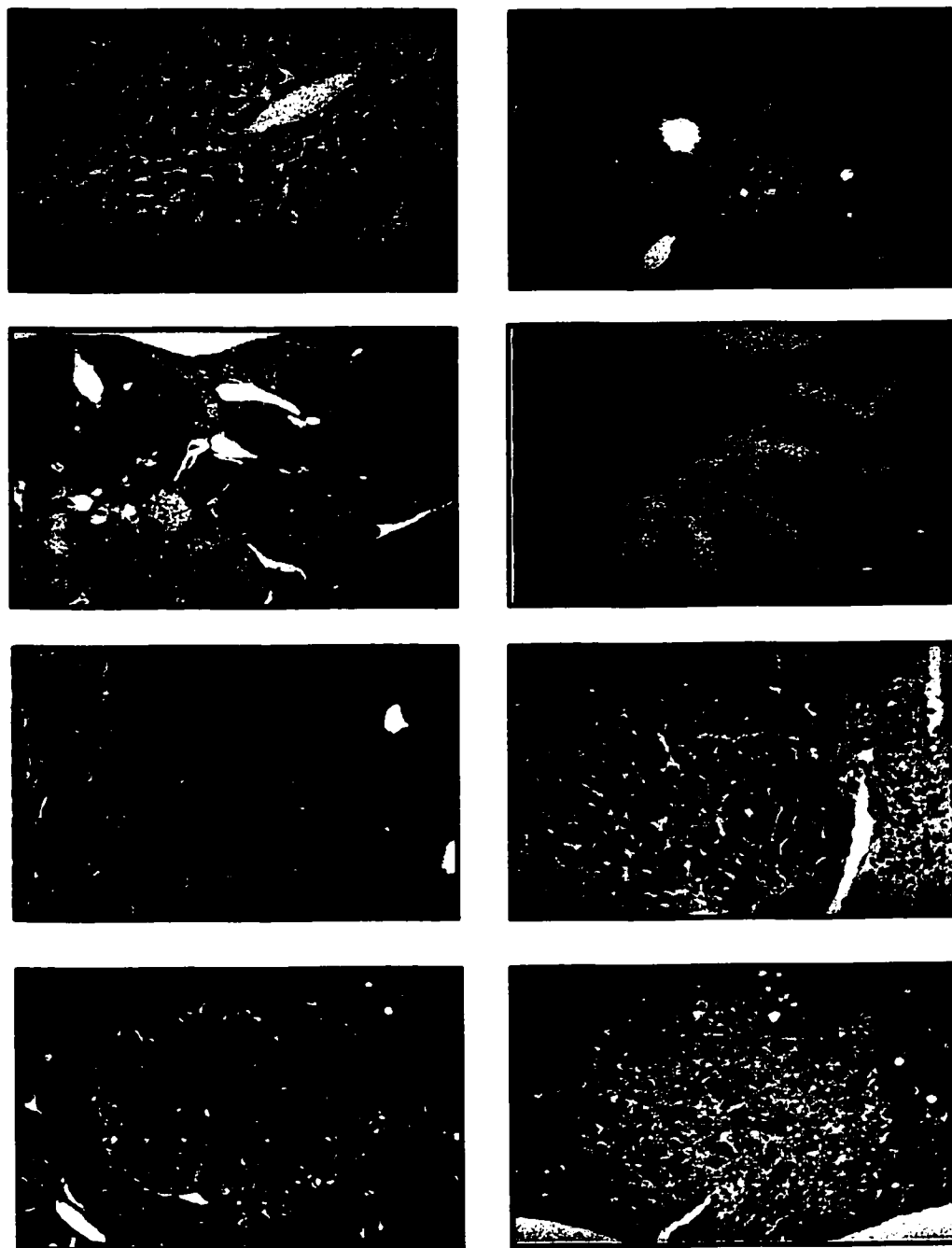


FIGURE 16. Immunohistochemistry with anti-human hepatocyte antibody (OCH1E5). Formalin fixed tissue was stained with an anti-human hepatocyte antibody as described in the methods section. (A) normal human liver; (B) non-transplanted homozygote SCID/uPA mouse; transplanted homozygote mouse at low power (C) - H&E, (D) - OCH1E5, and high power (E) - H&E, (F) - OCH1E5. Regenerative nodule in non-transplanted homozygote mouse (G) - H&E, (H) - OCH1E5.

TABLE 7
COMAPRISON OF SERUM ASSAY AND ESTIMATED PERCENT
HUMAN CHIMERISM IN LIVER FOR 8 SCID/uPA MICE

MOUSE	FRESH (F) OR CRYO (C) CELLS	WEEKS POST TRANSPLANT	SERUM hAAT (ug/ml)	ESTIMATED PERCENT HUMAN CHIMERISM IN LIVER (%) (SD)
1	C	5.5	90	9 (2.6)
2	F	8	104	17(2)
3	F	12	95	59 (9)
4	F	12	26	83 (6.6)
5	F	12	30	72 (10)
6	F	20	36	39 (13)
7	F	25	11	73 (6)
8	F	29	46	52 (7)

* hAAT = human alpha-1 antitrypsin
 * serum hAAT measured by quantitative ELISA method
 * percent liver chimerism estimated by manual quantification of multiple high power fields at 2.5 X magnification using IP LAB software package

FIGURE 17
PREDICTIVE VALUE OF 4 WK DOT BLOT > 200 ug/ml

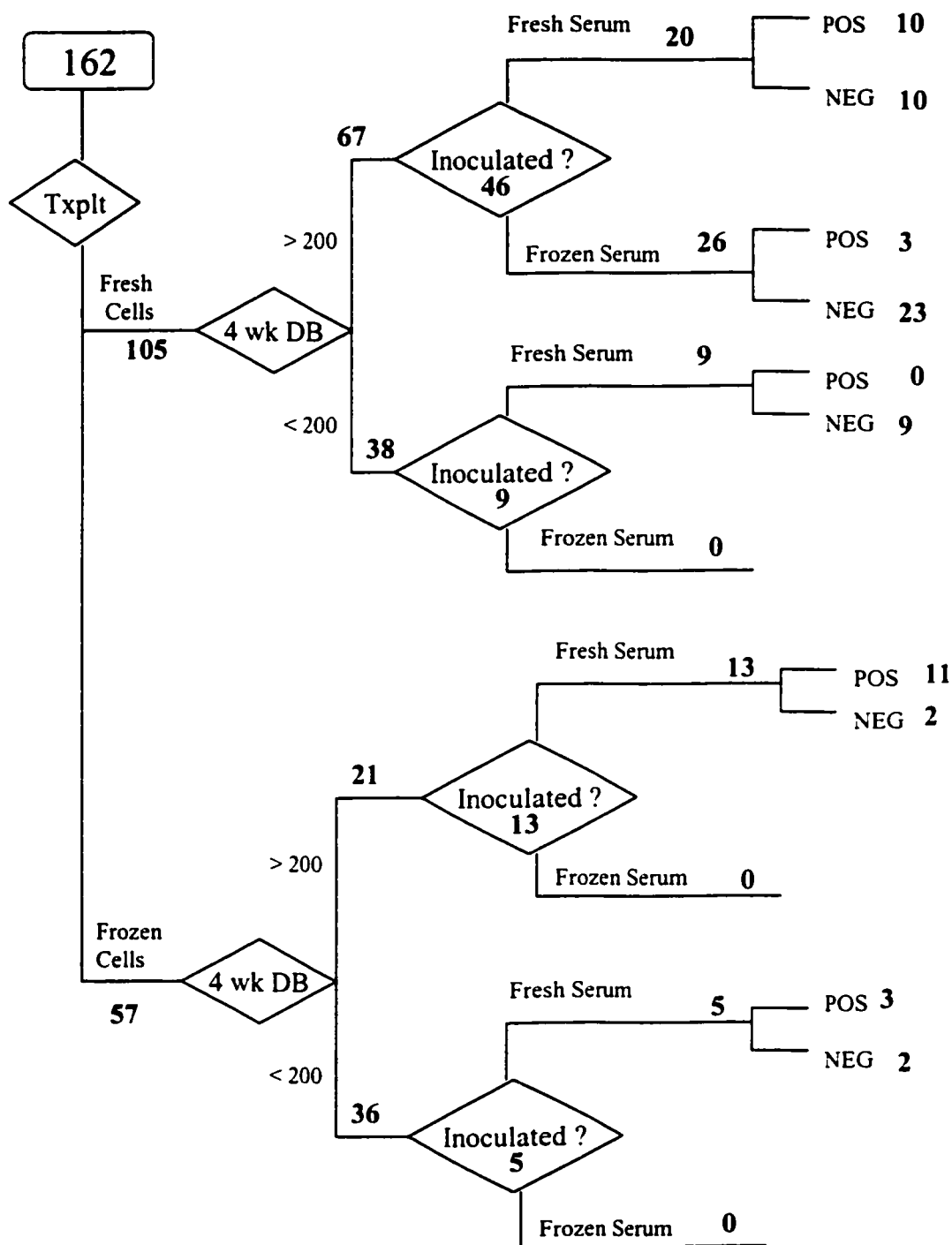


FIGURE 17. Predictive value of 4 week dot blot > 200 g/ml. 162 mice were transplanted with fresh or frozen / thawed human hepatocytes. All mice had serum collected at 4 weeks post-transplant for analysis by dot blot (DB) assay. 73 mice were inoculated with HCV.

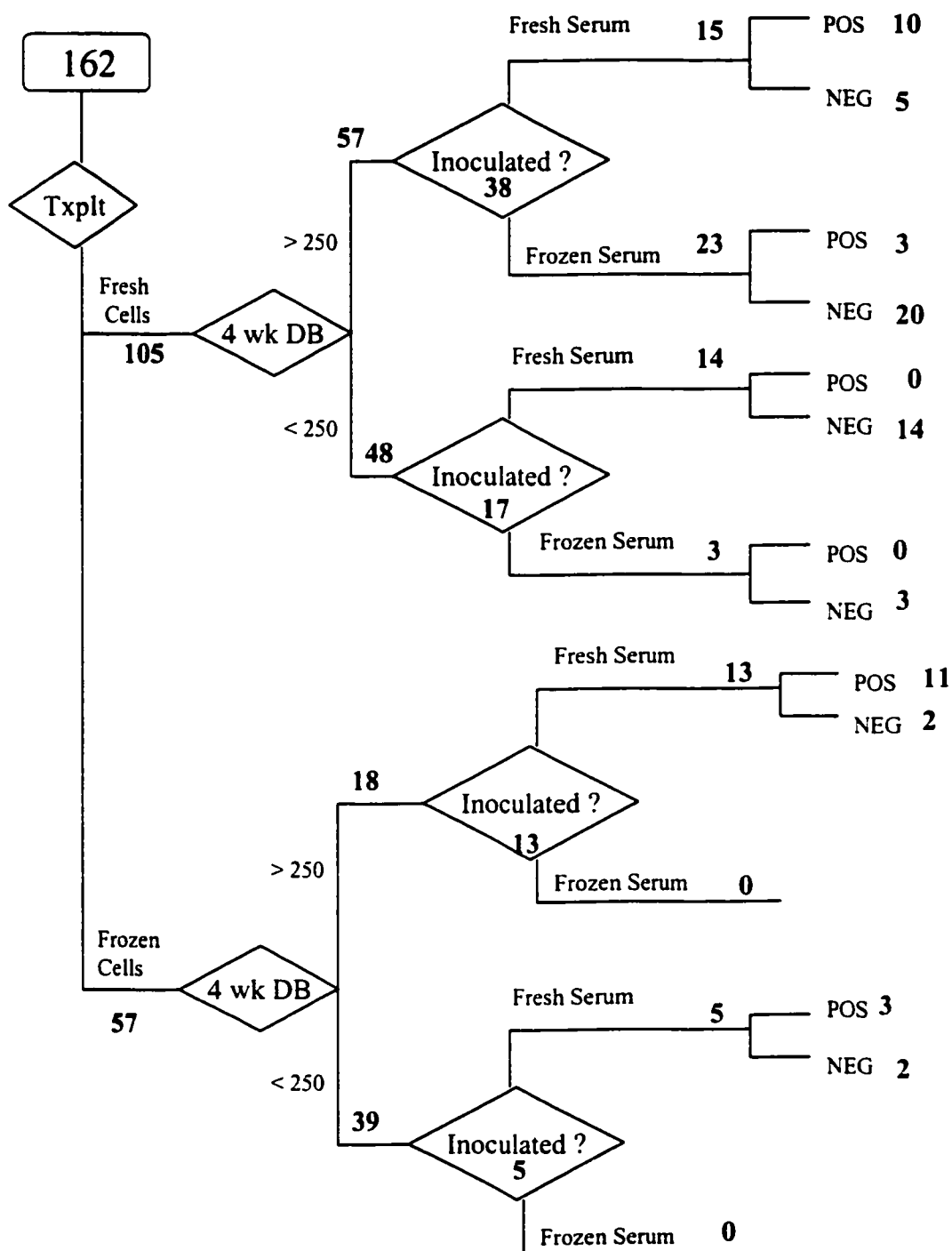


FIGURE 18. Predictive value of 4 week dot blot > 250 g/ml. 162 mice were transplanted with fresh or frozen / thawed human hepatocytes. All mice had serum collected at 4 weeks post-transplant for analysis by dot blot (DB) assay. 73 mice were inoculated with HCV.

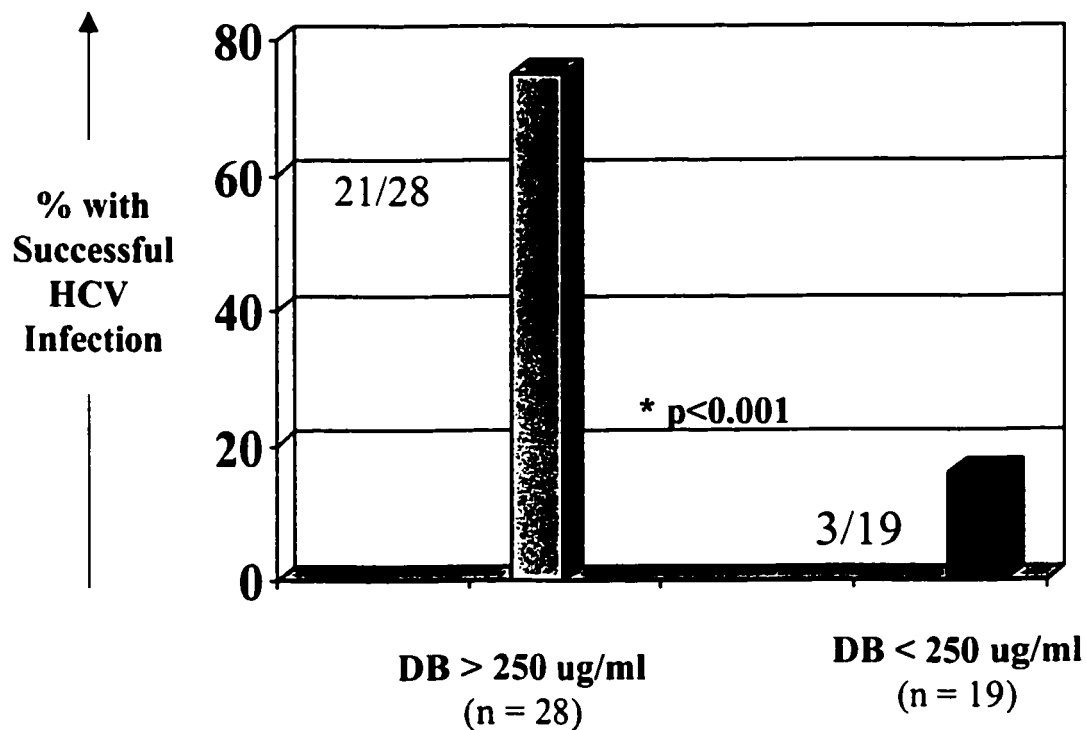


FIGURE 19. Correlating Graft Function at 4 weeks Post-Transplant with Success of HCV Infection: All mice that had a 4 week post-transplant (PT) serum human albumin level measured by dot blot assay that were also inoculated with freshly collected serum from an HCV-infected patient were analyzed (n=47). Mice with a signal > 250 g/ml at 4 weeks PT were successfully infected more often than mice with weaker signals (75% vs 16%, p<0.001 by Chi square analysis). HCV infection was determined by detection of HCV RNA in mouse serum.

VIII. Correlating Success of Infection with Fresh versus Frozen Serum

Of the transplanted mice with strong initial graft function (4 week PT serum DB result > 200 µg/ml) that were inoculated with fresh serum from an HCV infected patient, 64% became successfully infected, compared to only 12 % of similar mice who were inoculated with frozen/thawed serum ($p < 0.001$ by Chi square analysis). Considering mice with an early dot blot signal greater than 250 µg/ml, fresh serum resulted in a successful infection 75% of the time compared to only 13% for frozen serum ($p < 0.001$ by Chi square analysis). These results suggest that the infectivity of serum from HCV positive patients may be considerably decreased by the freezing and thawing process. To test this hypothesis, we used 6 animals that all had strong 4 week and 8 week PT dot blot signals and who failed to demonstrate an infection after inoculation with frozen/thawed serum. All 6 animals were re-inoculated with fresh serum 8 weeks after their initial inoculation, and 2 weeks later serum was drawn and analyzed for HCV RNA by qualitative RT-PCR. This time, 2 of the animals were found to be positive for HCV RNA, 1 was indeterminate and the remaining 3 were negative. This strongly suggests that frozen/thawed serum is not as infectious as freshly collected serum although genotype and HCV RNA titer differences between the two inocula are also possibilities.

IX. Long Term Study of Infected Animals:

Four infected animals were followed long-term to study graft function and HCV RNA levels in the SCID/uPA model over time. Two different patterns were seen. In 3 of the animals, both the graft signal and the levels of HCV RNA became undetectable between 24 and 30 weeks post-transplant. A close correlation is seen between graft signal and levels of HCV RNA. In the fourth animal, both the graft signal (hAAT) and the HCV RNA titers persist out past 49 weeks post-transplant which corresponds to 42 weeks post-inoculation (See Figure 20). Liver was harvested from these animals by partial hepatectomy at 27 weeks post-transplant and immunohistochemistry was performed as previously described. In one of these animals we were able to demonstrate the presence of HCV antigens in a human derived nodule using the TORDJI-22 antibody (Figure 21).

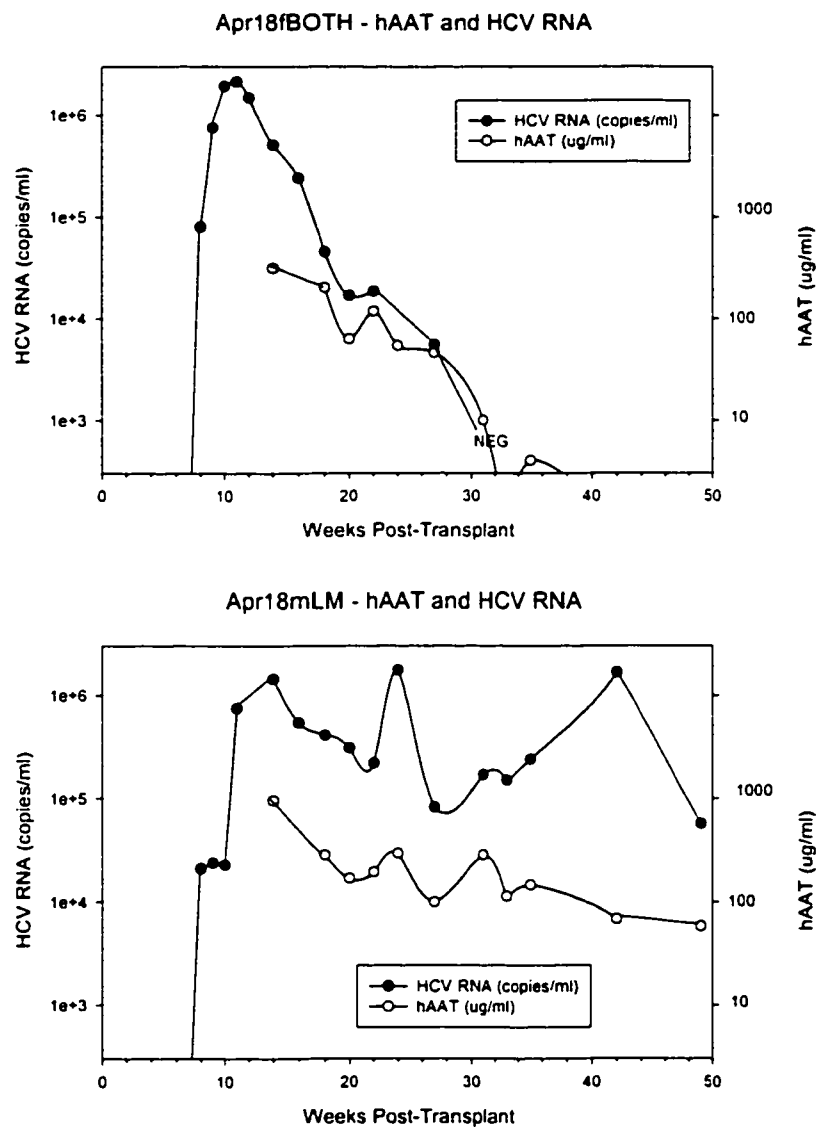


FIGURE 20. Long term follow up of infected SCID/uPA mice: Four animals were transplanted with 500,000 fresh human hepatocytes at 12 days of age, and inoculated at 7 weeks post-transplant with 250 μ l of freshly collected serum from an HCV-infected patient. With long term follow-up, 2 different patterns are seen. Three animals lost their graft signal and their HCV RNA signal between 24-30 weeks post-transplant. One mouse maintains a strong graft signal and high HCV RNA titers at 49 weeks PT = 42 weeks post-inoculation.

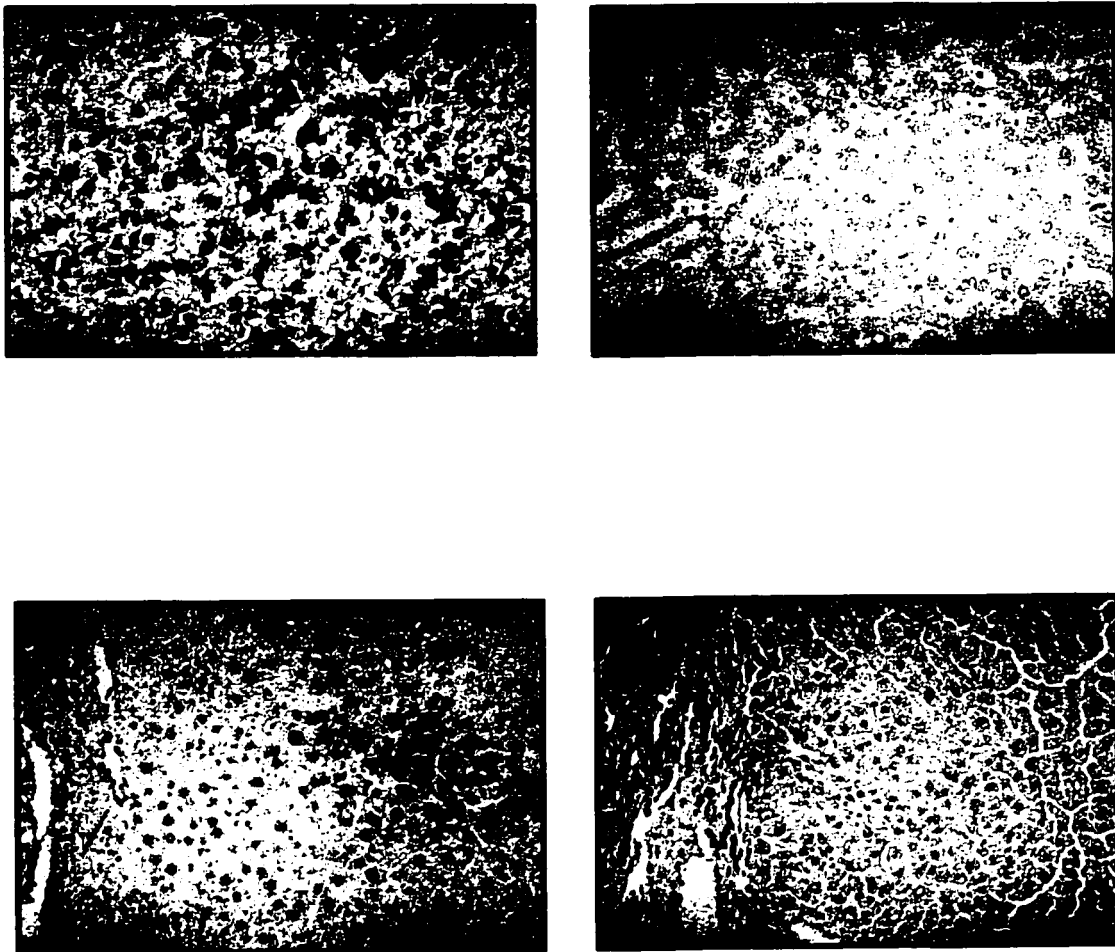


FIGURE 21. Immunohistochemistry with anti-HCV antibody (TORDJI-22) Formalin fixed tissue was stained with an antibody specific for the C-100 protein product of the NS4 region of the HCV genome as described in the methods section. **A)** patient with chronic HCV; **B)** normal human liver; **C)** transplanted and infected SCID/uPA mouse liver; **D)** transplanted but not infected SCID/uPA mouse liver.

X. Demonstration of Transmissibility

The results of this experiment are shown in Figure 22. In four separate transmissibility series, we were able to successfully transmit HCV infection from mouse to mouse and in one series we were able to demonstrate transmissibility through three generations of mice from the same initial viral inoculum. If we make the assumption that an adult mouse has an approximate blood volume of 1 ml, then this represents a greater than 4700 – fold increase in HCV RNA titers from mouse #1 to mouse #4.

XI. Effects of Interferon alpha on HCV Infected SCID/uPA mice

The results of this experiment are shown in tables 8 and 9. There does appear to be a treatment effect seen with administration of IFN α to infected SCID/uPA mice as seen in figure 23. The average level of HCV RNA before treatment was not significantly different in the control group ($4.07 \pm 1.96 \times 10^5$ copies/ml) compared to the treatment group ($2.44 \pm 1.03 \times 10^5$ copies/ml) (mean \pm SE, $p=0.624$ by Mann Whitney. After 2 weeks of treatment, HCV RNA titers in the control group increased (average change = $+ 6 \times 10^5$ copies/ml) while titers in the treatment group decreased (average change = -2.2×10^5 copies/ml) ($p=0.002$). The underlying graft function in the treatment group did not change significantly over the treatment period as determined by serum levels of hAAT (average pre-treatment level = 91.1 ± 19.6 mg/ml vs post-treatment level = 94.5 ± 15.6 mg/ml, $p=0.571$). After the end of treatment there does not appear to be a significant rebound effect in the levels of HCV RNA.

Figure 24 shows results of the experiment with the treatment mice grouped according to HCV genotype. There are 3 mice in the treatment group that were infected with genotype 3a: one mouse that received IFN 135 IU/g/d showed a drop in HCV RNA levels of approximately 1 log; 2 mice that received IFN 1350 IU/g/d cleared the infection and HCV RNA levels remained undetectable for the remainder of the study period. There were seven mice infected with genotype 1b that received IFN 1350 IU/g/d and on average showed a decrease in HCV RNA levels of approximately 1 log with treatment. There were no discernible adverse effects of the treatment observed in these mice.

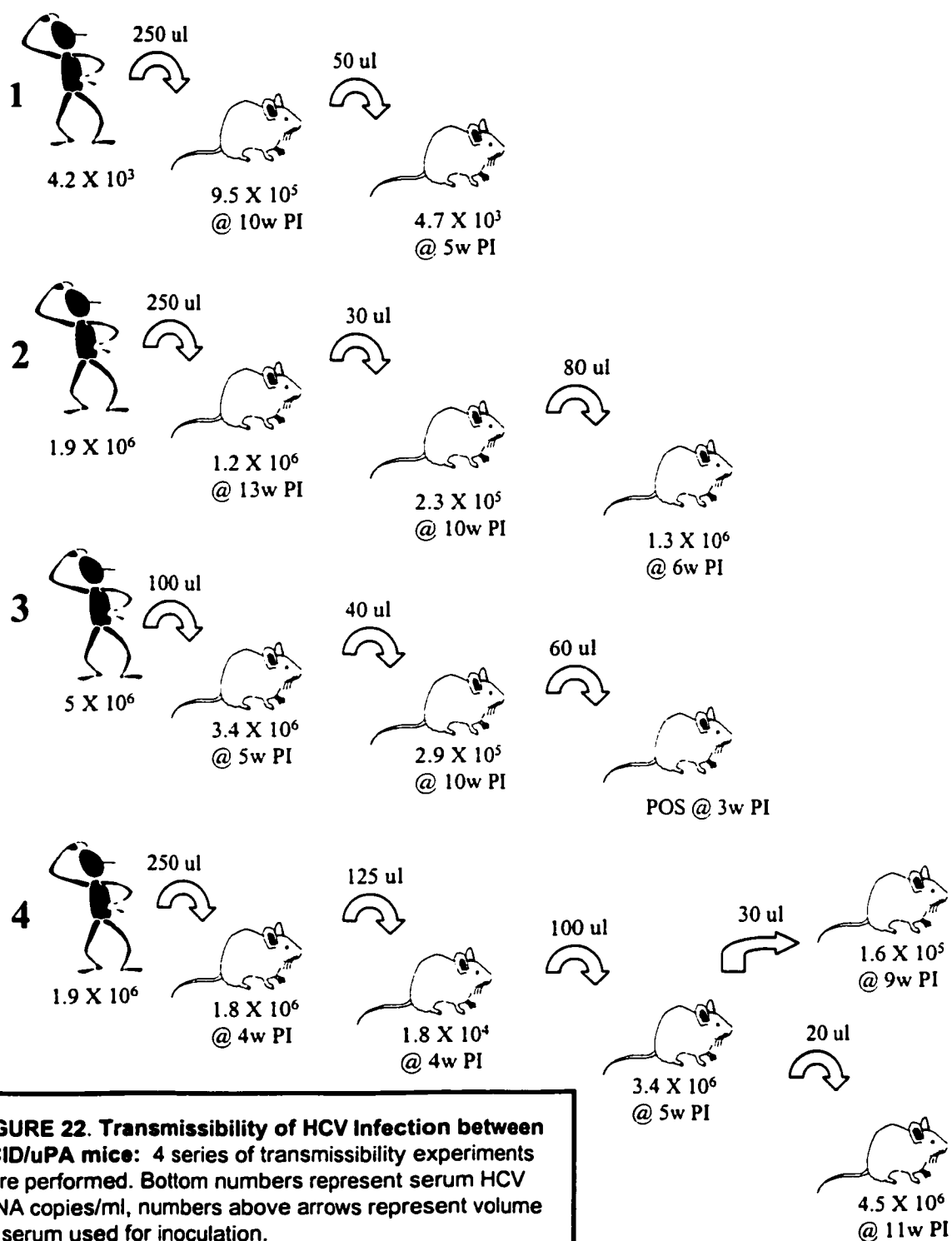


FIGURE 22. Transmissibility of HCV Infection between SCID/uPA mice: 4 series of transmissibility experiments were performed. Bottom numbers represent serum HCV RNA copies/ml, numbers above arrows represent volume of serum used for inoculation. (w = weeks) (PI = post-inoculation)

TABLE 8
EFFECT OF INTERFERON ON HCV RNA LEVELS OF
HCV-INFECTED SCID/UPA MICE

Mouse	HCV Genotype	IFN Dose (IU/g/d) or Control (C)	HCV RNA at 2w PI (copies/ml) (Start IFN)	HCV RNA at 4w PI (copies/ml) (End IFN)	HCV RNA at 6w PI (copies/ml)	HCV RNA at 8w PI (copies/ml)
Oct24fRM	3	C	1.10E+06	2.00E+06	1.50E+06	1.60E+06
Apr18mLP	3	C	2.80E+03	2.50E+04	6.60E+03	2.94E+03
Apr18mLM	3	C	2.40E+04	7.50E+05	1.4E+06	5.4E+05
Apr18fRA	3	C	1.60E+05	1.70E+05	9.0E+04	1.5E+04
Apr18fBOTH	3	C	7.50E+05	2.10E+06	1.5E+06	5.1E+05
MEAN			5.09E+05	1.26E+06	1.13E+06	6.67E+05
SE			2.20E+05	4.42E+05	3.49E+05	2.91E+05
CNov7fRA	3	135	2.00E+05	3.30E+04	4.20E+04	6.30E+03
ANov7fLA	3	1350	1.70E+03	0	0	0
BNov7mRA	3	1350	3.00E+04	0	0	0
ADec22fRP	pending	1350	2.10E+05	1.40E+04	5.09E+04	4.45E+04
ADec22mLA	pending	1350	2.30E+04	0	2.15E+03	3.93E+02
ADec22mLP	pending	1350	2.20E+05	1.40E+04	1.68E+04	1.12E+04
ADec22mLM	pending	1350	2.70E+04	1.40E+03	6.36E+03	3.34E+03
BDec22mLA	pending	1350	1.00E+06	1.50E+05	2.38E+05	2.40E+05
BDec22mRM	pending	1350	7.30E+05	2.20E+04	5.96E+04	7.75E+04
BDec22fBOTHp	pending	1350	1.10E+03	1.30E+03	0	0
MEAN			2.44E+05	2.36E+04	4.16E+04	3.83E+04
SE			1.03E+05	1.38E+04	2.18E+04	2.26E+04

• All HCV RNA quantification done by RT-PCR analysis.
 • 0 = below linear range of RT-PCR assay
 • SE = Standard Error
 • PI = post inoculation

TABLE 9
GRAFT FUNCTION DURING INTERFERON TREATMENT
IN HCV-INFECTED SCID/uPA MICE

Mouse	HCV Genotype	IFN Dose (IU/g/d) or Control (C)	hAAT level at 2w PI (ug/ml) (Start IFN)	hAAT level at 4w PI (ug/ml) (End IFN)	hAAT level at 6w PI (ug/ml)	hAAT level at 8w PI (ug/ml)
Oct24fRM	3	C	207	N/A	158	67
Apr18mLP	3	C	N/A	N/A	N/A	137
Apr18mLM	3	C	N/A	N/A	955	N/A
Apr18fRA	3	C	N/A	N/A	N/A	119
Apr18fBOTH	3	C	N/A	N/A	313	N/A
Experiment 2						
CNov7fRA	3	135	112	110	56	77
ANov7fLA	3	1350	79	150	65	64
BNov7mRA	3	1350	167	112	53	60
ADec22fRP	pending	1350	80	88	59	23
ADec22mLA	pending	1350	17	24	13	6
ADec22mLP	pending	1350	52	117	54	38
ADec22mLM	pending	1350	65	119	88	59
BDec22mLA	pending	1350	140	85	118	60
BDec22mRM	pending	1350	79	153	81	48
BDec22fBOTHP	pending	1350	0	0.6	0.2	0
MEAN			79.1	95.9	58.7	43.5
SE			15.4	14.9	10.2	7.8

* N/A = not available
* PI = Post Inoculation
* w = weeks
* IFN = Interferon

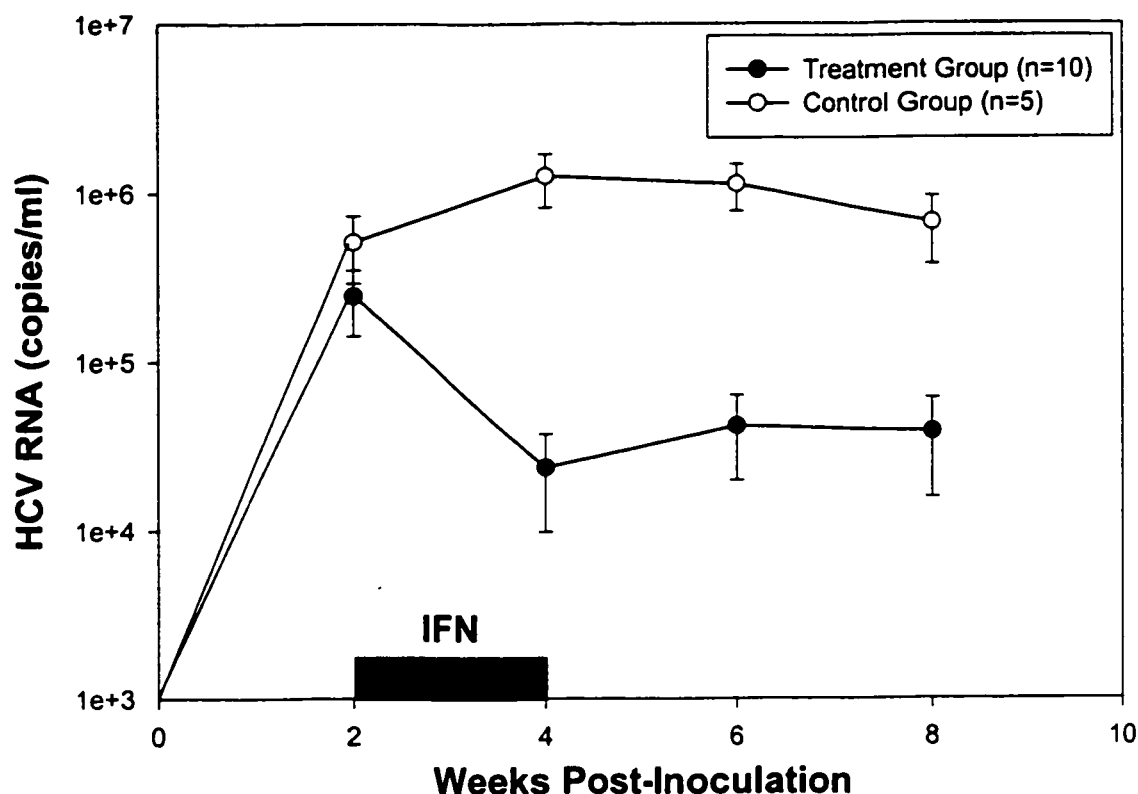


FIGURE 23. Effect of IFN on HCV-infected SCID/uPA mice – treatment vs controls. 15 mice with successful human hepatocyte engraftment were inoculated with 50 μ l of HCV-positive serum. Mice received 14 days of either IFN 135 IU/g/d (n=1), 1350 IU/g/d (n=9) or no treatment (n=5). Serum was analyzed for HCV RNA at the start of treatment, at the end of treatment, and at 2, and 4 weeks after the end of treatment. HCV RNA quantification was by RT-PCR analysis. There was no significant difference in the levels of HCV RNA between groups at the start of treatment. After treatment the HCV RNA levels in the control group increased (average change = $+6 \times 10^5$ copies / ml) while the levels in the treatment group decreased (average change = -2.2×10^5 copies/ml) ($p=0.002$).

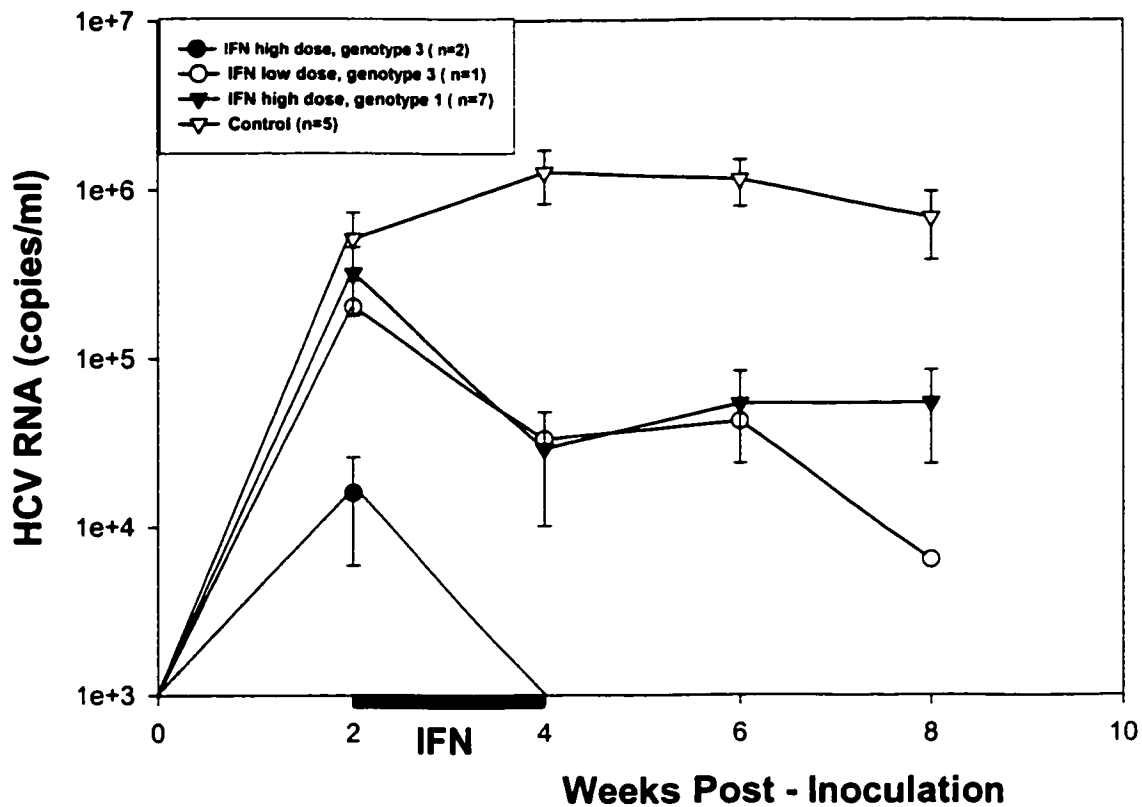


FIGURE 24. Effect of IFN on HCV-infected SCID/uPA mice – treatment effect according to genotype. 15 mice with successful human hepatocyte engraftment were inoculated with 50 μ l of HCV-positive serum. Mice received 14 days of either IFN 135 IU/g/d (n=1), 1350 IU/g/d (n=9) or no treatment (n=5). Serum was analyzed for HCV RNA at the start of treatment, at the end of treatment, and at 2, and 4 weeks after the end of treatment. HCV RNA quantification was by RT-PCR analysis. Of the 3 mice infected with genotype 3a: one mouse treated with low dose IFN showed a decrease in HCV RNA of 1 log, two mice treated with high dose IFN cleared the infection and remained negative for the remainder of the study period. Seven mice infected with genotype 1b showed a decrease of 1 log in HCV RNA..

DISCUSSION:

When fresh liver tissue is available from the operating theater, it is now possible to isolate in excess of 100 million viable human hepatocytes fairly consistently using Liberase HI collagenase. This enzyme is currently used at a concentration of 0.35 mg/ml of collagenase buffer and we have previously used concentrations as low as 0.18 mg/ml. The manufacturer product monograph reports that concentrations of 0.75 mg/ml, 1.5 mg/ml and 3.0 mg/ml have all been used successfully to isolate human islets. It is possible that higher concentrations may improve the yield of hepatocytes but this would be at the cost of using more of this very expensive enzyme.

Analysis of the graft function in mice receiving fresh hepatocytes versus frozen / thawed hepatocytes suggests that transplantation of fresh hepatocytes is superior in terms of graft function at 4 weeks PT. We have been able to demonstrate strong graft signals and subsequent HCV infections using cryopreserved hepatocytes, but our percentage of successful engraftment is significantly lower than what is seen with fresh hepatocytes (64% vs 37% using a cutoff DB signal of 200 μ g/ml serum HA). These results suggest that cryopreserved hepatocytes should only be used when there is no fresh human liver tissue available. With modifications to the cryopreservation protocol hopefully the yield and viability of thawed cells can be improved upon. Any centrifuge steps during the freezing and thawing process should be performed at speeds slower than 80g to avoid damaging the cells. The results show that cells that are cryopreserved immediately post-isolation have a better viability than cells that are kept overnight in UW solution. One would expect that the better post-thaw viability would translate into more successful hepatocyte engraftment in these mice but this has not yet been proven.

Over the course of the past 2 years we have experimented with different approaches to the question of optimal timing for transplant in this model. By transplanting the mice at a very early age one would hope that the human hepatocytes that engraft in the liver would undergo a higher number of doublings before the regenerative stimulus for liver growth decreases. This hypothetical advantage is offset by the very real problem of high intra-operative and post-operative mortality with very young mice. Transplanting older mice is technically much easier but beyond 16 days of age there appears to be a higher incidence of anesthetic-related deaths. One could argue

that these older mice with “un-rescued” livers were suffering from subclinical liver failure leading to peri-operative mortality from either a bleeding diathesis or from halothane toxicity. Hopefully that by transplanting the mice between 10-15 days of age with enflurane anesthesia (reported to be less hepatotoxic than halothane) we can reduce our post-operative mortality rates.

We currently inoculate these mice with HCV at 8 weeks PT. Since we do not infect the mice until 8 weeks PT, it would make sense to check their graft function closer to the time of inoculation instead of relying on the traditional 4 week PT result to predict success of infection. This is because mice with a 4 week DB signal $< 200 \mu\text{g/ml}$ may in fact have a signal well over $200 \mu\text{g/ml}$ by 8 weeks PT, and conversely, mice with an initially strong graft at 4 weeks may in fact lose their graft signal by 8 weeks and therefore not be able to support an HCV infection.

It is interesting to note that the group from Albert Einstein with the RAG/uPA mouse model for HBV inoculated their animals 2 days after transplant and then checked them for infection 8 weeks later. We have previously hypothesized that we needed a human hepatocyte graft of a certain “size” in order to support an active HCV infection in our SCID/uPA mice, supported by the fact that we have never documented an infection in a heterozygous SCID/uPA mouse which are known to have lower percent human hepatocyte engraftment. This is part of the reason that we do not infect our mice until 8 weeks after transplant (previously 4-6 weeks). It is very possible however that even heterozygous mice (who obviously have some viable engrafted human hepatocytes) may harbor HCV infections albeit at levels too low to detect with the currently available assays.

It would be interesting to inoculate the SCID/uPA mice with HCV several days after transplant. A current limitation of our model as it stands now is that most of our mice gradually lose their graft signal over time and inevitably show a parallel decline in the levels of HCV RNA. In order to be useful for the testing of antiviral agents, we need to be confident that control mice have a fairly stable level of HCV RNA during the treatment and follow up time period (most likely spanning several months). Infecting the mice earlier may allow us to achieve high levels of HCV RNA at an earlier age thus extending the window when these mice are useful for experiments before their graft

signal begins to fade. As a final thought, the bolus of human serum given soon after hepatocyte transplant may contain certain human specific growth factors that would transiently benefit the human cells trying to engraft and proliferate in a foreign environment.

The Western blot assay was shown to be very sensitive, perhaps overly sensitive in some cases. Mice that were shown on the quantitative assays to have minimal amounts of human proteins, still gave a moderate (++) or even strong (+++) signal on the western blot. Part of this may be due to the large amount of serum (20 μ l) that is used in this assay that may be exceeding the binding capacity of the nitrocellulose membrane (Figure 10).

The dot blot and ELISA assays both showed a similar trend in following the cohort of 21 homozygous and heterozygous animals transplanted with cryopreserved cells. Given the strong correlation between success of HCV infection and graft function and the fact that the average signal in the heterozygote group never exceeded 200 μ g/ml on the dot blot assay, it is likely that the lack of detectable HCV RNA in heterozygotes is due to poor engraftment of human hepatocytes. The Spearman rank correlation coefficient of 0.95 (0.01 level of significance) indicates that these two assays correlate very well with each other. Both assays were repeated numerous times for each sample (data not shown) and the dot blot assay was less reproducible from run to run. Another disadvantage associated with the dot blot assay is the dependence on expensive equipment such as the STORM 860 phosphorimager machine that is very expensive and prone to mechanical breakdown problems.

In the series of 21 mice presented here the homozygous animals demonstrated an average level of HA by dot blot of 57 μ g/ml (@ 3 weeks PT) to 1097 μ g/ml (@ 10 weeks PT) which corresponds to 0.1 – 2.7 % of normal human serum levels of albumin (normal human levels of albumin = 40 mg/ml). The highest recorded dot blot signal of 2283 μ g/ml corresponds to 5.7 % normal human levels.

The average serum level of hAAT demonstrated in the homozygous animals in this series was 13 μ g/ml (@ 3 weeks PT) to 149 μ g/ml (@ 10 weeks PT) corresponding to 0.7 % - 8.5 % of normal human AAT levels (the hospital lab reports normal serum levels of hAAT to be 0.9 – 2.6 mg/ml, mean = 1.75 mg/ml). The highest recorded level in this series of 306 μ g/ml corresponds to 17.5 % normal human levels.

It is unfortunate that immunohistochemistry was not available for the series of 21 mice transplanted with cryopreserved cells. We now know that tissue must be collected in formalin for optimum staining of human hepatocytes using the OCH1E5 antibody. From gross examination of SCID/uPA livers (Figure 14) and the increasing levels of human protein production seen in figures 11 and 12, it is reasonable to conclude that during the first 14 weeks after transplant, the human hepatocytes continue to proliferate and repopulate a substantial proportion of the mouse liver. As the mice get older, the picture becomes less clear. We know that in most mice the graft signal decreases with time. Whether the liver tissue is eventually replaced with regenerative mouse nodules or whether it remains largely replaced with human cells that slowly die off is unknown.

The results shown in Table 7 suggest that in some cases, up to 80% of the SCID/uPA mouse liver can be repopulated with human hepatocytes. This is only a rough estimate since the methods used to estimate percent human chimerism are not very precise. The estimated chimerism does not correlate well with the ELISA values suggesting that a) the method used to estimate chimerism is not very reliable or b) over time the human hepatocyte graft becomes less functional and produces less HA and hAAT although still staining positive with OCH1E5. Other groups working on chimeric human / mouse models estimate the percent human chimerism in the liver by DNA analysis which may be a more valid method. By comparing the chimeric liver DNA to mixtures of mouse / human DNA (i.e. 10% human: 90% mouse, 20% human : 80% mouse etc) the percent human tissue in the liver can be estimated. It would be very useful to analyze the livers of our transplanted mice with such an assay.

It is interesting to note that the authors who originally developed the uPA transgenic mouse have reported that virtually all of these mice develop hepatocellular carcinomas with age. We have observed 3 tumors in the SCID/uPA mice, 2 that were infected with HBV and 1 that was over 1 year old and had previously had a successful HCV infection. The question is whether these tumors are derived from human or mouse cells, and further work needs to be done to conclusively answer this question.

The results presented in Figure 19 support the hypothesis that success of HCV infection in these mice is strongly dependent upon repopulation of a substantial proportion of mouse liver with human cells as measured by production of human

proteins. This is not surprising since this hypothesis is what development of this mouse model was founded upon: in order for HCV to replicate in a rodent, one must first provide a viable engraftment of human (or alternatively chimpanzee) hepatocytes in that rodent. Although we use a dot blot serum level of HA at 4 weeks PT of 200 $\mu\text{g/ml}$ or 250 $\mu\text{g/ml}$ as our “threshold”, in reality mice with weaker grafts may still harbor HCV infections but with titers so low that even RT-PCR cannot detect them. By setting our “threshold” dot blot measurement higher (250 $\mu\text{g/ml}$ serum HA versus 200 $\mu\text{g/ml}$) we get a lower percentage of “successful” grafts (54% vs 64% with fresh hepatocytes) but a higher success rate of HCV infection (75% versus 64% with fresh serum). The 6 or 8 week graft signal may prove to be more predictive of infection success, and I also believe the hAAT ELISA assay to be more accurate and reproducible than the dot blot assay. Dot blot measurements of 200 $\mu\text{g/ml}$ and 250 $\mu\text{g/ml}$ correspond to hAAT ELISA values of approximately 25 $\mu\text{g/ml}$ and 31 $\mu\text{g/ml}$ respectively (from Figure 13)

Comparison of success of HCV infection using fresh versus frozen / thawed serum strongly suggests that the infectivity of frozen serum is less than that of freshly collected serum for the SCID/uPA mice. This is despite the presence of high levels of HCV RNA detectable in the thawed serum by RT-PCR. Since the serum is frozen without the use of any cryoprotectants, it is possible that an enveloped virus such as HCV suffers structural damage as the result of ice crystal formation. One approach that has been suggested is to freeze the serum in 10% DMSO in an effort to maintain infectivity, assuming that an intraperitoneal injection of 10% DMSO would not have any untoward effects in our mice. This has not been tried yet. Because we have fairly easy access to fresh serum from chronic carriers of HCV, we have decided to simply use fresh serum exclusively. The problem that this presents is that we will not necessarily know the genotype and HCV RNA titer of the serum that we are using to inoculate our mice until some time after the inoculation. This problem could be largely resolved if more HCV-infected patients were genotyped and had levels of serum HCV RNA quantified by RT-PCR.

Unfortunately using fresh serum for inoculation is not the final answer for the SCID/uPA model. Even using fresh serum we have observed instances where mice with seemingly strong graft signals are inoculated with fresh serum yet do not show any

evidence of HCV infection. Lanford *et al.* noticed similar results with their cultured primary chimpanzee hepatocytes (134) and hypothesized the possibility of neutralizing antibodies existing in some sera as possible reasons for lack of infectivity. There are obviously many variables dictating whether or not our mice are successfully infected with HCV including: (i) the genetic background of the individual mouse, (ii) the hepatocytes that are used for transplant, (iii) the technical success of the transplant, and (iv) the serum inoculum used. We have gained important insight into many of these aspects in the past 2 years but we have yet to explain why fresh serum from some HCV positive patients is successful in our model, while serum from other patients is not. From our early observations, neither the genotype nor the HCV RNA titers can satisfactorily explain this phenomenon since we have had successful infections using genotypes 1A, 3A and 6A and using serum with HCV RNA titers as low as 4.2×10^3 copies per ml. Just as our experience has taught us that “not all homozygotes are created equal”, I think that one of the major challenges in increasing the reproducibility of this mouse model lies in discovering what factors determine why serum from HCV-infected patients will or will not successfully infect our mice. Since LDL has been shown to inhibit endocytosis of HCV *in vitro* (15), is it not possible that patient serum with high levels of LDL may be less infectious in our mice compared to serum from a patient with lower levels of LDL? If cells from patients lacking the LDL receptor cannot bind HCV *in vitro* (15), are these patients immune to HCV infection? Our lab would have a significant advantage over other labs in exploring the association between HCV and LDL not only because we have the best small animal model for HCV but also because Dr. Donna Douglas already has experience in the area of lipid research. Other plausible explanations to explain the phenomenon of mice with apparently strong signals failing to become infected with HCV include defects or deficiencies in viral receptors on the human hepatocytes they have been transplanted with.

The finding that SCID/uPA mice transplanted with fresh human hepatocytes can maintain their graft for greater than 49 weeks PT and demonstrate HCV RNA levels that are in the same range as that seen in humans for 42 weeks post-inoculation is very encouraging. Once again the challenge will be to determine why some mice are more successful in terms of longevity of graft function and HCV infection than their littermates

receiving the same cells and same serum inoculum. While technical factors related to the transplant operation and different levels of IgG leakiness over time may play some role, it is more likely that there are subtle differences in the genetic makeup of individual transgenic mice that play a larger role. What is clearly evident once again from the follow up of these 4 infected animals is that an active HCV infection cannot be sustained in this model without a viable underlying human hepatocyte graft in which the virus can replicate. The 4 long-term followed mice demonstrated higher levels of human proteins in their serum than was seen in the series of 21 homozygote and heterozygote mice. The highest recorded hAAT level in the long term follow up group was 955 µg/ml (seen at 14 weeks post transplant) which corresponds to 55% of the normal level seen in humans.

The Albert Einstein group reported serum hAAT levels between 11 – 14% of the level found in normal human plasma (but don't give their reference level used for this calculation) in their RAG model of HBV transplanted with an immortalized human cell line that is transfected with HBV DNA *in vitro* (130). In their RAG/uPA model of HBV using transplantation of primary human hepatocytes, they estimate their serum albumin production to be 1-10% of normal human levels. It is difficult to compare these results directly with our own given the different assays used to quantify the human serum proteins and the possibly different reference levels used for calculations. It does seem however that our mice are capable of achieving much higher levels of human proteins in the serum compared to the RAG/uPA mouse model.

The group from Stanford (132) using the human encapsulated hepatocytes transplanted under the kidney capsule of a NOD/SCID mouse reported peak serum hAAT levels between 1-10 µg/ml in their model. Using essentially the same hAAT ELISA in our mice, we have demonstrated much higher levels of serum hAAT in our mouse model.

The results from the interferon experiment suggest that this drug does decrease HCV RNA titers in this model. This is very encouraging and suggests that this mouse model for HCV can be used for antiviral agent testing and that the virus responds at least somewhat similarly in our model as in humans. Although the numbers are small, it is interesting to note that two of the animals infected with genotype 3 had a sustained response with IFN administration since response to IFN is strongest for patients infected with genotypes 2 and 3. These results may provide some insight into the true mechanism

of action of interferon in HCV infections as our mice are immunodeficient and so any decrease in HCV RNA titers is presumably due to direct antiviral effects of IFN.

Combining the results of neonatal mortality, post-operative mortality, success of graft function and success of inoculation allows us to analyze the overall efficacy of our SCID/uPA mouse model. If we use a cutoff of 200 $\mu\text{g/ml}$ serum HA by 4 week PT DB assay and follow 100 mice from time of birth, we estimate that 75 will survive to time of transplant and 66 will survive the transplant procedure itself. If we transplant fresh hepatocytes, 42 of 66 (64%) will have a 4 week dot blot signal $> 200 \mu\text{g/ml}$ and if we inoculate all of these animals with fresh serum, 27 of 42 (64%) should be successfully infected with HCV. Using a cutoff of 250 $\mu\text{g/ml}$, we would generate 36 (54%) mice with “successful” grafts, and inoculating them would lead to 27 of 36 (75%) successfully infected mice. Although both cutoff levels ultimately generate the same number of successfully infected animals ($n=27$), using the lower cutoff level of 200 $\mu\text{g/ml}$ means that more animals will be inoculated and must therefore be analyzed by the Provincial Lab by either qualitative or quantitative RT-PC. Both of these assays are very costly. In the future it may be possible to perform “in-house” quantification of HCV RNA that should prove more cost effective.

In order to improve the efficacy of this model, a multifaceted approach is required. Starting at the breeding level, we need to try to breed younger animals so as to cut down on our neonatal mortality rates. We also need to be able to reliably distinguish heterozygous animals from homozygous animals, a task that has proven more difficult than was expected. We need to switch from halothane to enflurane anesthesia and transplant the baby mice between 10-15 days of age to decrease our post-operative mortality rates. We need to transplant the mice with fresh hepatocytes when available and only inoculate them with freshly collected infectious serum. We have already begun to check graft function immediately before inoculation to see if this predicts infection success better than the 4 week PT Dot Blot signal. Hopefully as we learn more about this model and HCV infections, our protocol can be modified and our efficacy significantly improved.

CONCLUSION

In conclusion, the quantitative serum assays have allowed us to confirm our hypothesis that repopulation of a substantial proportion of the liver with human hepatocytes is critical for successful HCV infection in the SCID/uPA mouse. Ultimately we would like to be able to produce a large number of mice with active HCV infections and high levels of serum HCV RNA. The results show that the single most important factor predicting success of the HCV infection is the viability of the underlying human hepatocyte graft. Quantitative serum assays provide a quick, reliable means of quantifying graft function using very small amounts of mouse serum. These assays allow us to evaluate the various aspects of our model in order to determine how we can make the model more efficient. To date we have learned that zygosity of the uPA transgene, transplantation of fresh versus frozen hepatocytes, and inoculation with fresh serum are all important determinants of success. Future projects such as the introduction of a hepatocyte growth factor (HGF) transgene, reconstitution with a human immune system and testing of new antiviral agents all rely on a means of evaluating the function of the underlying human hepatocyte graft. The quantitative serum assays should prove valuable tools in the ongoing development of this model.

REFERENCES

1. Choo Q, Kuo G, Weiner A, Overby L, Bradley D, Houghton M. Isolation of a cDNA Clone Derived from a Blood-Borne Non-A, Non-B Viral Hepatitis Genome. *Science* 244, 359-362. 1989.
2. Maddell GL, Bennett JE, Dolin R. Natural History of Hepatitis C. *The American Journal of Medicine* 107, 10S-15S. 1999.
3. Tong MJ, El-Farra NS, Reikes AR, Co RL. Clinical Outcomes After Transfusion-Associated Hepatitis C. *NEJM* 332(22), 1463-1466. 1995.
4. Bartenschlager R, Lohman V. Replication of hepatitis C virus. *Journal of General Virology* 81, 1631-1648. 2000.
5. Honda M, Kaneko S, Matsushita E, Kobayashi K, Abell G, Lemon S. Cell Cycle Regulation of Hepatitis C Virus Internal Ribosomal Entry Site-Directed Translation. *Gastroenterology* 118, 152-162. 2000.
6. Simmonds P. Variability of Hepatitis C Virus. *Hepatology* 21(2), 570-582. 1995.
7. Ito T, Mukaigawa J, Hirabayashi Y, Mitamura K, Yasui K. Cultivation of hepatitis C virus in primary hepatocyte culture from patients with chronic hepatitis C results in release of high titre infectious virus. *Journal of General Virology* 77, 1043-1054. 1996.
8. van Doorn L. Review: Molecular Biology of the Hepatitis C Virus. *Journal of Medical Virology* 43, 345-356. 1994.
9. Clarke BE. Approaches to the development of novel inhibitors of hepatitis C virus replication. *Journal of Viral Hepatitis* 2, 1-8. 1995.
10. Pileri P. Binding of Hepatitis C Virus to CD81. *Science* 282, 938-941. 1998.
11. Rice C. Is CD81 the key to Hepatitis C Virus Entry? *Hepatology* 29, 990-991 1999.
12. Petracca R, Falugi F, Galli G, Norais N, Rosa D, Campagnoli S, Burgio V, Di Stasio E, Giradina B, Houghton M, Abrignani S, Grandi G. Structure-Function Analysis of Hepatitis C Virus Envelope-CD81 Binding. *Journal of Virology* 74, 4824-4830. 2000.
13. Meola A, Sbardellati A, Bruni B, Cerretani M, Pezzanera M, Scarselli E. Binding of Hepatitis C Virus E2 Glycoprotein to CD81 Does Not Correlate with Species Permissiveness to Infection. *Journal of Virology* 74, 5933-5938. 2000.

14. Monazahian M, Bohme I Bonk S Koch A Scholz C Grethe S Thomssen R . Low Density Lipoprotein Receptor as a Candidate Receptor for Hepatitis C Virus. *Journal of Medical Virology* 57, 223-229. 1999.
15. Agnello V, Abel G Elfahal M Knight G Zhang Q . Hepatitis C virus and other Flaviviridae viruses enter cells via low density lipoprotein receptor. *Proc Natl Acad Sci USA* 96, 12766-12771. 1999.
16. Yoshikura H, Hijikata M Nakajima N Shimizu Y . Replication of hepatitis C virus. *Journal of Viral Hepatitis* 3, 3-10. 1996.
17. Takahashi M, Yamada G Miyamoto R Doi T Endo H Tsuji T . Natural Course of Chronic Hepatitis C. *The American Journal of Gastroenterology* 88(2), 240-243. 1993.
18. Shindo M, Di Bisceglie M Biswas R Mihalik K Feinstone S . Hepatitis C Virus Replication during Acute Infection in the Chimpanzee. *Journal of Infectious Diseases* 166, 424-427. 1992.
19. Saleh M, Tibbs C Koskinas J Pereira L Bomford A Portman B MacFarlane I Williams R. Hepatic and Extrahepatic Hepatitis C Virus Replication in Relation to Response to Interferon Therapy. *Hepatology* 20, 1399-1404. 1994.
20. Radkowski M, Wang L Vargas H Rakela J Laskus T . Detection of Hepatitis C Virus Replication in Peripheral Blood Mononuclear Cells After Orthoptic Liver Transplantation. *Transplantation* 66, 664-666. 1998.
21. Kakiuchi N, Komoda Y Komoda K Takeshita N Okada S Tani T Shimotohno K . Non-peptide inhibitors of HCV serine protease. *FEBS Letters* 421, 217-220. 1998.
22. G.Davis. Hepatitis C Virus Genotypes and Quasispecies. *The American Journal of Medicine* 107, 21S-26S. 1999.
23. Gross J. Clinician's Guide to Hepatitis C. *Mayo Clin Proc* 73, 355-361. 1998.
24. Fauci, Braunwald Isselbacher Wilson Martin . Harrison's Principles of Internal Medicine. 19th Edition, 1677-1692. 1999.
25. Donahue JG, Munoz a Ness PM Brown DE Yawn DH . The Declining Risk of Post-Transfusion Hepatitis C Virus Infection. *NEJM* 327(6), 369-373. 1992.
26. van der Peel C. Hepatitis C virus blood transfusion: past and present risks. *Journal of Hepatology* 31 (Suppl. 1), 101-106. 1999.
27. Colquhoun S. Hepatitis C - A Clinical Update. *Arch Surg* 131, 18-23. 1996.

28. Liang T, Rehermann B Seeff L Hoofnagle J . Pathogenesis, Natural History, Treatment, and Prevention of Hepatitis C. *Annals of Internal Medicine* 132, 296-305. 2000.
29. Missale G, Bertoni R Lamonaca V Valli A Massari M Mori C Rumi M Houghton M Fiaccadori Ferrari C . Different Clinical Behaviours of Acute Hepatitis C Virus Infection Are Associated with Different Vigor of the Anti-viral Cell-mediated Immune Response. *Journal of Clinical Investigation* 98, 706-714. 1996.
30. Lechman M, Ihlenfeldt H Braunschweiger I Giers G Jung G Matz B Kaiser R Sauerbruch T Spengler U . T- and B-Cell Responses to Different Hepatitis C Virus Antigens in Patients With Chronic Hepatitis C Infection and in Healthy Anti-Hepatitis C Virus-Positive Blood Donors Without Viremia. *Hepatology* 790-795. 1996.
31. Davis GL, Balart LA Schiff ER Lindsay K Bodenheimer H . Future Options for the Management of Hepatitis C. *Seminars in Liver Disease* 19, 103-111. 1999.
32. Farci P, Alter H Govindarajan S Wong D Engle R Lesniewski R Mushahwar I Desai S . Lack of Protective Immunity Against Reinfection with Hepatitis C Virus. *Science* 258, 135-140. 1992.
33. Farci P, Orgiana G Purcell R . Immunity Elicited by Hepatitis C Virus. *Clinical and Experimental Rheumatology* 13, S9-S12. 1995.
34. Kuo G, Choo Q Alter J Gitnick G Redeker G Purcell R Miyamura T Dienstag J Alter M Stevens C Tegtmeier G Bonino F Colombo M Lee W Kuo C Berger K Shuster J Overby L Bradley D Houghton M . An Assay for Circulating Antibodies to a Major Etiologic Virus of Human Non-A, Non-B Hepatitis. *Science* 244, 362-364. 1989.
35. Schiff E, de Medina M, Kahn R. New Perspectives in the Diagnosis of Hepatitis C. *Seminars in Liver Disease* 19, Suppl 1, 3-15. 1999.
36. Houghton M, Weiner A Han J Kuo G Choo Q . Molecular Biology of the Hepatitis C Viruses: Implications for Diagnosis, Development and Control of Viral Disease. *Hepatology* 14(2), 381-388. 1991.
37. Yu M, Chuang W Chen S Lin Z Hsieh M Wang L Chang W . Clinical application of the Quantiplex HCV RNA 2.0 and Amplicor HCV Monitor assays for quantifying serum hepatitis C virus RNA. *Journal of Clinical Pathology* 52, 807-811. 1999.
38. Sakamoto N, Enomoto N Kurosaki M Marumo F Sato C . Detection and quantification of hepatitis C virus RNA replication in the liver. *Journal of Hepatology* 20, 593-597. 1994.

39. Laskus T, Radkowski M Wang L Vargas H Rakela J. Search for Hepatitis C Virus Extrahepatic Replication Sites in Patients With Acquired Immunodeficiency Syndrome: Specific Detection of Negative-Strand Viral RNA in Various Tissues. *Hepatology* 28, 1398-1402. 1998.
40. Negro F, Pacchioni D Shimizu Y Miller R Bussolati G Purcell R Bonino F . Detection of intrahepatic replication of hepatitis C virus RNA by in situ hybridization and comparison with histopathology. *Proc Natl Acad Sci USA* 89, 2247-2251. 1992.
41. Krawczynski K, Beach M Bradley D Kuo G Di Bisceglie A Houghton M Reyes G Kim J Choo Q Alter M . Hepatitis C Virus Antigen in Hepatocytes: Immunomorphologic Detection and Identification. *Gastroenterology* 103, 622-629. 1992.
42. Negro F, Giostra E Krawczynski K Quadri R Rubbia-Brandt L Mentha G Colucci G Perrin L Hadengue A . Detection of intrahepatic hepatitis C virus replication by strand-specific semi-quantitative RT-PCR: preliminary application to the liver transplantation model. *Journal of Hepatology* 29, 1-11. 1998.
43. Brody R, End S Melamed J Mizrahi H Schneider R Tobias H Teperman L Theise N . Immunohistochemical Detection of Hepatitis C Antigen by Monoclonal Antibody TORDJI-22 Compared with PCR Viral Detection. *American Journal of Pathology* 110, 32-37. 1998.
44. Seeff LB. Natural History of Hepatitis C. *The American Journal of Medicine* 107(6B), 10S-15S. 1999.
45. Fried MW. Therapy of Chronic Viral Hepatitis. *Medical Clinics of North America* 80(5), 957-979. 1996.
46. Dhillon A, Dusheiko G. Pathology of hepatitis C Virus Infection. *Histopathology* 26, 297-309. 1995.
47. Terrault NA, Wright TL . Hepatitis C Virus in the Setting of Transplantation. *Seminars in Liver Disease* 15(1), 92-100. 1995.
48. Dusheiko GM, Khakoo S Soni P Grellier L . A Rational Approach to the Management of Hepatitis C Infection. *BMJ* 312, 357-364. 1996.
49. Peters M. Mechanisms of Action of Interferons. *Seminars in Liver Disease* 9(4), 235-238. 1989.
50. Pawlotsky J, Germanidis G Neumann A Pellerin M Frainais P Dhumeaux D . Interferon Resistance of Hepatitis C Virus Genotype 1b: Relationship to Nonstructural 5A Gene Quasispecies Mutations. *Journal of Virology* 72(4), 2795-2805. 1998.

51. Tilg H. New Insights Into the Mechanisms of Interferon Alpha: An Immunoregulatory and Anti-inflammatory Cytokine. *Gastroenterology* 112, 1017-1021. 1997.
52. Perelson A. Viral Kinetics and Mathematical Models. *The American Journal of Medicine* 107, 49S-52S. 1999.
53. Neumann AU, Lam NP Dahari H Gretch DR Wiley TE Layden TJ Perelson AS . Hepatitis C Virus Dynamics *In Vivo* And The Antiviral Efficacy of Interferon Alfa Therapy. *Science* 29, 103-107. 1998.
54. Yasui K, Okanoue T Murakami Y Itoh Y Minami M Sakamoto S Sakamoto M Nishoji K . Dynamics of Hepatitis C Viremia following Interferon-alpha Administration. *The Journal of Infectious Disease* 177, 1475-1479. 1998.
55. Zeuzem S, Schmidt J Lee J von Wagner M Teuber G Roth W . Hepatitis C Virus Dynamics In Vivo: Effect of Ribavirin and Interferon Alfa on Viral Turnover. *Hepatology* 28, 245-252. 1998.
56. Ahmed A, Keefe E . Treatment of Chronic Hepatitis C. *Clinics in Liver Disease* 3, 757-773. 1999.
57. Tong M, Reddy R Lee W Pockros P Hoefs J Keefe E Hollinger F . Treatment of Chronic Hepatitis C With Consensus Inteferon: A Multicenter, Randomized, Controlled Trial. *Hepatology* 26, 747-754. 1997.
58. Wong J. Cost-Effectiveness of Treatments for Chronic Hepatitis C. *The American Journal of Medicine* 107 (6B), 74S-78S. 1999.
59. Gutfreund K, Bain V. Chronic Viral Hepatitis C: management update. *CMAJ* 162, 827-833. 2000.
60. Hoofnagle J, Di Bisceglie A . The Treatment of Chronic Viral Hepatitis. *NEJM* 336, 347-356. 1997.
61. Shiffman M, Hofmann C Thompson E Ferreira-Gonzalez A Contos M Koshy A Luketic V Sanyal A Mills A Garrett C . Relationship Between Biochemical, Virological, and Histological Response During Interferon Treatment of Chronic Hepatitis C. *Hepatology* 26, 780-785. 1997.
62. Davis GL, Balart LA Schiff ER Lindsay K Bodenheimer H . Treatment of Chronic Hepatitis C With Recombinant Interferon Alfa - A Multicenter Randomized, Controlled Trial. *NEJM* 321(22), 1501-1505. 1989.
63. Gavier B, Martinez-Gonzalez M Riezu-Boj J Lasarte J Garcia N . Viremia After One Month of Interferon Therapy Predicts Treatment Outcome in Patients With Chronic Hepatitis C. *Gastroenterology* 113, 1647-1653. 1997.

64. Chemello L, Bonetti P Cavalletto L Talato F Donadon V Casarin P Belussi F . Randomized Trial Comparing Three Different Regimens of Alpha-2a-Interferon in Chronic Hepatitis C. *Hepatology* 22(3), 700-705. 1995.
65. Glue P, Rouzier-Panis R Raffanel C Sabo R Gupta S Salfi M Jacobs S Clement R. A Dose-Ranging Study of Pegylated Interferon Alfa-2b and Ribavirin in Chronic Hepatitis C. *Hepatology* 32, 647-653. 2000.
66. Neddermann P, Tomei L Steinkuhler C Gallinari P Tramontano A . The Nonstructural Proteins of the Hepatitis C Virus: Structure and Functions. *Biol.Chem.* 378, 469-476. 1997.
67. Taylor D, Shi S Romano P Barber G Lai M . Inhibition of the Interferon-Inducible Protein Kinase PKR by HCV E2 Protein. *Science* 285, 107-109. 1999.
68. Fukuma T, Enomoto N Marumo F Sato C. Mutations in the Interferon-Sensitivity Determining Region of Hepatitis C Virus and Transcriptional Activity of the Nonstructural Region 5A Protein. *Hepatology* 28, 1147-1153. 1998.
69. Patterson JL, Fernandez-Larson R . Molecular Mechanisms of Action of Ribavirin. *Reviews of Infectious Diseases* 12(6), 1139-1145. 1990.
70. Lai M, Kao J Yang P Wang J Chen P Chan K Chu J . Long-term Efficacy of Ribavirin Plus Interferon Alfa in the Treatment of Chronic Hepatitis C. *Gastroenterology* 111, 1307-1312. 1996.
71. Levine R. Treating Histologically Mild Chronic Hepatitis C: Monotherapy, Combination Therapy, or Tincture of Time? *Ann Intern Med* 129(4), 323-326. 1998.
72. Di Bisceglie A. Chronic Hepatitis C Viral Infection in Patients With Normal Serum Alanine Aminotransferases. *The American Journal of Medicine* 107, 53S-55S (1999).
73. Jacobson I. Management of Interferon Relapsers. *The American Journal of Medicine* 107, 62S-66S (1999).
74. Bacon B. Available Options for Treatment of Interferon Nonresponders. *The American Journal of Medicine* 107, 67S-69S (1999).
75. Younossi Z, Perrillo R . The Roles of Amantadine, Rimantadine, Ursodeoxycholic Acid and NSAIDS, Alone or in Combination With Alpha Interferons, in teh Treatment of Chronic Hepatitis C. *Seminars in Liver Disease* 19, 95-101 (1999).
76. Khalili M, Denham C Perrillo R . Interferon and Ribavirin Versus Interferon and Amantadine in Interferon Nonresponders With Chronic Hepatitis C. *The American Journal of Gastroenterology* 95, 1284-1289 (2000).

77. Brillanti S, Levantesi F Masi L Foli M Bolondi L . Triple Antiviral Therapy as a New Option for Patients With Interferon Nonresponsive Chronic Hepatitis C. *Hepatology* 32, 630-634 (2000).
78. Mangia A, Minerva N Annese M Leandro G Villani M Santoro R Carretta V Bacca D . A Randomized Trial of Amantadine and Interferon Versus Interferon Alone as Initial Treatment for Chronic Hepatitis C. *Hepatology* 33, 989-993 (2001).
79. Lemon S, Thomas D . Vaccines to prevent Viral Hepatitis. *NEJM* 336(3), 196-204. 1997.
80. Farci P, Shimoda A Wong D Cabezon T De Gioannis D Strazzera A Shimizu Y . Prevention of hepatitis C virus infection in chimpanzees by hyperimmune serum against the hypervariable region 1 of the envelope 2 protein. *Proc Natl Acad Sci USA* 93, 15394-15399. 1996.
81. Mosier D, Gulizia R Baird S Wilson D . Transfer of a functional human immune system to mice with severe combined immunodeficiency. *Nature* 335, 256-259. 1988.
82. Choo Q, Kuo G Ralston R Weiner A Chien D Van Nest G Han J Berger K Thudium K Kuo C Kansopon J McFarland J Tabrizi A Ching K Moss B Cummins L Houghton M Muchmore E . Vaccination of chimpanzees against infection by the hepatitis C virus. *Proc Natl Acad Sci USA* 91, 1294-1298. 1994.
83. Sakamoto N, Wu C Wu G. Intracellular Cleavage of Hepatitis C Virus RNA and Inhibition of Viral Protein Translation by Hammerhead Ribozymes. *Journal of Clinical Investigation* 98, 2720-2727. 1996.
84. Lieber A, He C Polyak S Gretch D Barr D Kay M . Elimination of Hepatitis C Virus RNA in Infected Human Hepatocytes by Adenovirus-Mediated Expression of Ribozymes. *Journal of Virology* 70, 8782-8791. 1996.
85. Wakita T, Wands J . Specific Inhibition of Hepatitis C Virus Expression by Antisense Oligodeoxynucleotides. *Journal of Biological Chemistry* 269, 14205-14210. 1994.
86. Araya V, Rakela J Wright T . Hepatitis C After Orthoptic Liver Transplantation. *Gastroenterology* 112, 575-582. 1997.
87. Di Martino V, Saurini F Samuel D Gigou M Dussaix E Reynes M Bismuth H Feray C . Long-Term Longitudinal Study of Intrahepatic Hepatitis C Virus Replication After Liver Transplantation. *Hepatology* 26, 1343-1350. 1997.
88. Gane E, Nauomov N Qian K Mondelli M . A Longitudinal Analysis of Hepatitis C Virus Replication Following Liver Transplantation. *Gastroenterology* 110, 167-177. 1996.

89. Chazouilleres O, Kim M Combs C Ferrell L Bacchetti P Roberts J Ascher N Neuwald P Wilber J Urdea M Quan S Sanchez-Pescador R Wright T . Quantitation of Hepatitis C Virus RNA in Liver Transplant Recipients. *Gastroenterology* 106, 994-999. 1994.
90. Forman LM, Lucey M. Orthoptic Liver Transplantation for Hepatitis C: Analysis of Allograft Survival Using the UNOS Database. *American Journal of Transplantation* Vol 1 (Suppl 1), 156. 2001
91. Berenguer M, Wright TL . Hepatitis C and liver transplantation. *Gut* 45, 159-163. 1999.
92. Bizollon T, Ducerf C Trepo C . Hepatitis C virus recurrence after liver transplantation. *Gut* 44, 575-580. 1999.
93. Vargas H, Laskus T Wang L Lee R Radkowski M Dodson F Fung J Rakela J . Outcome of Liver Transplantation in Hepatitis C Virus-Infected Patients Who Received Hepatitis C Virus-Infected Grafts. *Gastroenterology* 117, 149-153. 1999.
94. Mercer D. Development of an Animal Model of Hepatitis C. PhD Thesis, 1999.
95. Mercer DF, Schiller DE, Elliott JF, Douglas DN, Hao C, Rinfret A, Addison WR, Fischer KP, Churchill TA, Lakey JRT, Tyrrell DLJ, Kneteman NM. Hepatitis C Virus Replication in Mice with Chimeric Human Livers. *Nature Medicine* August 2001. (accepted for publication)
96. Heckel J, Sandgren EP Degen JL Palmiter RD Brinster RL . Neonatal Bleeding in Transgenic Mice Expressing Urokinase-Type Plasminogen Activator. *Cell* 62, 447-456. 1990.
97. Sandgren EP, Palmiter RD Heckel JL Daugherty CC Brinster RL Degen JL . Complete Hepatic Regeneration after Somatic Deletion of an Albumin-Plasminogen Activator Transgene. *Cell* 66, 245-256. 1991.
98. Rhim JA, Sandgren EP Degen JL Palmiter RD Brinster RL . Replacement of Diseased Mouse Liver by Hepatic Cell Transplantation. *Science* 263, 1149-1152. 1994.
99. Rhim JA, Sandgren EP Degen JL Palmiter RD Brinster RL . Complete reconstitution of mouse liver with xenogeneic hepatocytes. *Proc Natl Acad Sci USA* 92, 4942-4946. 1995.
100. Sandgren E, Palmiter R Heckel J Brinster R Degen J . DNA rearrangement causes hepatocarcinogenesis in albumin-plasminogen activator transgenic mice. *Proc Natl Acad Sci USA* 89, 11523-11527. 1992.

101. Jamal H, Weglarz T Sandgren E . Cryopreserved Mouse Hepatocytes Retain Regenerative Capacity In Vivo. *Gastroenterology* 118, 390-394. 2000.
102. Hendrickson E. The SCID Mouse: Relevance as an Animal Model System for Studying Human Disease. *American Journal of Pathology* 143, 1511-1522. 1993.
103. Alt F, Oltz E Young F Gorman J Taccioli G Chen J . VDJ Recombination. *Immunology Today* 13(8), 306-314. 1992.
104. Nonoyama S, Smith F Bernstein I Ochs H . Strain-Dependent Leakiness of Mice with Severe Combined Immune Deficiency. *Journal of Immunology* 150, 3817-3824. 1993.
105. Roder J, D.A. The beige mutation in the mouse selectively impairs natural killer cell function. *Nature* 278, 451-453. 1979.
106. Spritz R. Genetic Defects in Chediak-Higashi Syndrome and the beige mouse. *Journal of Clinical Immunology* 18, 97-104. 1998.
107. Seglen P. Preparation of rat liver cells. Enzymatic requirements for tissue dispersion. *Exp Cell Res* 82, 391-398. 1973.
108. Berry M. High-Yield Preparation of Isolated Rat Liver Parenchymal Cells. Friend D. *Journal of Cell Biology* 43, 506-520. 1969.
109. Caruana M. Isolation of Human Hepatocytes sfter Hepatic Warm and Cold Ischemia: A Practical Approach Using University of Wisconsin Solution. Battle T, Fuller B Davidson B. *Cryobiology* 38, 165-168. 1999.
110. Reese J. Isolation and Culture of Adult Hepatocytes from Liver Biopsies. Byard J. *In Vitro* 17(11), 935-939. 1981.
111. Ballet F. Isolation, Culture and Characterization of Adult Human Hepatocytes from Surgical Liver Biopsies. Bouma M, Wang S Amit N Marais J Infante R. *Hepatology* 4(5), 849-854. 1984.
112. Gerlach J. Comparison of Four Methods for Mass Hepatocyte Isolation from Pig and Human Livers. Brombacher J, Kloppel K Schnoy N Neuhaus P. *Transplantation* 57(9), 1318-1322. 1994.
113. Kreamer B. Use of a Low-Speed, Iso-Density Percoll Centrifugation Method to Increase the Viability of Isolated Rat Hepatocyte Preparations. Staecker J, Sawada N Sattler G Hsia S Pitot H. *In Vitro Cellular & Developmental Biology* 22(4), 201-211. 1986.

114. Dorko K, Freeswick PD, Bartoli F, Cicalese L, Bardsley BA, Tzakis A, Nussler AK. A New Technique for Isolating and Culturing Human Hepatocytes from Whole or Split Livers not used for Transplantation. *Cell Transplantation* 3(5), 387-395. 1994.
115. Novicki D, Irons G, Strom S, Jirtle R, Michalopoulos G. Cryopreservation of Isolated Rat Hepatocytes. *In Vitro* 18(4), 393-399. 1982.
116. Loretz LJ, Li AP, Flye MW, Wilson GE. Optimization of cryopreservation procedures for rat and human hepatocytes. *Xenobiotica* 19(5), 489-498. 1989.
117. Adams R, Wang M, Crane A, Brown B, Darlington G, Ledley F. Effective Cryopreservation and Long-Term Storage of Primary Human Hepatocytes with REcovery of Viability, Differentiation, and Replicative Potential. *Cell Transplantation* 4(6), 579-586. 1995.
118. Gomez M. Biochemical Functionality and Recovery of Hepatocytes after Deep Freezing Storage. Lopez P, Castell J. *In Vitro* 20(11), 826-833. 1984.
119. Chesne C, Guyomard C, Fautrel A, Poullain M, Fremond B, De Jong H, Guillouzo A. Viability and Function in Primary Culture of Adult Hepatocytes from Various Animal Species and Human Beings After Cryopreservation. *Hepatology* 18, 406-414. 1993.
120. Gupta S, Bhargava K, Novikoff P. Mechanisms of Cell Engraftment During Liver Repopulation with Hepatocyte Transplantation. *Seminars in Liver Disease* 19, 15-26. 1999.
121. Gupta S, Rajvanshi P, Bhargava K, Andrew Kerr. Hepatocyte Transplantation. *Progress in Liver Diseases* 14, 199-222. 1996.
122. Shimizu Y, Igarashi H, Kiyohara T, Shapiro M, Wong D, Purcell R, Yoshikura H. Correlation between the infectivity of hepatitis C in vivo and infectivity in vitro. *Proc Natl Acad Sci USA* 90, 6037-6041. 1993.
123. Bassett S, Thomas D, Brasky K, Lanford R. Viral Persistence, Antibody to E1 and E2, and Hypervariable Region 1 Sequence Stability in Hepatitis C Virus-Inoculated Chimpanzees. *Journal of Virology* 73, 1118-1125. 1999.
124. Xie Z, Riezu-Boj J, Lasarte J, Guillen J, Su J, Civeira M, Prieto J. Transmission of Hepatitis C Virus Infection to Tree Shrews. *Virology* 244, 513-520. 1998.
125. Major M, Mihalik K, Fernandez J, Seidman J, Kleiner D, Kolykhalov A, Rice C, Feinstone S. Long Term Follow-Up of Chimpanzees Inoculated with the First Infectious Clone for Hepatitis C Virus. *Journal of Virology* 73, 3317-3325. 1999.

126. Galun E, Burakova T Ketzinel M Lubin I Shezen E Kahana Y Eid A Ilan Y Rivkind A Pizov G Shouval D Reisner Y . Hepatitis C Virus Viremia in SCID/BNX Mouse Chimera. *Journal of Infectious Diseases* 172, 25-30. 1995.
127. Ilan E, Burakova T Dagan S Nussbaum O Lubin I Eren R Ben-Moshe O Arazi J Berr S Neville L Yuen L Mansour T. The Hepatitis B Virus-Trimera Mouse: A Model for Human HBV Infection and Evaluation of Anti-HBV Therapeutic Agents. *Hepatology* 29[2], 553-561. 1999.
128. Notatangelo L, Villa A Schwarz K. RAG and RAG defects RAG and RAG defects. *Current Opinion in Immunology* 11, 435-442. 1999.
129. Petersen J, Dandri M, Gupta S, Rogler C. Liver repopulation with xenogenic hepatocytes in B and T cell-deficient mice leads to chronic hepadnavirus infection and clonal growth of hepatocellular carcinoma. *Proc Natl Acad Sci USA* 95, 310-315. 1998.
130. Brown J. A Long-Term Hepatitis B Viremia Model Generated by Transplanting Nontumorigenic Immortalized Human Hepatocytes in Rag-2-Deficient Mice. *Hepatology* 173-181. 2000.
131. Dandri M, Burda M Torok E Pollok J Iwanska A Sommer G Rogiers X Rogler C Gupta S Will H Greten H Petersen J . Repopulation of Mouse Liver With Human Hepatocytes and In Vivo Infection with Hepatitis B Virus. *Hepatology* 33, 981-988. 2001.
132. Ohashi K, Marion P, Nakai H, Meuse L, Cullen J, Bordier B, Scwall R, Greenberg H, Glenn J, Kay M. Sustained survival of human hepatocytes in mice: A model for in vivo infection with human hepatitis B and hepatitis delta viruses. *Nature Medicine* 6(3), 327-331. 2000
133. Iacovacci S, Manzin A Barca S Sargiacomo M Serafino A Valli M Macioce G Hassan J Ponzetto A Clementi M Peschle C Carloni G . Molecular Characterization and Dynamics of Hepatitis C Virus Replication in Human Fetal Hepatocytes Infected *In Vitro*. *Hepatology* 26, 1328-1337. 1997.
134. Lanford R, Sureau C Jacob J White R Fuerst T . Demonstration of *In Vitro* Infection of Chimpanzee Hepatocytes with Hepatitis C Virus Using Strand-Specific RT/PCR. *Virology* 202, 606-614. 1994.
135. Yoo B, Shelby M Choe J Suh B Choi B Joh J Nuovo G Lee H Houghton M Han J. Transfection of a Differentiated Human Hepatoma Cell Line (Huh 7) with In Vitro-Transcribed Hepatitis C Virus (HCV) RNA and Establishment of a Long-Term Culture Persistently Infected with HCV. *Journal of Virology* 69, 32-38. 1995.

136. Dash S, Halim A Tsuji H Hiramatsu N Gerber M . Transfection of HepG2 Cells with Infectious Hepatitis C Virus Genome. *American Journal of Pathology* 151, 363-372. 1997.
137. Pietschmann T, Lohmann V Rutter G Kurpanek K Bartenschlager R . Characterization of Cell Lines Carrying Self-Replicating Hepatitis C Virus RNAs. *Journal of Virology* 75, 1252-1264. 2001.
138. Shmizu Y, Iwamoto A Hijikata M Purcell R Yoshikura H . Evidence for in vitro replication of hepatitis C virus genome in a human T-cell line. *Proc Natl Acad Sci USA* 89, 5477-5481. 1992.
139. Kato N, Nakazawa T Mizutani T Shimotohno K . Susceptibility of Human T-Lymphotropic Virus Type 1 Infected Cell Line MT-2 to Hepatitis C Virus Infection. *Biochemical and Biophysical Research Communications* 206, 863-869. 1995.
140. Nakajima N, Hijikata M Yoshikura H Shimizu Y . Characterization of Long-Term Cultures of Hepatitis C Virus. *Journal of Virology* 70, 3325-3329. 1996.
141. Shimizu Y, Igarashi H Kiyohara T Shapiro M Wong D Purcell R Yoshikura H . Infection of a chimpanzee with hepatitis C virus grown in cell culture. *Journal of General Virology* 79, 1383-1386. 1998.
142. Kullander S, Nilsson I. Human Placental Transfer of an Antifibrinolytic Agent (AMCA). *Acta Obstet Gynec Scand* 49, 241-242. 1970.
143. Yolken R. Enzyme Immunoassays for the Detection of Infectious Antigen in Body Fluids: Current Limitations and Future Prospects. *Reviews of Infectious Diseases* 4(1), 35-60. 1982

APPENDIX:**1. HEPATOCYCE ISOLATION:****SOLUTIONS:**

- Collagenase Base (make ~450 cc first, pH to 7.5, and then top up to 500 cc)
 - 500 cc double-filtered H₂O
 - 1.95 g NaCl
 - 0.25 g KCl
 - 0.35 g CaCl₂
 - 12000 mg HEPES buffer
 - pH to 7.5 with NaOH
- Dulbecco's Phosphate Buffered Saline (DPBS) (Sigma, #D-5652):
 - 1 pkg of CMF (Ca²⁺-Mg²⁺ free) DPBS + 1 liter of double-filtered H₂O

OR

- 1 pkg of DPBS with Ca-Mg + 1 liter of double-filtered H₂O + 0.1861 g Na₂EDTA
- Percoll 1.127 stock (make in fumehood):
 - 16 ml of 10X Isolation Media + 184 ml Percoll stock
- Percoll 1.04 working solution (make in fumehood):
 - 31.5 ml of 1.127 Percoll stock + 68.5 ml of 1X Isolation Media
- Collagenase Working Solution:
 - Liberase HI: 52.5 mg + 150 ml Collagenase Base (0.75 mg/ml MAX)

OPERATING ROOM PROCEDURE:

1. Bring to OR:
 - 250 cc of DPBS on ice
 - Sterile specimen container
2. After receiving tissue from surgeon:
 - Flush dominant vessels with DPBS using 10 cc syringe and 14 gauge angiocath

- Flush until pale
 - Place in sterile container with remaining DPBST
3. Obtain sticker from chart, record warm ischemia time and cold ischemia time

HEPATOCYTE ISOLATION:

1. Cannulate dominant vessel(s) by sewing in angiocath (cut to 1 cm length) with 5-0 silk / dextron. Flush with CMF DPBS until pale – IMPORTANT to get rid of all RBCs if possible – blood inhibits collagenase!.
2. Weigh piece of liver with cannulas in – record weight
3. Place tissue in funnel and flush with CMF DPBS through 37 degree water jacket until pale – trying to flush out as much blood as possible before perfusing with collagenase
4. Mix up collagenase in small beaker.
5. Flush circuit with CMF DPBS without EDTA – unhook cannulas from tubing while doing this to avoid big air emboli into liver tissue
6. Hook up circuit with collagenase in recirculating fashion with pump set at 25 = 50 cc/hr.
7. Perfuse with collagenase for 45-60 min
8. Stop pump. Gently remove tissue into shallow dish and manipulate with sterile pipette tips to liberate hepatocytes – ideally leave just vascular skeleton.
9. Wash tissue during manipulation with 50 cc warm Hanks Buffered Salt Solution (HBSS) or with collagenase solution. Pipette resulting cell suspension into two 50 ml conical tubes (Falcon)
10. Weigh remaining liver tissue with cannula – can throw carcass into third conical tube to shake in water bath as well.
11. Shake tubes in 37 degree water bath for 30 minutes
12. Place on ice for 5-10 minutes and continue shaking
13. Pour over coarse (200 μ m) then fine (80 μ m) screens
14. Centrifuge at 500 rpm (80g) for 4 min. Pipette off supernatant and re-suspend in 20 cc cold HBSS. Repeat this step (centrifuge – pipette – re-suspend) X 2.
15. Re-suspend in HBSS

16. Pipette equal amounts of Percoll 1.04 solution and cell suspension into 50 ml conical tubes. Put percoll in first and then gently pipette in cell suspension so as not to disrupt liquid interface. MAX of 5 cc of percoll and 5-8 cc of cell suspension per tube
17. Centrifuge in -5 degrees centrifuge at 1500 rpm (400 g) for 4 minutes.
18. Pipette off supernatant and leave cell pellet in tube
19. Re-suspend cells with HBSS and centrifuge at 500 rpm (80g) for 3 minutes
20. Pipette off supernatant and re-suspend cells in University of Wisconsin (UW) solution (~ 5-10 ml)
21. Place final solution on ice
22. Count cells in hemocytometer. Record number of live cells, number of dead cells. Calculate total number of live cells and viability% with trypan blue

CELL VIABILITY COUNTING:

1. Using 50 μ l pipette, pipette 100 μ l of trypan blue into endorph tube
2. Pipette 50 μ l of cell suspension into endorph tube. Total volume of cell suspension is V
3. Mix by pipetting up and down several times
4. Pipette up 50 μ l of mixture and place onto hemocytometer plate
5. Count inside double-line grid the number of live cells (L1) and the number of dead cells (D1)
6. Repeat for the other side of the hemocytometer plate to get L2 and D2
7. $L = (L1 + L2) / 2$; $D = (D1 + D2) / 2$
8. Total number of live cells per mL of solution = $(L * 3 * 10000)$ cells/mL
9. Total number of live cells = $(L * 3 * 10000)$ cells/mL * V mL
10. Viability % = $L / (L + D)$

2. HEPATOCYTE CRYOPRESERVATION:

1. Turn on programmable freezing bath (Dr. Lakey's Lab) – put holder in EtOH bath, fill up bath with EtOH, THEN turn on 2 switches on front of the machine. Make sure that

- machine is in PTN1 mode – to get to this mode press Reset – PTN1 – Run (This is the mode that cools down the EtOH bath by 1 degree celsius / min)
2. Spin hepatocytes down at 500 rpm for 1 minute at -4 degrees celsius to remove supernatant. Then add “Freeze/Thaw” medium to make up volume to equal 1cc per tube frozen (want minimum of 5-10 Million cells per tube frozen!)
 3. Prepare the hepatocytes at 1.5 M DMSO by stepwise addition of the DMSO solution as follows: at time = 0 add 0.5 ml of 2M DMSO, at time = 5 minutes add 0.5 ml of DMSO, at time = 30 minutes add 2 ml of 2M DMSO. Important to keep the hepatocytes on ice at all times and write on the cryo-tubes with PENCIL, not pen.
 4. After the time = 45 minutes, put the tubes in the EtOH bath (which should be at -7.4 ° C) for 5 minutes
 5. Fill Liquid N₂ flask, and put superconducting rod in it
 6. Nucleation: Touch each tube to the superconducting rod at the level of the air-liquid interface until ice crystals are seen – shake tube gently and then put back in EtOH bath.
 7. Once all tubes have been nucleated – push “STEP” button on the stepper machine and this starts the cooling process down to -40 ° C – when the temperature reaches -38 ° C, remove the tubes from the bath, put them in the metal brackets, label the metal brackets and place them in liquid nitrogen dewars.

Freeze / Thaw Medium :

50 cc fetal calf serum (FCS) + 2.5 cc pen-strep (P-S) -> fill up to 500 cc volume with M199 media

OR

28 cc human albumin (HA) + 2.5 cc pen-strep (P-S) -> fill up to 500 cc volume with M199 media

2M DMSO: 15.62 cc DMSO -> fill up to 100 cc with M199 + SUP

3. HEPATOCYTE THAW:

- A. Fill liquid nitrogen flask. Remove tubes from dewar into liquid nitrogen flask. Once out of the liquid nitrogen, the tube contents begin to rapidly expand as they warm up so put tubes into liquid nitrogen flask quickly or they can EXPLODE!
- B. Take tubes out of liquid nitrogen one at a time and quickly unscrew top of tube to allow liquid nitrogen to escape. Then immerse tube in a 37 °C water bath and gently shake until there is just a small ice crystal left – place tube on ice. Repeat for all the tubes.
- C. Spin tubes at 500 rpm (80g) for 1 minute and discard the supernatant
- D. Keep tubes on ice, add 1 ml of 0.75 M sucrose to each tube at time = 0.
- E. At time = 30 minutes, add 1 ml of freeze / thaw media and shake
- F. At time = 35, add 1 ml of freeze / thaw media and shake
- G. At time = 40, add 4 ml of freeze / thaw media and shake
- H. At time x spin the tubes again at 500 rpm (80g) and discard the supernatant
- I. Re-suspend cells in cold UW solution (5-10 mls) and assess **yield** (number of viable cells upon thawing / number of viable cells that were frozen) and **viability** (percent of thawed cells that are viable)

4. WESTERN BLOT ASSAY:

- A. For each mouse to be tested, add 20 µl of serum to an eppendorph with 1000 µl of 0.2 % NP.40 in TBS, 1 µl of monoclonal mouse anti-human albumin antibody (clone HSA-9, Sigma, # A-2672) and 25 µl of Protein G agarose (Boehringer-Mannheim, # 1 243 233). Place in slow shaker in cold room (4 ° C) overnight.
- B. Spin each eppendorph at 7000 rpm for 1 minute and aspirate supernatant. Add 1 ml of b% NP40/TBS, shake for 1 minute and repeat X 6 times.
- C. After aspirating the supernatant for the last time, add 20 µl of reducing buffer (20% glycerol, 14mM sodium dodecyl sulphate (SDS), 200mM

dithiotreitol (DTT) and bromophenol blue) to each eppendorph. Also add 1 μ l of HA standard (1 mg/ml of HA in TBS, diluted 1:800 in TBS) to an eppendorph with 20 μ l of reducing buffer – this is the positive control.

- D. Heat the eppendorphs for 5 minutes at 100 ° C.
- E. Using a gel loading pipette tip, aspirate the solution from each eppendorph, leaving the beads behind, and load into a 10-well gel. Load the 2 outside lanes with plain reducing buffer, load the first lane with the HA standard, and the last lane with the non-transplanted negative control mouse. Therefore a 10-well gel can be used for 6 mice.
- F. Run the gel at 18mA per gel for 90-100 minutes until blue buffer solution approaches the bottom of the gel
- G. Remove gel from gel apparatus and cut one corner to keep orientation right.
- H. Trim top and bottom of gel and soak in transfer buffer for 5 minutes.
- I. Place gel in transfer apparatus along with fibre mats, filter paper, and a piece of nitrocellulose membrane (Schleicher & Schuell, # 1040259) which has been cut to size.
- J. Attach transfer apparatus to power pack and run at 200 mA for 45 minutes. **Note** – this part can be run overnight and left for a.m. Run transfer in ice bucket as it can generate heat.
- K. Remove nitrocellulose membrane and place in small plastic dish, with the correct side facing up. Tape edges down.
- L. Block for 1 hour with phosphate buffered saline / 3 % v/v Tween-20 (3 % PBST)
- M. Biotinylated primary antibody HSA-11 (Sigma, # A6684) in 0.5% PBST at 1:5000 for 2 hours (30 cc volume)
- N. 3 twenty minute washes with 1% PBST (30 cc volume per wash)
- O. SA-HRP at 1:10000 in 0.1% PBST for 1 hour (30 cc volume)
- P. 6 X 10 minute washes with 0.1% PBST (30 cc volume per wash)

- Q. Mix SuperSignal Chemiluminescent Substrate (Pierce, #34080) reagents as per manufacturers directions (need 2 mls of solution per membrane)
- R. Wrap membrane in saran wrap and take along with Kodak Biomax XL film (Kodak, #868 9358) to darkroom for development. Exposure time of 1-3 seconds is usually sufficient.

5. DOT BLOT ASSAY:

STANDARDS:

To make standards, first dissolve 20 mg of human albumin (Sigma, A1887) into 1 ml of Tris Buffered Saline (TBS). Then dilute this stock solution of 20 mg/ml by a factor of 25 in blank, non-transplanted SCID/uPA mouse serum to get $20 / 25 = 0.8$ mg/ml human albumin in mouse serum. Alternatively can use some other non-transplanted mouse serum as diluent but theoretically should use SCID/uPA mouse serum.

Now dilute the 0.8 mg/ml = 800 µg/ml standard 1:1 repeatedly in blank mouse serum to get the series of standards ranging from 800 – 25 µg/ml human albumin in mouse serum. Aliquot and freeze. Over time with repeated freeze / thaw cycles the signal in the standards can decrease significantly, so it is important to aliquot the standards out before freezing. Also, remember to include an aliquot of blank serum in the standard series to serve as a negative control for the assay.

1. Add 2 µl of serum and 40 µl of reducing buffer in eppendorph. Vortex
2. Heat at 100 °C for 5 min
3. Cool for 2 min at room temperature
4. Blot 2 µl of mixture onto DRY nitrocellulose membrane. Use new tip for each blot. Vortex tube before each blot. Blot each standard in triplicate and each mouse sample in duplicate.
5. Allow membrane to dry for 20 min
6. Soak membrane for 10 minutes in Western Transfer Buffer (allows membrane to expand in size before being taped down in plastic dish)

7. Block with 3% PBST for 1 hr (30 cc volume per membrane)
8. Biotinylated HSA-11 in 0.5% PBST at 1:5000 for 2 hours (30 cc volume)
9. 3 twenty minute washes with 1% PBST (30 cc volume per wash)
10. SA-HRP at 1:10000 in 0.1% PBST for 1 hour (30 cc volume)
11. 6 X 10 minute washes with 0.1% PBST (30 cc volume per wash)
12. Mix ECL-PLUS (Amersham) reagents as per manufacturers directions (need 2 mls of solution per membrane)
13. Apply 2 ml of ECL-PLUS evenly to membrane for 1-1.5 minutes – or until standard signal becomes visible.
14. Place membrane face down on STORM 860 phosphorimager – make sure there are no air bubbles trapped beneath membrane.
15. Scan in image with “Blue Chemifluorescence” setting. This generates a “gel” file. Select each blot with identical sized circle / ellipse and then choose “Volume Analyze” and have results stored in an excel file.
16. Average the fluorescent readout number for each blot (discard obvious outliers) and use kinetics formula to generate best fit standard curve and equation. Calculate the HA values for the sampled mice off of the linear portion of the standard curve.

6. HUMAN ALPHA-1-ANTITRYPSIN ELISA ASSAY:

SOLUTIONS:

Dialysis Buffer (to dialyze primary Antibody out of azide):

50mM K_2HPO_4 , dibasic, adjust to pH 8.0 with 50mM KH_2PO_4 monobasic

Coating Buffer:

0.1 M $NaHCO_3$, titrated to pH 9.5 with 0.1 M Na_2CO_3

Tris Buffered Saline – Tween (TBST):

20X stock: 1M Tris, adjusted to pH 7.5 with concentrated HCl

Working Buffer: 50 ml 20X stock, 5.84 g NaCl, 0.5 ml Tween 20

Milk Buffer:

1 g Low Fat Dry Milk Solids / 20 ml TBST

Dialysis Buffer (for conjugation of HRP to primary Ab):

50 mM NaH₂PO₄, adjusted to pH 6.8 with 50mM Na₂HPO₄; 0.9 % NaCl; 0.2%

Thimerosal (Sigma T-5125)

Citrate / Phosphate Buffer (make fresh each time):

2.4 ml 0.1 M citric acid (1.92g/100ml)

2.6 ml 0.2 M Na₂HPO₄ (2.84g/100ml)

5 ml ddH₂O – pH to 5.0 before using

PREPARATION OF ANTIBODIES:

- 1) Dialyze azide out of primary antibody (Diasorin, Goat anti-human-alpha-1-antitrypsin, # 81902) by dialyzing through 3 changes of 500 cc volumes with dialysis buffer in spectraphor tubing, MW 12,000 – 14,000. Measure protein concentration with spectroscopy at 280 nm. OD of 1.44 at 180 nm corresponds to 1mg/ml of protein. Freeze half of the antibody to be used as the primary=capture antibody
- 2) Using dialyzed antibody, follow steps in Pierce EZ link Plus Activated Peroxidase Kit (Pierce, #31489) (use the carbonate – bicarbonate buffer pack, not the phosphate buffered saline pack.)
- 3) After linking, dialyze into the Thimerosal containing dialysis buffer through 3 changes of 500 cc volumes with the spectraphor tubing, MW 12,000 – 14,000. Aliquot and freeze as secondary buffer.

ELISA PROCEDURE:

1. Coat plates overnight at 4 degrees, 50 μ l per well of primary antibody diluted 1:1000 in coating buffer
2. Wash plate X 1 with TBST. Slam to remove fluid.
3. Coat plate with milk buffer, 200 μ l /well overnight at 4 degrees
4. TO PREPARE SAMPLES:
 - a. Dilute Calibrator-4 in milk buffer to get a final concentration of 100 ng/ml.
 - b. In clean 96-well plate, add 150 μ l / well of milk buffer to all wells in rows B-H. Add 150 μ l of milk buffer to well A1. Column 1 is your blank column.
 - c. Dilute mouse samples 1:100 in milk buffer (2 μ l mouse serum + 198 μ l milk buffer. Run a non-transplanted mouse as a negative control.
 - d. In wells A2 and B2 add 300 μ l of Calibrator 4 / milk buffer 100 ng/ml solution. Columns 2 and 3 will be your Calibrator standard columns to generate a standard curve from.
 - e. In the remaining columns (3-12) add 200 μ l of the mouse serum / milk buffer solution which is at 1:100 dilution
 - f. Serially transfer 150 μ l down the plate in columns 2 and 3 – this results in the top row at 100 ng/ml with 1:2 dilutions from there giving 50 ng/ml, 25 ng/ml, 12.5 ng/ml etc.
 - g. For the columns 4-12, (mouse samples), serially transfer 50 μ l down the plate. This results in 1:4 dilutions (50 μ l + 150 μ l) giving dilutions of 1:100, 1:400, 1:1600 etc.
5. Wash blocked plate X 2 with TBST. Slam to remove fluid.
6. Once the entire plate has been mixed, carefully transfer 50 μ l from the mixed plate to the coated + blocked plate. Incubate for 2 hours at Room Temp covered
7. Wash plate X 3 in TBST. Slam to remove fluid
8. Dilute HRP-linked secondary 1:300 in milk buffer and add 50 μ l / well. Incubate for 2 hours at Room Temp.

9. Prepare TBMD solution: For each plate need: 2.4 ml 0.1 M Citric acid + 2.6 ml 0.2 M Na₂HPO₄ + 5 ml of H₂O → pH this solution to 5.0. Add 1 tablet of TBMD and shake until dissolved. Filter using syringe and filter tip. Add 3 µl of 30% H₂O₂ immediately before use.
10. Wash plate X 3 with TBST. Slam to remove fluid.
11. Add 50 µl of TBMD solution in TIMED additions.
12. Allow reaction to run for 5 minutes
13. Stop reaction by adding 50 µl of 1 M H₂SO₄ in TIMED additions.
14. Read on plate reader at wavelength 450 nm.

7. BIOTINYLATION OF ANTIBODIES:

- Use “Ultra-Free MC Millipore Centrifuge Tubes”, 10,000 NMWL (Nominal Molecular Weight Limit)
- Need 0.1 M NaHCO₃, pH 8.4 (0.1 M = 0.84g in 100cc or 0.42 g in 50 cc)
- Need to Sterile Filter before use.
This is used to dialyze the antibody out of the azide. Azide interferes with the biotinylation.
- Put antibody into top cup of Centrifuge Tubes, top up with 0.1 M NaHCO₃, pH 8.4
- Centrifuge at 7000 rpm for 5 minutes. Top up again with NaHCO₃.
- **NOTE:** Don't let volume get too small in top cup – if antibody gets too concentrated then antibody will precipitate out.
- Repeat Centrifuge / Top-up and spin at 7000 rpm for: 2min, 2min, 5 min, 8 min, 10 min, 10 min, 15 min. When finished, remove antibody from top cup of centrifuge tube and rinse membrane to get any antibody stuck to the membrane.
- Weigh out Biotin – approximately 1 mg – easiest to weigh out directly into an eppendorph
- (Molecular Probes Inc, Eugene, OR, USA. 503-465-8300.)

- 6-(((6-((biotinoyl)amino)hexanoyl)amino)hexanoic acid, succinimidyl ester.
MW=567.7)
- Mix Biotin in dimethylsulfoxide (DMSO) to concentration of 10 mg / ml = 10 $\mu\text{g} / \mu\text{l}$ = 10mg / 1000ul = 1mg / 100 ul DMSO
- Add Biotin / DMSO solution to Antibody/ NaHCO_3 solution – need to add 80 μg of Biotin per mg of antibody = 8 μl of Biotin / DMSO solution
- Vortex
- Incubate for 4 hours at Room Temperature
- Dialyze back into PBS.NaNO_3 – exchange 5 volumes using Millipore Centrifuge Tubes as in step 1.
- Aliquot and store at 4°C